CONSEQUENCES OF PROTEOLYTIC MODIFICATION OF THE MOLECULAR CHAPERONE ALPHA-CRYSTALLIN

by

Mary-Jane Kelley

A DISSERTATION

Presented to the Department of Biochemistry and Molecular Biology

and

the Oregon Health Sciences University

School of Medicine

in partial fulfillment of

the requirements for the degree of

Doctor of Philosophy

May 1994

TABLE OF CONTENTS

ACKNOWLEDGEMENTS

First and foremost, I would like to thank my advisor, Dr. Tom Shearer, for allowing me to work in his laboratory, for providing a positive research opportunity, for conducting some of the chaperone assays, especially in Figure 4, and for advice and general support. I would also like to thank members of the Shearer laboratory for their help and support. Particularly, I would like to thank Jay Wright for helping with computer graphics, calpain preparation and purification of rat crystallins; Dr. Naoki Iwasaki for computer assistance and help with some of the chaperone assays; Dr. Ruth Anderson and Dr. Wes Bullock for advice and for criticizing this document; Dr. Mike Meredith for graciously sharing his equipment and chemicals; Dr. Walter Gabler for the same; and Dr. Larry David for help with equipment, advice on methods and data analysis, help with Figures 5 and 6, and for helpful discussions and criticisms. I am grateful to Jackie Powell for retyping the introduction at the last minute. I would also like to thank my advisory committee for advice, support and suggestions.

In addition, I thank my friends and fellow graduate students, who made me laugh, who amused and bemused me, and most of all encouraged and inspired me when I sorely needed it. Finally, I thank my family for not disowning me through missed birthdays, weddings, reunions, and celebrations, during this process, and for their continued love and attention.

ABSTRACT

Cataracts are a primary cause of blindness worldwide, thus optimum preventive treatments are of considerable interest. The molecular etiology of cataractogenesis is not well-understood, although a variety of mechanisms have been implicated. Several animal models have been developed to determine this etiology, including the selenite rat cataract model. The focus of this dissertation is upon an understanding of the role of α-crystallin chaperone function in the molecular etiology of cataractogenesis in an animal model. The working hypothesis is that calcium enters into the lens. This calcium elevation activates calpain II, a proteolytic enzyme implicated in cataract formation. Activated calpain II acts on lens α-crystallins, compromising their ability to serve as chaperones for the β- and γ-crystallins when they are exposed to denaturation stress. These unprotected crystallins then aggregate and become insoluble, producing the opacity, which serves as a hallmark of nuclear cataracts.

This hypothesis is supported by several critical pieces of evidence. First, *in vitro* incubation of α-crystallin with calpain II caused loss of the C-terminus, and diminished chaperone activity. Second, *in vivo,* the action of calpain on α-crystallin caused reduction in chaperone activity of α-crystallin from selenite cataract. The *in vivo* data implicated a specific enzyme found in the lens, calpain II, as responsible for removal of the C-terminus, and established the first evidence of diminished chaperone function in a model of cataract. The *in vitro* information demonstrated that intact α-crystallin was proteolyzed by calpain II in a manner that was the same as that of *in vivo* α-crystallin isolated from the lens of animals with selenite nuclear cataract. From these

investigations, the chaperone behavior of α-crystallins and of cataract formation has been better elucidated.

Additional supporting evidence supplied by these studies defined the interactions between α-and β-crystallins. When exposed to heat, βH-crystallins precipitated more readily than did βL-crystallins, in the absence of α-crystallin. βH-crystallin required more α-crystallin to prevent heat-induced protein precipitation than did βL-crystallins. Precipitating subunits differed between the two β-crystallin aggregates. Precipitates of heated βH-crystallin contained an increased proportion of subunits βB1a and βB1b, while precipitates of heated βL-crystallin contained an increased proportion of subunits βB2 and βB3, when analyzed by two-dimensional gel electrophoresis.

We also studied the factors that were important in the maintenance of α-crystallin chaperone activity. Preheating reduced the ability of α-crystallin to serve as a chaperone of βL-crystallin. LMW α-crystallins are more efficient chaperones of βL-crystallin than HMW α-crystallin. A concentration dependence for optimal chaperone activity of α-crystallin subunits was determined with αA serving as the most efficient chaperone at higher concentrations, and αt serving as the most efficient chaperone at lower concentrations. For α-crystallins the optimum subunit ratio for chaperone activity was found to be 2:1 (αA:αB). Alpha A chaperone activity was the most severely decreased by calpain proteolysis of the α-crystallin subunits. HMW α-crystallin appeared resistant to calpain proteolysis and had little effect upon chaperone activity. The data lead to the conclusion that, in animal models, α-crystallin is an important factor in helping to maintain the solubility of crystallins in lens.

LIST OF ABBREVIATIONS USED

αA	alpha A crystallin subunit
αB	alpha B crystallin subunit
αinsert	alpha A insert crystallin subunit
αt	native or unfractionated α-crystallin fraction
βA_1	acidic subunit of βH-and βL-crystallin aggregates
βA_2	acidic subunit of βH-and βL-crystallin aggregates
βA_3	acidic subunit of βH-and βL-crystallin aggregates
βA_4	acidic subunit of βH-and βL-crystallin aggregates
βB_2	basic subunit of βH-and βL-crystallin aggregates
βB_3	basic subunit of βH-and βL-crystallin aggregates
βB_{1a}	basic subunit of βH-crystallin aggregates
βB_{1b}	basic subunit of βH-crystallin aggregates
βH	Beta heavy crystallin fraction from gel filtration
βL	Beta light crystallin fraction from gel filtration
BSA	bovine serum albumin
CC	cortex fraction of the lens from control animals
CN	nuclear fraction of the lens from control animals
DEAE	diethylaminoethyl (anion exchange resin)
dpi	dots per inch
DTE	dithioerythritol
E64	synthetic cystein protease
ELISA	enzyme linked immunosorbant assay
FAB	fast atom bombardment (mass spectrophotometry)
γ	gamma-crystallin fraction from gel filtration
HMW	high molecular weight (minor α-crystallin fraction)
HPLC	high-pressure liquid chromatography
HSP	heat shock protein
LMW	low molecular weight (major or normal α-crystallin fraction)
mOD	10^{-3} (milli-) optical density units
PTH	phenylthiohydantoin
PVDF	polyvinylidene difluoride
SDS-PAGE	sodium dodecylsulfate-polyacrylamide gel electrophoresis
SC	cortical fraction of the lens from selenite cataract animals
SN	nuclear fraction of the lens from selenite cataract animals
TFA	trifluoroacetic acid

INTRODUCTION

GOAL: TO INVESTIGATE THE BIOCHEMICAL MECHANISM FOR CHAPERONE FUNCTION OF LENS ALPHA-CRYSTALLIN AND TO UNDERSTAND THE ROLE OF ALPHA-CRYSTALLIN CHAPERONE ACTIVITY IN CATARACT DEVELOPMENT.

LENS FUNCTION.

From the earliest light-sensitive patches of primitive creatures to the structure found in most mammals today, the eye has provided not only vision, but sensitivity to light and photoperiodism of diurnal rhythms, as well as more subtle aspects of mood and affect. The normal lens of the eye, one of a number of refractive media, is a clear, transparent structure that allows light rays to pass through and focus on the retina. This happens without loss of information from light scattering (126). The intermolecular organization and interactions of lens components, are critical for transparency, refractive properties, and ability to accommodate (12,128,147,151,169). To focus light, the lens must have a higher refractive index than the surrounding medium. Very high concentrations of soluble structural proteins, the crystallins, are thought to be responsible for this high refractive index (2). These lens proteins are not inherently more transparent than other proteins, but, since these proteins persist without replacement, they resist large-scale aggregation and maintain structural organization for the visual lifetime of the individual (167).

Opacification, the process whereby the normal transparency of the lens is disrupted because of structural and functional changes is termed cataractogenesis. The lens becomes occluded and unable to transmit light. Cataract is the major cause of blindness in developing countries (113); lack of treatment in the Third World causes untold misery and malfunctioning. Cataract may often be treated by a brief surgical procedure in this country, and is generally successful outpatient surgery. However, this expensive surgery is unavailable for many in poorer countries. The most prevalent type of cataract is senile cataract. Since 50% of the elderly over 75 show some incidence of cataract, the development of a drug to delay or prevent the onset of cataract would be of quite beneficial. The studies described herein were designed to examine the molecular changes that occur during cataractogenesis. A molecular understanding of the mechanism of cataractogenesis should allow the development of rational treatments or prevention of this common disease. Knowledge gained studying animal cataract models will help in understanding the less experimentally accessible human forms of cataract. The relationships of protein aggregation and denaturation involved in cataract will facilitate understanding of the biochemistry of this disease.

LENS STRUCTURE.

Basic anatomical features.

The human lens is described as a biconvex structure; the anterior surface, which faces the cornea, has less curvature than the posterior surface, which faces the vitreous. The lens is not static. It is capable of changing shape rapidly, depending upon the desired visual focus, although these changes in shape become restricted with aging (126).

Located between the aqueous and vitreous humours of the eye, the lens is held by suspensory ligaments that connect the poles of the lens to the ciliary body of the pigmented iris diaphragm. The suspensory ligaments are utilized in lens accommodation, allowing the lens to change shape for near and far vision. The innermost region of the lens is known as the nucleus, while the outer region surrounding the nucleus is called cortex. The lens is avascular and receives its nutrients from the aqueous humour, which also removes waste products, such as lactic acid (64).

Development.

Developing lens fibers are laid down in concentric layers as the cells differentiate. Initially the lens develops as an ectodermal thickening that invaginates and pinches off as a spherical lens vesicle surrounding a central cavity. When the developing optic vesicle makes contact with the lens vesicle, the epithelial cells of the lens begin synthesis of lens-specific proteins. At the equator, a central region of the lens, cells quickly elongate and differentiate to lens fibers, losing their nuclei as well as the majority of their organelles. Complete differentiation of the inner lens fiber cells results in loss of protein synthesis, active cation transport, cell division, and secretion of capsular precursors (126).

Fibers: Shape, Size, and Contents.

In the adult body, there are only a few structures containing cells that are preserved without turnover of their proteins; one of these is the lens. The epithelial cells differentiate as they migrate into the lens, and the innermost, oldest cells become the lens nucleus. As the lens develops and grows, the epithelial cells increase lens

protein production until they differentiate into fibers. Elongated fibers lie side by side to form the thick refractile body of the lens. Throughout life, there is a migration and an addition of fibers to the layers which are already present and these decrease gradually(96). Therefore, the core of proteins laid down in the embryonic lens nucleus are the among the oldest proteins in an individual. As new layers of fibers are added to the cortex throughout life, no proteins are lost from the inner fiber layers.

A non-cellular capsule surrounds the lens (126). This capsule contains sulfated glycosaminoglycans (161) and has several layers; the outermost layer is composed of collagen and zonular elastic microfibrils (29,30,43). The lens increases in volume as it grows throughout life, and the lens capsule expands as well (56).

Lens Proteins.

With the growth of the lens, two major types of proteins are synthesized: insoluble and soluble. The transformation of epithelial cells into fiber cells at the equator is characterized by the massive accumulation of soluble crystallins and de novo synthesis of membrane proteins, lipids and other components for insertion into the fiber cell plasma membrane. The mature fiber cell contains two compartments: the structural soluble (and insoluble) crystallins and cytoskeletal components (2).

Given the absence of new protein synthesis, posttranslational modifications play a primary role in changing the composition of the mature lens. Methods such as SDS-PAGE gel electrophoresis have been used to analyze these lens proteins, and show that the crude plasma membrane fraction consists of several components that are classified as insoluble proteins. The most abundant of these is a membrane polypeptide of 25-27

kDa (1,24). This protein was present in a wide variety of species and was named MP26 (membrane protein 26) (18). There are numerous other proteins classified as insoluble, but MP26 is the most abundant.

Soluble Proteins:

Enzymes.

The lens contains several proteolytic enzymes (65). In most tissues proteolysis is initiated by endopeptidases, with the aminopeptidases (exopeptidases) completing the cleavage peptide fragments to individual amino acids. The major exopeptidase of the lens is leucine aminopeptidase, which catalyzes the hydrolysis of N-terminal amino acids from a wide range of synthetic peptides (65). The primary focus in this document will be on the neutral endopeptidase, calpain.

Calpain

Endopeptidases include the calpains, which are sulfhydryl (cysteine), calcium-dependent, neutral endopeptidases ubiquitously distributed in mammalian and avian tissues. The action of calpain is one of limited proteolysis. Two distinct forms of the enzyme have been identified: calpain I, which is activated at a low (approximately 10 μM) concentration of calcium, and calpain II, which requires high (500 μM) calcium for activity. The first evidence that calpain was proteolytic in the lens was noted by several groups studying lens cytoskeletal preparations (88,130,132,133) and in lens homogenates (133).

Purified calpain II from rat lens is a protein of Mr approximately 120,000, composed of 80-and 28-kDa subunits (35). Several endogenous substrates for calpain

have been isolated and characterized in rat (35) and bovine (88) lens; these include vimentin, intrinsic membrane proteins, and crystallins. Calpain II partially proteolyzes α- and β-crystallins, but not γ-crystallin. In human lens, calpain II activity has also been detected, but the specific activity is only about 3% of that present in rat lens (38). Calpastatin, an endogenous inhibitor of both types of calpain, is also found in most tissues. High levels of inhibitor calpastatin are present in human lens, especially in the nuclear region.

Crystallins.

The soluble crystallins of the lens are substrate for calpain II. Based on their elution during molecular sieve chromatography, the structural crystallins are classed as α, β-heavy (βH), β-light (βL) or (γ), and comprise approximately 90% of the lens dry weight. The high concentration of crystallins (about 30%) produces the high refractive index needed for the proper functioning of the lens (126). Lens crystallins comprise two superfamilies, α, and β-γ-crystallins (48,119,120,123). Interestingly, the non-mammalian crystallins seem to be enzymes recruited for structural purposes (120). For nearly a century α, β, and γ-crystallins have been known, and most mammalian lenses examined have only α, β, and γ-crystallins (82). Recently, δ-crystallin, which is present exclusively in birds and reptiles, has been identified. Guinea pig lens contains another crystallin, ϵ (82).

Crystallins are usually isolated from lens homogenates, and then purified using a combination of physical methods: ion-exchange chromatography, gel filtration, isoelectric focusing, SDS-PAGE, and chromatofocusing. Except for the six γ and βs

crystallins, which are monomeric, all crystallins are multimeric subunits. Gamma-crystallins are differentially distributed across the lens, with the concentration increasing from the cortex to the nucleus.

LENS BIOCHEMISTRY

Types of Crystallins.

βγ-Crystallins.

Composition.

The mammalian crystallins in solution, largely the α-, β-, and γ-crystallins, are comprised of monomers and oligomers in an array of sizes. The βγ family is composed of β- and γ-crystallins that have many similarities as well as differences. While α- and β-crystallins exist in a multimeric state, the γ-crystallins are monomers. The β-crystallins individual subunits are only slightly larger than the γ-crystallins (50-200 kDa) (58), while the aggregates are of different sizes and are smaller than α-crystallin aggregates (103). At physiological pH, the crystallins have a range of net charges. Gamma-crystallins are the most positive while α-crystallins are the most negative (103). Despite these differences, amino acid compositions and molecular studies demonstrate an homology between γ-crystallins and certain β-crystallins. The similarities that the β- and γ-crystallins share have resulted in their classification as a single protein superfamily (103). In addition to homology, the β- and γ-crystallins show similarities in intermolecular interactions, charge stabilization, secondary and tertiary structure, and location of sulfhydryl groups (103). From the gel filtration profiles, β-crystallins are classified as βH (heavy) and βL (light). The β- and γ-crystallins have similar secondary

and tertiary structures: Four antiparallel β-strands in each of four 'Greek Key' motifs divided between two domains (64). The basic β-crystallins have both N- and C-terminal peptides extending from their four-motif core structures, while the acidic β-crystallins have only prominent N-terminal peptide extensions (13). Three-dimensional models of β-crystallins using interactive computer graphics, also show that a number of the β-crystallins share a common origin with γ-crystallin.

The γ-crystallins are very prominent in most vertebrates, and all of the primary sequences and tertiary structures for the γ-crystallins have been established. The γ-crystallin secondary structures are composed of β-pleated sheets, and are very symmetrical.

Location.

It is thought that an ancestral βγ gene was duplicated to produce the β-crystallin subunit family as well as the closely-related family of γ-crystallin monomers. This is based on evidence from their gene structures and their protein structures deduced from x-ray crystallography. All β-crystallins are thought to be organ specific to the eye and are found in a gradually increasing concentration gradient from the cortex to the nucleus. The chromosomal location of most β-crystallin genes is not known (13). The location of two linked βB2 genes is known, they are mapped to chromosome 22. Another β-crystallin, BA3/A1, is on chromosome 17. The γ-crystallins are enriched in the nucleus, but undergo extensive insolubilization with aging (13).

Heterogeneity.

While the β-crystallin heteropolymers are 50-200 kDa, each of the polypeptides

is composed of 20-30-kDa subunits in varying numbers. There are eight β-crystallin primary gene products, and these have been assigned as βA (acidic) and βB (basic). Both the βH-and βL-crystallins contain basic and acidic primary gene products, some of which they share and some of which are found only in βH-crystallin (13). The γ-crystallins comprise six homologous proteins of about 21 kDa. They contain seven cysteine residues, which is thought to be important in lens transparency (13).

Alpha Crystallin.

Composition.

Alpha crystallins, which can bind and protect other crystallins from heat-induced denaturation, are macromolecular weight aggregates with an Mr of 600-900 kDa in the native state (40). The wide range of molecular weights observed for α-crystallins is related to variations of isolation procedures involving temperature (148,149), ionic strength, and pH of the extracting buffers. Other factors important for this heterogeneity of molecular weight are the age of the lens (154) as well as post-translational modifications. Alpha-crystallin is an aggregate of 20 kDa monomers composed of an acidic chain, αA-2, and a basic chain, αB-2. These normally occur in a ratio of 2:1, respectively (159).

The two chains, αA-2 and αB-2 (often referred to now as αA and αB), are held together in the native state by noncovalent interactions (140). In some rodents, such as rat, α-crystallin also contains an αAinsert subunit, which is identical to αA2, except for an additional 23-residue peptide inserted between residues 63 and 64 (30). The amino acid sequences of αA-2 and αB-2 are known and are 57% homologous (155). The αA2

chain has 173 amino acids, with a molecular weight of 19,830, whereas the αB2 chain has 175 residues with a molecular weight 20,070 (138). Alpha-A and αB polypeptides likely arose by gene duplication from a single α-crystallin gene. An important feature is a sequence homology with small heat shock proteins, suggesting that the ancestral α-crystallin gene and heat shock genes shared a common origin (65).

Location.

Originally, α-crystallin was thought to be exclusively a lens protein, but now it has been identified in numerous other tissues in the body. In the mid-1980's using specific antibodies against αA or αB, Bhat and Nagineni (14,15) were the first to show clearly that αB is present in non-lenticular tissues such as heart, brain, skeletal muscle, skin, spinal cord, and lung. Using Northern blot analysis, Dubin, Wawrousek, and Piatigorsky (49) also showed that the αB gene is expressed in non-lens tissues. Until 1991, αA was believed to be lens-specific, but it is now known that the highest concentration of αA is in the spleen and thymus (91).

Within the lens itself, α-crystallin is located in both the cortex and the nucleus, and its concentration increases gradually from the outside layers to the core. The amounts of truncated αA2 and αB2 changes in bovine lens, which suggests a step-wise breakdown from the C-terminus (157,157). In addition, since the C-terminal shortened A and B chains increase from the cortex to the nucleus, this suggests an age-dependent degradation process (138).

As for the chromosomal location, the subunits are encoded by single copy genes located on different chromosomes (71,81). The genes for human and rat αA have been

mapped to chromosomes 21 (53) and 17 (13) respectively, while human αB gene has been mapped to chromosome 11 (23,114).

Heterogeneity.

A primary cause of the molecular weight heterogeneity of α-crystallin is post-translational modifications (16). Such posttranslation modification may occur through cAMP-dependent phosphorylation of serine residues in both the A and B chains (140). Others (65) have determined that truncated forms of α-crystallin are produced spontaneously by nonenzymatic cleavage of the primary gene products at the C-terminal end of αA and αB. Recent work clearly shows that the αA1 and αB1 chains are examples of posttranslationally modified polypeptides (65,140). In addition to phosphorylation and truncation, other conditions also contribute to the heterogeneity of size found in the range of α-crystallin molecular weights, such as oxidative conditions. Oxidative crosslinking of crystallins occurs in bovine crystallins (59), which contain both αA and αB chains (104).

Posttranslational modifications also contribute to the considerable polymerization of native α crystallin (16), including the formation of HMW aggregates. In aging and in cataractous conditions, HMW aggregates are common; these are non-disulfide cross-linked crystallins that have been found to be composed of 1 αA: 2 αB chains, with molecular weights in excess of 1 million. Another type of non-disulfide cross-linked crystallin, a 43 kDa crystallin aggregate isolated from human cataractous lenses was also found (131). Sequence analysis of a 30 kDa fragment cleaved from the 43 kDa crystallin by limited proteolysis showed that it is composed of three distinct components

corresponding to A and B chain polypeptides in the ratio of 1:2. These investigations provided compelling evidence that the A and B chains in the parent 43 kDa aggregate are held together by covalently cross-linked nonreducible bonds (40).

Domains of α-crystallin.

The αA-crystallin monomer can be divided into at least two functionally distinct domains. Recent work indicates that the N-terminal domain is relatively hydrophobic and suggests that it may mediate interactions between α-crystallin and the lens membrane (84). What is responsible for the ability of α-crystallin to bind and protect other crystallins against precipitation, has not been studied. One of the functions of a chaperone protein is to prevent precipitation of other proteins, as α-crystallin does. It is not known if α-crystallin chaperone activity is functional because of the conformation of the entire structure, or a specific region or if a sequence of the protein is able to bind and prevent aggregation and precipitation of other crystallins. The C-terminus of αA may be involved in the binding to other crystallins or may interact with other parts of the αA and/or αB chains resulting in a configuration that directly binds to and stabilizes other lens proteins against further denaturation (109,146). Expansion of this hypothesis is the major theme of this thesis.

Crystallin Interactions.

Calpain and Cataract.

Cataract is the opacification of the lens, and may occlude a part of the lens or the total lens. Some common types of cataract are diabetic or sugar cataract, steroid-induced cataract, ultra-violet and radiation cataracts, and the most common type of cataract,

senile cataract. Cataracts may occur for a variety of reasons, including disease, exposure to toxic substances, injuries, congenital anomalies, or aging (13). In addition, various types of experimental cataracts have been developed in animal models, by agents such as galactose, radiation, or injection of selenite (35,136).

Selenite cataract is an experimental cataract produced in suckling rat pups by a single subcutaneous injection of sodium selenite at ten days of age (34). Within three to five days, severe opacity of the nucleus of the lens appears; a temporary cortical opacity forms within 15-30 days after the injection. While the cortical opacity clears, the nuclear opacity does not. The current hypothesis for the mechanism of action of selenite cataract, as developed in our lab, is that the lens epithelial membranes contain crucial sulfhydryl groups that are oxidized by selenite. Calcium homeostasis is impaired by the oxidation of the sulfhydryl groups, which results in an accumulation of calcium in the nucleus of the lens. Calpain II, a calcium-dependent proteolytic enzyme, is activated by the increased calcium in the lens. Calpain produces limited proteolysis of crystallins, resulting in insolubilization of β-crystallin, increased light scattering, and abnormal interactions between the crystallins (135,136).

Calpain is a calcium-activated, non-lysosomal neutral cysteine protease (34,135). Strong evidence exists for activation of calpain as a causal factor in rodent cataracts: 1) Calpain II is found in the lens, and calcium levels are sufficiently high (mM) to activate calpain II; 2) The cleavage sites found on insoluble β-crystallins during cataractogenesis are identical to the cleavage sites produced by incubation of β-crystallins with calpain *in vitro*; 3) Many rodent models of cataract, including selenite cataract *in vivo*, have

patterns of proteolysis typical of calpain substrate specificity; 4) Calpain proteolysis of crystallins causes insolubilization *in vitro*, thereby mimicking opacity in cataract (68).

Molecular Chaperone Concept.

Three-dimensional structures govern the biological activities of proteins. Twenty years ago, Anfinsen (4,5,32,33), based on critical *in vitro* studies of reversible unfolding of ribonuclease A, proposed that proteins are self-organizing molecules and that the amino acid sequence contained all of the information required for a polypeptide to fold to its native three-dimensional conformation. How proteins fold into complex formations has been examined recently in more detail. Anfinsen's experiments led to the view that, in principle, protein folding *in vivo* also occurs by a spontaneous process (4). Although the self-organizing model for renaturation seemed appropriate for many proteins, further data emerged that seemed to conflict with the model of spontaneous folding. Examples of proteins that do not fold spontaneously include α-lytic protease and subtilisin (139). The inability of some proteins to spontaneously refold complicated the problem of protein folding and suggested that other factors may be required to mediate folding for those specific proteins. Subsequently, this phenomenon was noted in proteins other than subtilisin (139), but does not seem to be necessary for the majority of protein folding. Concurrently, a protein was identified whose function was to facilitate folding. This protein was GroEL, which is a member of a very large family of proteins now called molecular chaperones (52).

Although spontaneous folding could easily happen if there were only one or a few

possible final forms, there are many conformations to which proteins can refold. Proteins often refold to the native conformation in a matter of seconds. However, the time required for a large polypeptide to sample all possible conformations on the way to the native state has been calculated to be on the order of the agè of the universe (101). Therefore, the study of protein folding has focused on folding intermediates on the way to the final tertiary structure, and the characterization of pathways during the refolding of denatured proteins (4,5,28,32,46,47). *In vitro* folding/unfolding studies clearly establish that rapid, unassisted protein folding is a common event. Folding competes with the other major reaction, aggregation of early folding intermediates. Refolding of most proteins can be favored if proper conditions are chosen, such as low protein concentration and low temperature (73). Recently, biochemists have concentrated on the relationship of the protein folding of the denatured state and protein folding as it occurs in the cell (15,55,58,60,68,129).

The consensus is emerging that many newly made, unfolded, or partially folded proteins are bound and released through: (a) specific protein modulators of the binding (and ATP hydrolyzing) activities of chaperones and b) the synergistic interaction and cooperation of different chaperones with each other. As a result, these proteins are transferred in an orderly manner to the various polypeptide-handling systems of the cell (101).

WHAT IS A CHAPERONE?

The term "molecular chaperone" originated to describe the function of nucleoplasmin, a protein in *Xenopus* oocytes that binds tightly to histones and donates the

bound histone to assembling chromatin. Eventually, the usage of the term was broadened to apply to a larger group of proteins. At present, a more comprehensive usage is that a molecular chaperone is " a protein that binds to and stabilizes an otherwise unstable substrate protein, and by controlled binding and release, facilitates its correct fate *in vivo*: be it folding, oligomeric assembly, membrane insertion, transport to a particular subcellular compartment, or controlled switching between active and inactive conformations (73)." Molecular chaperones are generally not components of the functional assembled structures (29,51,53,61). Molecular chaperones are involved in a host of processes that act in different cellular compartments to stabilize proteins under stress conditions, to achieve the folded state of proteins, and to regulate their activity state. They are comprised of several apparently structurally unrelated protein families, and are ubiquitous (60,73).

Normal Cellular Functions of Chaperones.

The term "molecular chaperone" has been extended to include proteins that bind to and stabilize the non-native conformations of other proteins, thereby facilitating their correct folding by releasing them in a controlled manner at the appropriate time (73). An important function of molecular chaperones is to bind to proteins and prevent their premature folding, as during translocation between cellular compartments, such as in proteins entering mitochondria. The chaperone binds to the protein in the unfolded state to prevent it from folding before it crosses the mitochondrial membrane, and subsequently releases the protein to allow folding after tranversing the membrane. A shared property common to the molecular chaperones in unfolded or partially denatured

proteins is the recognition of exposed structural elements. Thus they interact with many different polypeptide chains without exhibiting a specific sequence preference (51,60,73). Chaperones generally recognize structural elements which are exposed by proteins in non-native conformations (73). Non-functional structures are prevented from forming because chaperone proteins promote the self-assembly of polypeptides by inhibiting intermolecular aggregation, or inappropriate alternative folding pathways. Chaperones act by recognition of certain features that are common to intermediates formed during folding or unfolding. Earlier studies on folding had suggested that recognition occurred through an α-helical conformation, mediated by another molecular chaperone, GroEL (100). Recent work, however, shows that the molecular chaperone hsp70 binds to its substrate, probably via hydrogen bonds, when the polypeptide backbone of the substrate is in an extended conformation (99).

Heat-Shock Proteins.

Among the molecular chaperones are several classes of heat-shock proteins (hsps). A variety of cellular stresses can induce the expression of many molecular chaperones, causing them also to be classified as stress or heat-shock proteins. Under normal cellular conditions, most 'stress proteins" also have essential functions.

All organisms, in response to various environmental stresses, including temperature, synthesize heat-shock proteins. Until recently, the functions of heat-shock proteins (hsps) have been fairly obscure, although the phenomenon of increased synthesis of heat-shock proteins upon subjection to a stress has been known for about 30 years. Over the last few years, it has become clear that hsps are critical players in protein

biogenesis processes, such as protein synthesis and translocation into subcellular compartments. Such events temporarily require the protein to exist in a conformation that is unfolded or partially folded.

Some hsps act during heat shock or other stresses when proteins become unfolded. This prevents aggregation, which is detrimental to the cell. Hsps act by binding to the partially unfolded or nascent proteins to protect their surfaces from interactions with other partially unfolded proteins. Other hsps may bind to interactive sites on folded proteins for regulation (29). Probable candidates for assisting protein folding are the HSP 70's and HSP 60's, because of their ability to bind polypeptides. These proteins were once considered as temporary partners of unassembled subunits of oligomeric enzymes, but are now thought to be components that function to control or direct the folding of many monomeric polypeptide chains (69,76). HSP 60 proteins are a highly conserved family of approximately 60 kDa that are usually found as a 14-subunit oligomer (26,72,75,83,105). HSP 60 proteins are known as chaperonins, a subclass of sequence-related molecular chaperones, which include stress-inducible members found in bacterial cytosol, and the inner space of mitochondria and chloroplasts (72). Mitochondrial HSP 60 is one of the few proteins made in response to stress in Tetrahymena (105); these are chaperones that appear to help proteins to fold (73). HSP 70 proteins are a family of stress-inducible proteins that are approximately 70 kDa in size and have diverse roles in the cell. They have an ATP-dependent release mechanism, whereby the protein is allowed to refold upon release from the chaperone (73). They reversibly bind portions of polypeptide chains and are interactive with a number of

protein modulators that respond to other signals in the cell. HSP 90 is a chaperone that regulates protein function. It may bind to receptors, hold them in a stabilized state, and promote high affinity binding of hormones.

Other Chaperones.

The word "chaperone" in this thesis is used specifically to mean a protein which interacts with an unfolded protein to reduce its propensity to aggregate and precipitate during or following environmental stress, such as heat treatment. We presume that the type of interactions involved in this type of chaperone activity are very similar to those involved in preventing early folding following protein translation, for example, to allow cellular targeting of mitochondrial or membrane proteins. This event is probably similar to that of "stress" or "heat shock" proteins in a variety of systems. However, beyond some sequence similarity, the parallelism of these systems with the effect we are studying has not been clearly established. Thus, we will use the term chaperone with the select meaning described above.

Intermolecular Chaperones and Molten Globules.

That all proteins do not spontaneously refold was first shown with subtilisin E, an alkaline serine protease from *Bacillus subtilis,* in 1987. Subsequently, subtilisin was found to be produced as a precursor, pre-pro-subtilisin. The signal peptide of 29 residues corresponded to the pre- region, while the propeptide contained 77 residues, and protein folding was found to be facilitated by the propeptide of denatured subtilisin (85). Further work has suggested that in addition to rendering the proenzymes catalytically inactive, the function of propeptides is also to mediate correct folding without being

components of the final three-dimensional structure. Instead, they act as co-translational chaperones. This particular class of helpers was noted with a number of other proteins as well, such as α-lytic protease. In this group of molecular chaperones the propeptides, covalently attached to the amino terminus of proteins, mediate folding of that molecule. In this way they differ from other molecular chaperones and are called intramolecular chaperones (87).

The mechanisms by which intramolecular chaperones mediate protein folding are well-studied. Studies of α-lytic protease (9) and subtilisin (50) have shown that these proteins can fold into stable partially folded intermediates in the absence of its propeptide *in vitro*. Investigation of the secondary structure of the intermediate by far UV circular dichroism (CD) spectrum has shown that it is similar to that of the native state, but that there was a significant loss of tertiary structure. This intermediate structure was more compact than the unfolded chain, but less compact than the fully folded protein. This type of intermediate has been popularly called the "molten globule" intermediate (97). The intermediate state collapses to a compact, three-dimensional conformation in the presence of the propeptide, which is thought to lower a kinetic barrier between the two states (37).

Differences Between in vitro and in vivo Folding.

Refolding of early intermediates is often accomplished in terms of milliseconds, while translocation across a membrane or ribosomal extrusion of a protein often takes seconds to minutes. Refolding experiments suggest that there is a rapid equilibrium between early elements of folded structure and the unfolded state (32,46,94). Additional

studies have shown that a complete protein domain is required for the formation of a stable structure. Ribonuclease A and staphylococcal nuclease, in their C-terminally truncated form, can be regarded as *in vitro* mimics of a ribosome-associated chain. Although these fragments show compact conformations, they do not fold to an enzymatically active state (3,57). Similarly, a nascent polypeptide could neither adopt a stable structure, nor retain an extended conformation. The rapid collapse of a polypeptide chain into a compact state in an aqueous milieu is promoted by hydrophobic forces (25). Arising from the hydrophobic collapse are kinetic intermediates thought to possess properties similar to the equilibrium "molten globule" state of some proteins: 1) they are slightly larger than the native state, but compact in size; 2) they have substantial secondary structure, with few persistent tertiary interactions; and 3)they have a conformational flexibility more like the unfolded than the native state (28,97,108,122), and 4) hydrophobic areas are transiently exposed on the surface, facilitating a tendency to aggregate in both the early intermediates and the molten globule state (45). One of the functions of a healthy, active cell is to maintain and access nascent and newly synthesized intracellular polypeptide pools. This supply of proteins must be kept in a folding-competent state, yet not aggregate over a wide range of temperatures, stresses, and high protein concentrations in the cell (77), and for some proteins, the presence of a molecular chaperone to assist such processes is essential.

α-Crystallin as a Molecular Chaperone.

Evidence.

Originally, α-crystallin was thought to have a purely structural role in the

maintenance of protein-protein interactions necessary for the transparent properties and refractive index of the normal lens (45). However, the function of α-crystallins appears to be more complex than initially proposed. Using an *in vitro* assay, Horwitz (77,79) determined that α-crystallin inhibited the heat-induced denaturation and aggregation of lens β-and γ-crystallins (79). This behavior, as well as the known sequence homology of α-crystallin with small heat shock proteins (42,86), suggested that α-crystallin might also serve as a molecular chaperone in the intact lens. In many cells undergoing stress, increased amounts of these polypeptides are synthesized putatively to protect against the denaturing effects of high temperature, abnormal pH, osmotic shock, etc. Since they have protective functions, both the heat shock proteins and the α-crystallins preferentially bind to partially denatured forms of many proteins to prevent further denaturation and precipitation (127,62).

Based upon transmission electron microscopy of negatively stained protein preparations, it has been hypothesized that partially denatured proteins bind to a central, electron dense cavity present in the oligomeric complex of the GroE chaperonins (33). Recently, immunolocalization has been used to demonstrate that partially denatured forms of γ-crystallin do indeed bind to the central region of the α-crystallin complex (22).

Evolutionary evidence links α-crystallin and the small heat shock proteins, implicating α-crystallin as a molecular chaperone. Ingolia and Craig (8) discovered that the small heat-shock proteins of *Drosophila melanogaster* are evolutionarily related to the lens protein α-crystallin. Until 1985, it was thought that α-crystallin was lens-specific. However, evidence from many research groups indicates that αB is found in a variety

of non-lenticular tissues and especially prevalent in certain neurological diseases (20,65,66,80,81,121,134). Subsequently α A was found at high levels in spleen and thymus (78). Recent evidence with both α-crystallin and small hsps reconfirm that both are molecular chaperones. Jakob, et.al. (89) showed that small hsps (Hsp25, Hsp27, and bovine αB) all prevented aggregation of citrate synthase and alpha-glucosidase under heat shock conditions, as well as promoting refolding after urea denaturation. Merck, et.al. (110) in a comparison of circular dichroism experiments determined that α-crystallin and Hsp25 resemble each other in secondary structure and can form mixed polymers from any αA, αB, or Hsp25 combination. All function as molecular chaperones involving the protection of other proteins under conditions of stress.

Other researchers found that αB was particularly prevalent in neurological cells which were responding to a heat or other stress. Aoyama, et. al. (6) showed that αB crystallin is a small heat shock protein that accumulates transiently in response to heat, glucocorticoids, and other kinds of stress in NIH 3T3 fibroblasts, and protects these cells from thermal shock (6). In a similar study, Kato, et. al.(90) also established that αB crystallin was overexpressed in response to heat in human astroglioma U373 MG cells and was associated with Hsp28 in these cells (90). Head, et.al.(71) found that αB and Hsp27 were coregulated as stress proteins in CNS astrocytes in a neurological pathology, Alexander's disease. All of these similarities in function of α-crystallin and hsps suggest that common structural elements may be present in small heat shock proteins and α-crystallin. Recently, evidence was presented that this was correct, and was an amino acid sequence homology.

The most common distinguishing feature of α-crystallin and small heat shock proteins is the presence of an homologous sequence of 90-100 residues. This family includes αA and αB, a group of 15-30 kDa heat shock proteins, a major egg antigen of *Schistosoma mansoni,* and two mycobacterial surface antigens, as well as a number of members in plants. Alpha-B in particular is noted to behave like a small heat shock protein (43).

HYPOTHESIS OF THE MANUSCRIPT.

After a survey of the literature, a number of important questions remained unanswered. Can α-crystallin act as a chaperone *in vivo* as well as *in vitro*? Is it possible to show that α-crystallin has chaperone activity in the lens in an established animal model of cataract? What makes α-crystallin unable to act as a chaperone? What subunits of β-crystallin are subject to precipitation and aggregation without α-crystallin? What factors affect the optimum functioning of α-crystallin as a chaperone? Are such events *in vivo* important in cataractogenesis? Is it possible that a drug treatment for cataract could be developed for inhibiting reactions that interfere with α-crystallin? From these questions, a hypothesis may be formulated.

HYPOTHESIS: THE CHAPERONE ACTIVITY OF A-CRYSTALLIN IS A CRITICAL FEATURE IN THE MAINTENANCE OF NORMAL LENS CLARITY. COMPROMISED CHAPERONE ACTIVITY OF A-CRYSTALLIN CAUSES AGGREGATION AND PRECIPITATION OF CRYSTALLINS IN THE CATARACTOUS LENS.

MATERIALS AND METHODS

Production of Selenite Cataract.

Cataracts were induced in 10-day-old Sprague-Dawley rats (purchased from B & K International, Fremont, CA) by a single subcutaneous injection of 30 μmoles sodium selenite/kg body weight (34). Five days after injection, the cortex and nucleus of lenses were isolated by dissection, as previously described (34,92). All animals used in this study were treated in accordance with the Declaration of Helsinki and NIH guidelines.

Gel Filtration of Crystallins.

To separate the individual crystallin fractions, cortical and nuclear regions from 40 young rat lenses were homogenized in buffer I (20 mM imidazole (pH=6.8), 0.1 mM EGTA, 2 mM DTE, and 0.01% azide). Homogenates were centrifuged at 8000 X g for 15 min at room temperature (to prevent cold precipitation of crystallins). Following centrifugation, the supernatant was chromatographed on a 2.5 x 90 cm Bio-Gel A1.5 M gel filtration column (Bio-Rad, Richmond, CA), and eluted with 20 mM Tris (pH=7.5), 1 mM EGTA, 1 mM EDTA, 10 mM 2-mercaptoethanol, and 100 mM NaCl at a flow rate of 25 ml/hr. After pooling the appropriate fractions (Fig. 1), α- and βL-crystallins were concentrated by ultrafiltration (YM-5 membrane, Amicon, Beverly, MA) and the gel filtration buffer was exchanged for buffer I. For the α-crystallin preheating studies with rat crystallins, whole homogenates of 8 week-old rat lenses were subjected to homogenization, centrifugation, and chromatography as above, and then lypophilized before use. Protein concentrations were determined by Bio-Rad protein assay (Bio-Rad,

Richmond, CA) using BSA as standards.

Bovine lenses from 3-6 month old fetal calves *in utero* were obtained from a local abattoir. Bovine HMW α-, α-, β-, and γ-crystallins were purified by the same method used for rat crystallins, as described above, on either the Bio-Gel A1.5 M or a 2.5 x 90 cm Sephacryl HR-300 (Pharmacia, Piscataway, NJ) column.

Proteolysis of Lens Proteins with Calpain.

Calpain II was purified from porcine cardiac muscle as previously described (39). Porcine cardiac muscle calpain II cleaved crystallins at the same sites as those cleaved by calpain purified from rat lens (36,92). Partial proteolytic cleavage of α-crystallin was achieved by incubating 17 units of purified calpain II with 0.48 mg normal α-crystallin and 2 mM $CaCl_2$ in a total volume of 0.4 ml buffer I at 37° C. The reaction was terminated after 1 hour by the addition of 0.1 ml 25 mM EGTA.

Chaperone Experiments.

As a model for protein denaturation in the eye, heat-induced aggregation of β-crystallin was measured by a plate reader for an enzyme-linked immunoabsorbant assay (Anthos ht11, Anthos Labtec Instruments, Salzburg, Austria). The crystallin mixtures were preincubated at 37° C for 5 minutes prior to heat-induced aggregation. The plate reader shaker was activated for 10 seconds at a setting of medium before and after preincubation as well as before every 15 minute time point. Heat-induced aggregation of βL-crystallin was then studied by heating at 60 or 64° C in a total volume of 0.25 ml buffer I containing 0.08 M NaCl. Turbidity was measured as an increase in light absorbance at 340 nm. Control studies, using identical β-crystallin solutions in all wells,

indicated that the outer rows and columns of plates exhibited uneven heating, thus these wells were not used. For the chaperone experiments, various α- and β-crystallins were preincubated together prior to the heat-induced aggregation.

Electrophoresis.

One-dimensional SDS-PAGE (98) of lens proteins was performed on 12% (0.75 mm thick) acrylamide gels. Low (14-97 kDa) and broad-range (7-200 kDa) molecular weight standards (Bio-Rad) were used at 6.2 μg protein/lane. Two-dimensional gel electrophoresis using a non-equilibrium pH gradient in the first dimension and SDS-PAGE with 12% gels in the second dimension was conducted as previously described (16,37). Gels were stained with Coomassie blue. Other gels were electroblotted to PVDF membranes (Immobilon P, Millipore, Bedford, MA), and the membranes were subsequently stained with Ponceau S before being subjected to computer image analysis (Image 1.44, National Technical Service, Springfield, VA.). Images were digitized using flat bed scanning (LaCie Silverscanner, Beaverton, OR.) with green lamp illumination, at either 150 or 200 dpi resolution, and 256 grey scale levels per pixel.

Tryptic Mapping.

Following incubation with calpain, putative breakdown products of αA and αB crystallins were identified by tryptic mapping. The lenses of 14-day old rats were dissected and homogenized at a ratio of 1 mg lens wet weight/2.5 μl buffer I. The lens homogenates were centrifuged at 8000 X g for 15 min at 25° C to remove the insoluble protein. Soluble lens protein (30 mg/ml) was incubated for 60 min at 37° C in buffer I containing 2.4 units of calpain II/mg lens protein and 1.2 mM $CaCl_2$, and centrifuged at

8000 X g for 15 min. The supernatant was removed, dried in a vacuum centrifuge and frozen at -70° C. Aliquots (250 μg) of the lens proteins proteolyzed with calpain and non-proteolyzed control samples were subsequently subjected to two-dimensional gel electrophoresis, as described above, except that 125-250 μg total protein was applied. The proteins from 4 gels were blotted onto PVDF membranes, the membranes were stained with Ponceau S, and protein spots were excised from the membrane. The excised protein spots were then destained in 1mM NaOH. Subsequently, the membranes were blocked by incubation in 0.5% polyvinylprolidone-40, 0.1M acetic acid for 30 min, followed by ten rinses with MilliQ water. Blotted polypeptides were subjected to in-situ digestion with 4 μl of 1 mg/ml sequencing grade modified trypsin (Promega Corporation, Madison, WI) dissolved in 0.1% TFA plus 50 μl 0.1 M NH_4HCO_3 (pH=8.0) with 10% acetonitrile. Trypsinization released the tryptic fragments from the membranes, and they were dried by vacuum centrifugation. Following this, the tryptic fragments were solubilized in 0.1% TFA, and separated by reverse phase chromatography on a C_{18} HPLC column (150 x 2.1 mm Vydac, Hesperia, CA) (36). Chromatography was conducted at 50°C, using a 0.2 ml/min flow rate, and a linear 0-55% acetonitrile gradient containing 0.1% TFA for 75 min. Detection of tryptic fragments was by absorbance at 216 nm and one minute fractions were collected. Sequence analysis of 6-10 amino-terminal amino acid residues was used to identify the parent protein of the tryptic fragments. The protein/peptide sequencer (Applied Biosystems Model 477A Protein-Peptide Sequencer, Foster City, CA) utilized the Edman degradation technique to remove amino acids sequentially from the amino terminus (37). The molecular weights of tryptic

fragments of αA-crystallin were measured using fast atom bombardment mass spectroscopy, using a Kratos model MS-50 RF FAB mass spectrophotometer with a continuous flow probe in the laboratory of Dr. Jean Smith, Purdue University (118).

Insolubilization Studies of β-Crystallins.

Since the insolubilization studies of β-crystallins and two-dimensional analysis of the supernatants and the precipitates required large quantities of crystallins, fetal calf lenses the species was changed from rat to bovine. The amino acid residues were well-conserved and the substitution was not problematic for these studies. Alpha-, βL-, and βH-crystallins from the cortex of fetal calf lenses (6-8 months *in utero*) were used to examine the insolubilization of lens β-crystallins. Twenty-five μg α-crystallin/ml plus 75 μg βL-crystallin/ml and 50 μg α-crystallin/ml plus 50 μg βL-crystallin/ml. The control sample was 75 μg βL-crystallin/ml. The samples were centrifuged in a microfuge at 4° C for 15 minutes at 16,000 rpm prior to incubation. Supernatants containing the three mixtures of crystallins were then either heated to 64° C or maintained at 4° C for 30 minutes, followed by a second centrifugation. The resulting Supernatants and pellets were assayed with the Pierce BSA protein assay (Pierce, Rockford, Ill.) using BSA as the standard.

Preheating Studies with α-Crystallin.

Lyophilized α- and βL-crystallins from 8-week old Sprague-Dawley rat lenses were used to determine the effect of preheating on the ability of α-crystallin to prevent heat-induced aggregation of βL-crystallin. Alpha-crystallins were preheated at 60° C for 10, 30, 60, or 90 minutes prior to their incubation with βL-crystallin in the standard heat

aggregation assay. All of the preheated α-crystallins were removed from heat at the same time and allowed to stand on the bench at room temperature for approximately 20 minutes, prior to initiating the βL-crystallin aggregation assays. Preheated α-crystallins (61 μg α-crystallin/ml) were then incubated with 100 μg βL-crystallin/ml in buffer I (pH=6.8) containing 0.1 M NaCl.

Isolation of αA and αB Polypeptides from the α-Crystallin Aggregate.

The ability of the individual α-crystallin monomers (αA and αB) in the α-crystallin aggregate to act as chaperones was studied. Purified rat lens α-crystallin aggregate (MW ≈ 700,000) served as the starting material. Alpha-crystallin subunits were separated by HPLC (Waters 501 pumps and Waters Absorbance Detector, Model 441, Milford, MA) ion exchange chromatography on a 7.5 x 75 mm DEAE 5-PW column (Bio-Rad). Fifteen mg lyophilized rat α-crystallin was dissolved in 500 μl 10 mM Tris (pH=8.5) containing 10 mM DTE and incubated at 37° C for 105 minutes. Subsequently, 1.7 ml 9 M urea (ultra-pure, BDH, Poole, England) was then mixed with the α-crystallin solution to dissociate the αA and αB subunits, and the sample was injected into the HPLC . The mobile phase was 10 mM Tris, with 2 mM DTE and 6 M isocyanate-free urea (pH=8.5), with a flow rate of 1 ml/min. Elution of αA and αB was performed with a linear 100 mM NaCl gradient for 60 min. Fractions containing protein peaks were then extensively dialyzed against buffer I (pH=6.8), and protein concentrations were determined by a Bio-Rad protein assay, as described above. The α-polypeptides in the peaks were identified by SDS-PAGE, and the purified αA and αB polypeptides were then utilized in the βL-crystallin heat aggregation assay. The procedure was

repeated using α-crystallin from bovine fetal lens, except that 24 mg of fresh α-crystallin aggregate was used.

RESULTS

Isolation and Purification of Rat Lens Crystallins.

Crystallins from the lenses of rats were purified by gel filtration chromatography. After dissection of the lenses from the eyes and homogenization procedures, α- and βL-crystallins were isolated from the soluble protein fraction of 14-15 day old rat lens cortex. (Fig. 1). A two-dimensional electrophoretic gel (Fig. 1, inset) showed that normal intact α-crystallin is composed of three subunits in the rat, αA, αB, αAinsert. SDS-PAGE confirmed that α-crystallin was composed of the same three major polypeptides migrating at 20-23 kDa (Fig.2A, lane 2), and that βL-crystallin was composed of two major and two minor polypeptides migrating between 26 and 31 kDa (Fig. 2A, lane 8). A comparable purification was conducted to isolate the α-and βL-crystallins from rats with an experimentally-induced selenite nuclear cataract.

Comparison of Rat Lens Crystallins from Normal and Selenite Cataract.

Compared to controls, selenite cataract crystallins showed additional bands at lower apparent molecular weight on SDS-PAGE gels. This suggested proteolysis. The α-crystallin from normal control cortex (Fig. 2A, lane 2) was unproteolyzed, and only small amounts of α-crystallin in selenite cortex and control nucleus (CN) were proteolyzed (lanes 3 & 4). Marked degradation of the α-crystallin fraction occurred in the nucleus of lenses with selenite nuclear cataract (lane 5). Proteolytic fragments are shown below the arrow in Fig. 2A, denoting the partially degraded α-crystallins.

Fig. 1: Gel filtration chromatography of water-soluble proteins from lens cortex of 14-day old rats. The heavy vertical bars on this representative chromatogram enclose α-crystallin and βL-crystallin peaks. The inset shows a portion of a two-dimensional electrophoretic gel of the proteins in the α-crystallin peak, indicating αA, αB, and αA insert polypeptides. The matrix used for the gel filtration chromatography was Bio-Gel A1.5 M.

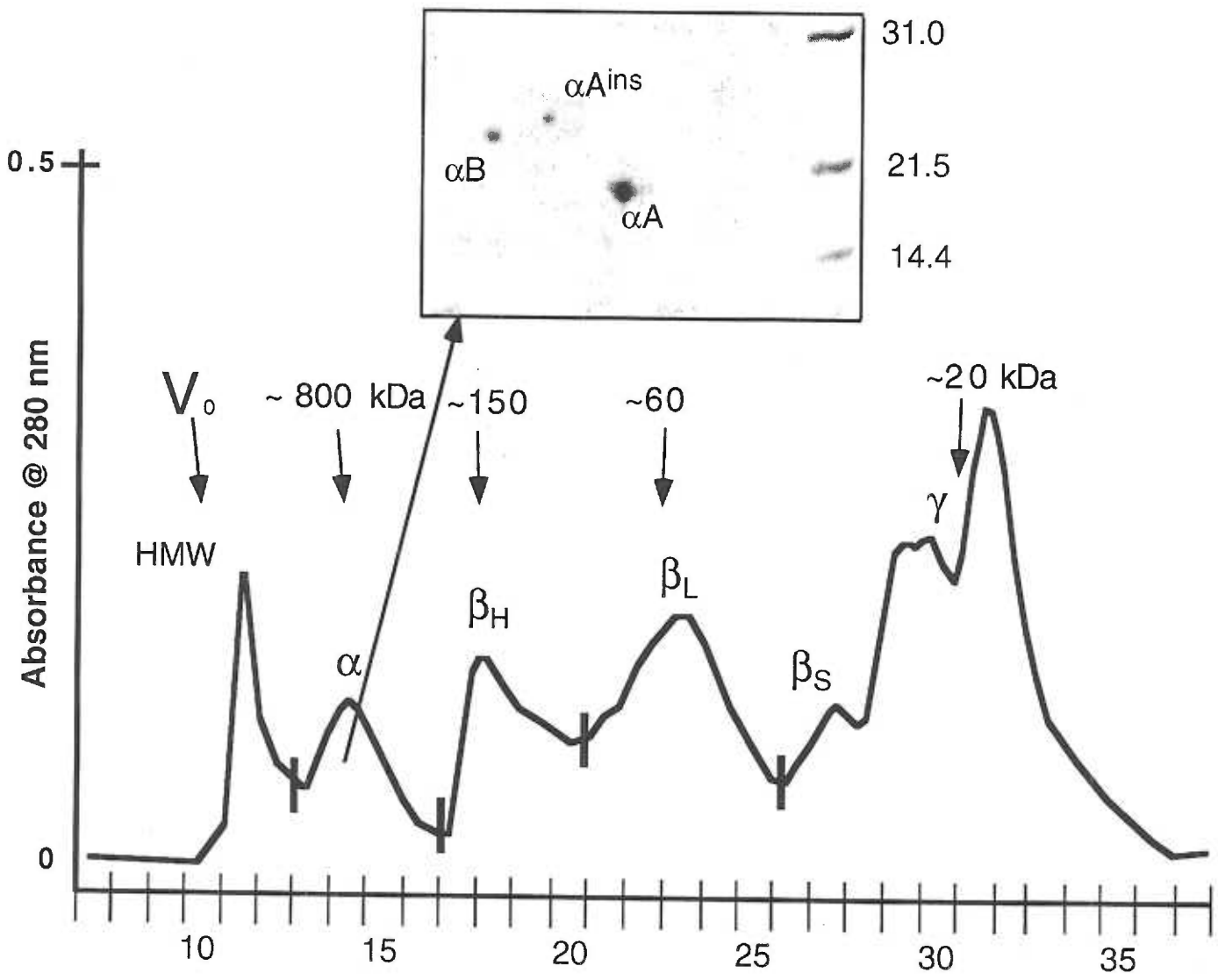
0.5
0
Absorbance @ 280 nm
V_o
HMW
~ 800 kDa
α
~150
β_H
~60
β_L
β_S
~20 kDa
γ
αA^ins
αB
αA
31.0
21.5
14.4
10
15
20
25
30
35

Fig. 2, Panel A: SDS-PAGE of α-crystallin preparations. Lanes 1 and 9: Molecular weight standards labeled in the margin in kDa; lane 2: α-crystallin from control cortex (CC); lane 3: α-crystallin from selenite cortex (SeC); lane 4: α-crystallin from control nucleus (CN); lane 5: α-crystallin from selenite nucleus (SeN); lane 6: α-crystallin from control cortex incubated with calpain (CALP); lane 7: α-crystallin from control cortex incubated with both calpain and a synthetic protease inhibitor, E64 (E64); lane 8: βL-crystallin (βL) isolated from the control cortex by gel filtration and used in the heat-induced aggregation and scattering assay. All sample lanes were loaded with 5 μg of protein/lane. Note the appearance of proteolytic fragments below the arrow, especially in lanes 5 and 6.

Fig. 2 Panel B: Percentage of α-crystallin fragments. Percentages were calculated by densitometric scanning of the gel shown in panel A and dividing the density of bands below 20 kDa by the total density of each lane, then multiplying by 100.

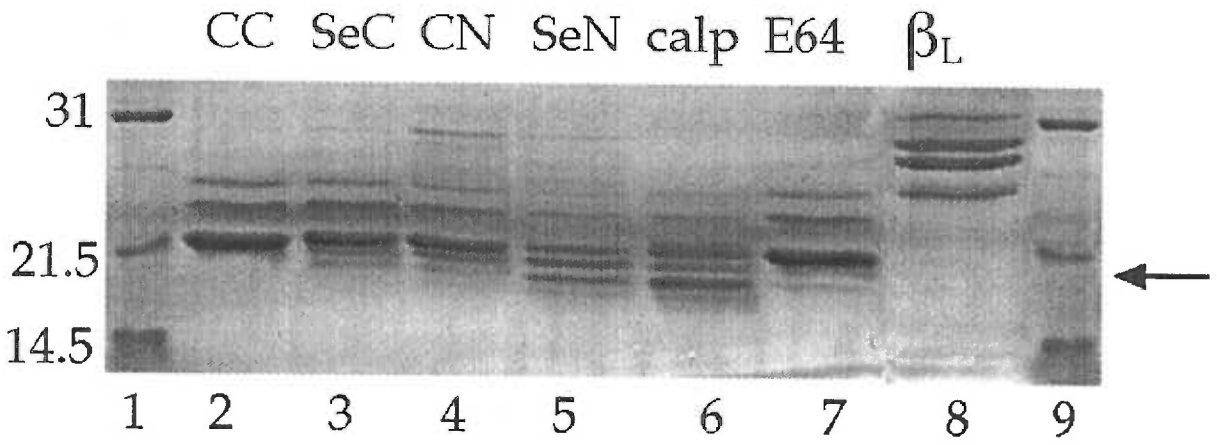
CC
SeC
CN
SeN
calp
E64
β_L
31
21.5
14.5
1
2
3
4
5
6
7
8
9

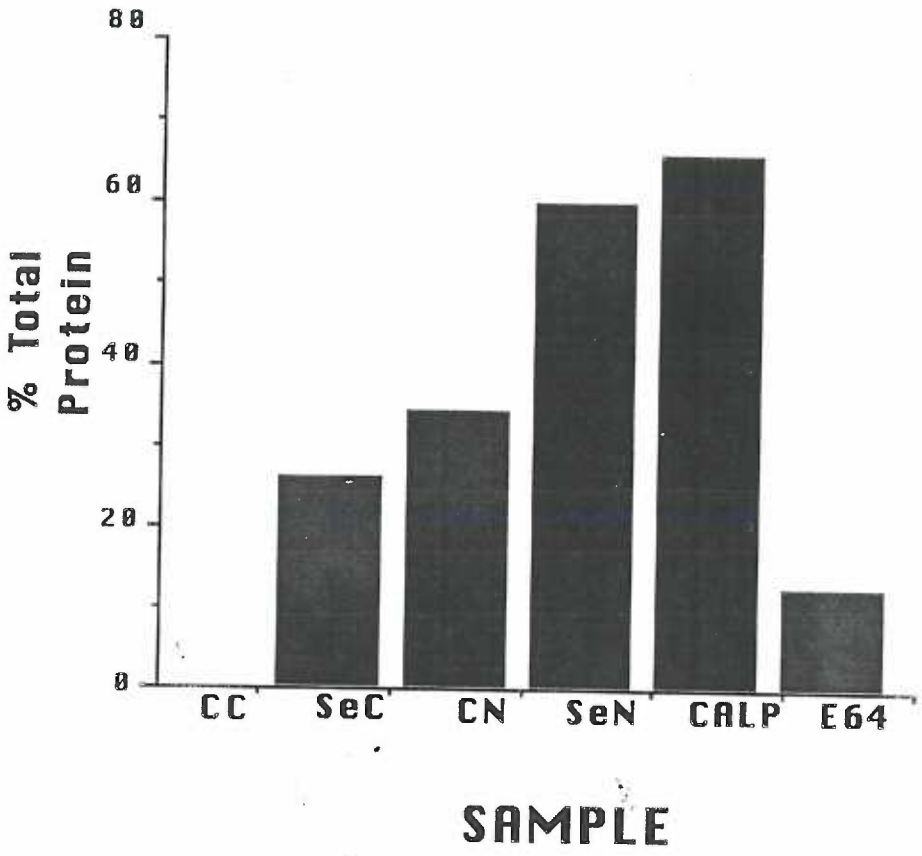
80
60
40
20
0
% Total Protein
CC
SeC
CN
SeN
CALP
E64
SAMPLE

These fragments were quanitated by densitometric analysis (Fig. 2B). Approximately 60% of α-crystallin fragments from selenite nuclear cataract were partially degraded.

Comparison of α-Crystallins from in vivo Selenite Cataract with in vitro Calpain-Treated.

The extent of proteolysis of α-crystallin during formation of selenite cataracts *in vivo* was compared with that which occurred following incubation of normal α-crystallin with calpain *in vitro*. The degradation of α-crystallin in SN was similar to the degradation of α-crystallin incubated with calpain (Fig. 2A, lane 6), suggesting that calpain cleaves α-crystallin *in vitro* and selenite nuclear cataract may result from the same proteolysis of α-crystallin *in vivo*. The cleavage of α-crystallin by calpain *in vitro* was inhibited by the cysteine protease inhibitor, E64 (Fig. 2A, lane 7).

Effects of Heating βL-Crystallin and α-Crystallin Chaperone Activity.

Since α-crystallin had been shown to have chaperone activity (77), one functional consequence of this proteolysis could be loss of this activity. Therefore, the relationship between chaperone activity and this proteolysis was investigated. Heating βL-crystallin from the cortex of rat lens in the absence of α-crystallin caused aggregation, as measured by an increase in light scattering at 340 nm (Fig. 3, "β-L"). The extent of aggregation of βL-crystallin was directly related to both the concentration of βL-crystallin (Fig. 3, insert) and the duration of heating.

Addition of normal α-crystallin from the lens cortex of young rats caused a marked protective effect against the heat-induced aggregation and light scattering of βL-

Fig. 3: Rate of heat-induced aggregation and scattering of βL-crystallin (200 μg/ml) in the presence (75 μg/ml) and absence of α-crystallin isolated from the lens cortex and nucleus of control 14-day old rats. Control cortical α-crystallin (CC) was more effective than control nuclear α-crystallin (CN) in preventing the heat-induced aggregation and scattering of βL-crystallin. βL-crystallin without α-crystallin aggregates and precipitates most rapidly. The inset shows a time course of heat-induced aggregation and scattering of successively higher concentrations of βL-crystallin at 64° C. The y-axis (mOD increase) is the increase in light scattering measured at 340 nm and the x-axis is incubation time (min) for both figures. The higher concentrations of βL-crystallin showed increased precipitation and light scatter during heating. Error bars for this figure are not shown because the mean range for multiple determinations (n=2 to 4) for all points on this figure was ± 10%. Also, at each time point, none of the individual values within a group overlapped individual values in another group. This experiment was performed several times with different concentrations, but the pattern was the same for all the experiments. This graph shows a repeatable, typical example.

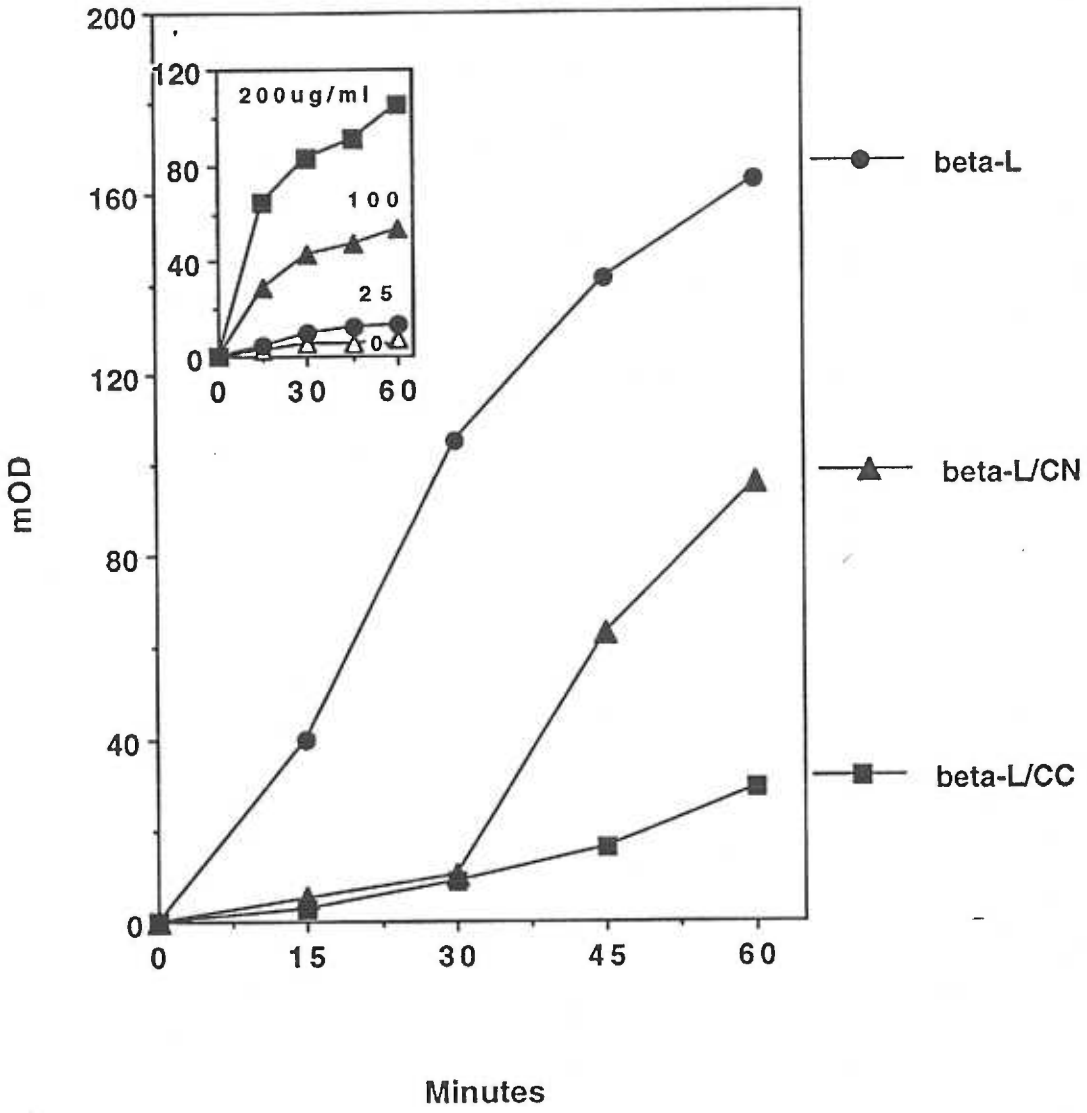
200
160
120
80
40
0
mOD
0
15
30
45
60
Minutes
120
80
40
0
200ug/ml
100
25
0
0
30
60
beta-L
beta-L/CN
beta-L/CC

crystallin (Fig. 3,"βL/CC"). This ability of rat α-crystallin to act as a molecular chaperone to attenuate the heat precipitation of βL-crystallin was similar to the chaperone activity observed in other species (77,10). Chaperone activity of α-crystallin depended upon three factors, temperature, concentration of α-and βL-crystallins, and purity of the α-crystallin preparation. The chaperone activity of α-crystallin from the cortex of rat lens shown in Fig. 3 was 91% effective against heat-induced aggregation and scattering of βL-crystallin at 30 min, and 82% effective even after 60 min of heating at 64° C (Fig. 3).

Note that α-crystallin from the nucleus of rat lens was also an effective chaperone for the first 30 min of heating of βL-crystallin (Fig. 3, "β-L/CN"). However, after 30 min, α-crystallin from the nucleus tended to lose chaperone effectiveness faster than α-crystallin from the cortex. The α-crystallin from control cortex (CC), and control nucleus (CN) were both effective chaperones (Fig. 4A), although the α-crystallin from the control cortex (CC, Fig. 4A) was slightly more effective than control nucleus (CN) at lower concentrations.

Chaperone Activity of α-Crystallin from Normal and Selenite Cataract.

To determine if the chaperone effect of α-crystallin was altered in a model of cataract, α-crystallin from rats with selenite cataracts (see Fig. 2A) were tested in the standard heat aggregation (chaperone) assay. After 30 minutes at 64° C, the α-crystallin from the nucleus of lenses with selenite cataract showed reduced chaperone activity (Fig. 4A, SN). In contrast, α-crystallin from control cortex (CC), selenite cortex (SC), and control nucleus (CN) were all more effective chaperones (Fig. 4A).

Fig. 4, Panel A: Comparison of the chaperone activity of α-crystallins from normal lens and selenite cataract. Alpha crystallins from selenite nucleus (SN), selenite cortex (SC), control nucleus (CN), and control cortex (CC) were used at the concentrations indicated to suppress the heat-induced aggregation and scattering of 200 μg/ml βL-crystallin at 64° C. In this experiment, α-crystallins from selenite nucleus (SN) were ineffective chaperones when compared with the other groups shown. The mean range for duplicate determinations for each point within this experiment was ± 8%. None of the individual values at 25, 50, and 75 μg α-crystallin from SN overlapped with any value from the CN, SC, or CC groups. This experiment was performed with duplicates several times with different concentrations, and the conclusion was similar for all experiments.

Fig. 4, Panel B: Treatment of α-crystallin with calpain decreased chaperone activity. Prior to incubation with 200 μg/ml βL-crystallin at 64° C for 30 min, α-crystallin was incubated for 1 hour at 37° C in the presence of calpain, both with and without the protease inhibitor E64. The α-crystallin treated with calpain was an ineffective chaperone of βL-crystallin. E64, however, inhibited calpain proteolysis and allowed the α-crystallin to act as a chaperone to prevent precipitation of βL-crystallin. The mean range for replicates within this representative experiment was ± 3%. None of the individual values at 25, 50, and 75 μg α-crystallin overlapped between the calpain and E64 groups. This experiment was performed with duplicates several times with different concentrations, but the pattern was the same for all the experiments. Since the experiments differed from each other slightly, a range was determined for each

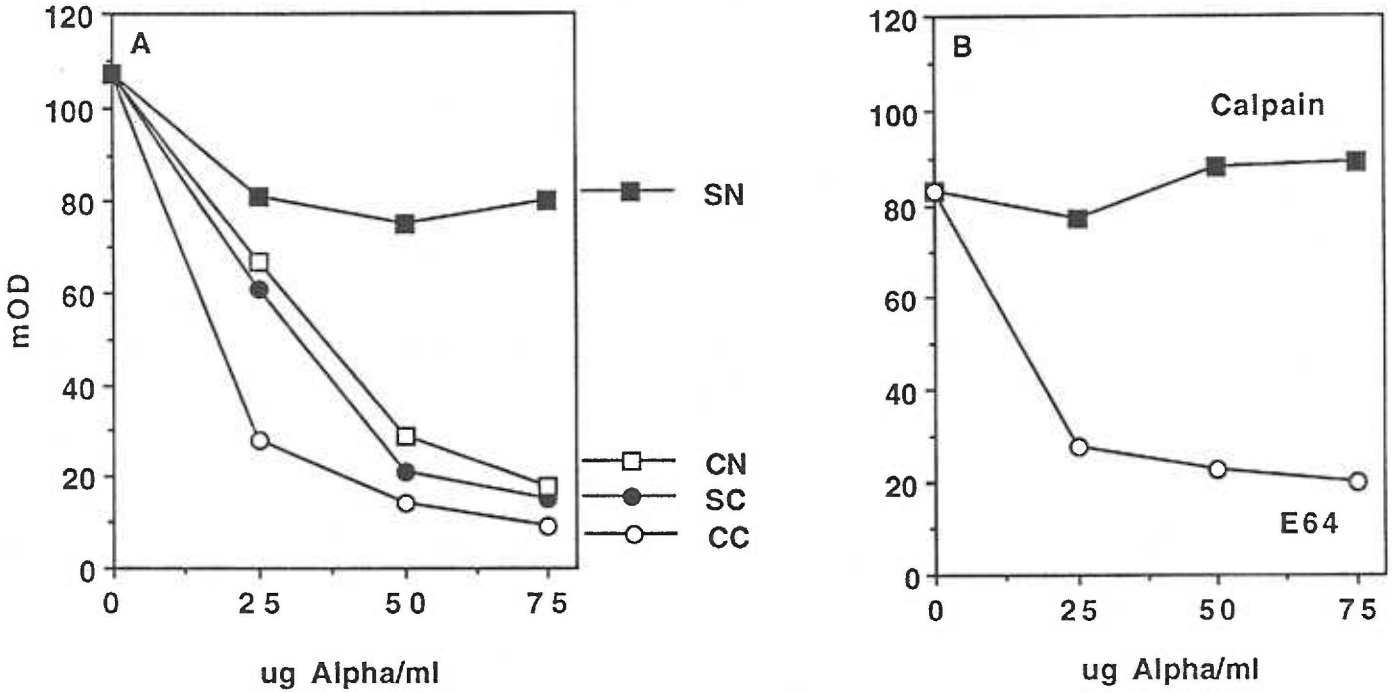
A
mOD
120
100
80
60
40
20
0
0
25
50
75
ug Alpha/ml
SN
CN
SC
CC
B
Calpain
E64
120
100
80
60
40
20
0
0
25
50
75
ug Alpha/ml

experiment separately. This graph shows a repeatable, typical example.

There was a relationship between the extent of proteolysis of α-crystallin and the loss of chaperone function (Fig. 4A). The chaperone-defective α-crystallin aggregates from the cataractous nucleus of selenite-treated (SN) rats showed specific, selective proteolysis of αA, αB, and αA insert polypeptides, resulting in new proteolytic fragments appearing at approximately 18 and 19 kDa (Fig. 2A, lane 5). The proteolytic fragments of α-crystallins at 18 and 19 kDa comprised approximately 58% of the total α-crystallin isolated from the selenite cataractous nucleus (Fig. 2B); this α-crystallin preparation exhibited the lowest chaperone activity. In contrast, control nucleus (CN) and selenite cortex (SC), which exhibited only slightly reduced chaperone activity, showed lesser levels of proteolysis (Fig. 2A, lanes 3 and 4) with fragments comprising only 25 and 33 % of the total protein (Fig. 2B). This suggested that limited proteolysis of α-crystallin *in vivo* reduced chaperone activity.

Chaperone Activity of α-Crystallin Incubated with Purified Calpain II.

Much, if not all, of the proteolysis observed in selenite cataract is caused by activation of calpain II, which is present in rat lens (37). Thus, it was conceivable that the loss of chaperone activity observed in selenite cataract was a result of proteolysis of α-crystallin by calpain. In order to test this hypothesis, normal α-crystallin from the clear cortical region of rat lenses was incubated with purified calpain II (Fig. 2A, Lane 6), as noted earlier. This resulted in a pattern of proteolysis similar to that observed in selenite cataract (Fig. 2A, lane 5), with similar proportions of proteolytic fragments migrating to positions below 20 kDa (Fig. 2B). As a control, the cysteine protease inhibitor E64 was added at the beginning of the incubation in order to inhibit calpain.

The resulting α-crystallin preparation showed only minor proteolysis (Fig. 2A, lane 7 and Fig. 2B), resembling normal α-crystallin. The α-crystallin preparation resulting from incubation of α-crystallin with calpain showed markedly reduced chaperone activity ("calpain" curve, Fig. 4B). This was compared to the chaperone activity of α-crystallin incubated with calpain inhibited by E64 ("E64" curve, Fig. 4B), which retained effective chaperone activity. Unlike βL-crystallin, normal intact α-crystallin showed no appreciable increase in light scattering when heated to 64° C, indicating the thermal stability of normal intact α-crystallin.

Nature of α-Crystallin Cleavage: Isolation of α-crystallin fragments.

Two-dimensional electrophoresis was used to examine the specific changes occurring in α-crystallin, which resulted in loss of chaperone activity. Soluble protein from normal lenses, soluble protein incubated *in vitro* with calpain, and soluble protein from selenite cataract were compared (Fig. 5). The gel of normal soluble protein showed the subunits of α-crystallin, αA and αB (Fig. 5A). After calpain treatment, the parent αA and αB subunits were diminished, while new fragments appeared (Fig. 5B). There were three αA fragments, αA-1, αA-2 and αA-3, and one αB fragment, αB-1. The selenite cataract soluble protein (Fig. 5C) exhibited a pattern essentially identical to that seen with the *in vitro* calpain treatment.

Tryptic Mapping of α-Crystallin Subunits and Fragments.

Tryptic mapping was used to compare and verify the identification of the α-crystallin subunits and fragments. The peptides from these two-dimensional gels (Fig. 5) were electrophoretically transferred to PVDF membranes, individual spots were

Fig. 5: Two Dimensional Electrophoresis of Soluble Lens Proteins from Normal, Calpain-treated and Selenite Cataract Rats. Soluble protein from normal control lenses without (A) and with (B) calpain treatment are compared to those from the nuclear selenite cataract (C). The positions of intact αA and αB polypeptides are indicated in A. These polypeptides were identified by sequencing tryptic fragments as shown in Fig. 6. Calpain treatment produced partially degraded αA and αB polypeptides indicated by αA-1, αA-2, αA-3, and αB-1 (B). These polypeptides were identified by comparison of their tryptic maps with the tryptic maps of intact αA andαB polypeptides (Fig. 6). Soluble proteins from the nucleus of rats with selenite-induced cataract contained partially degraded polypeptides (C, αA-1, αA-2, αA-3, αB-1). These polypeptides migrated to the same position as the partially degraded αA and αB polypeptides produced by calpain (B). The most basic pH of the first dimension (isoelectric focusing) gel is to the left side of each figure. The molecular weight marker sizes in the second dimension are also shown on the left as 21.5 and 31.0 kDa.

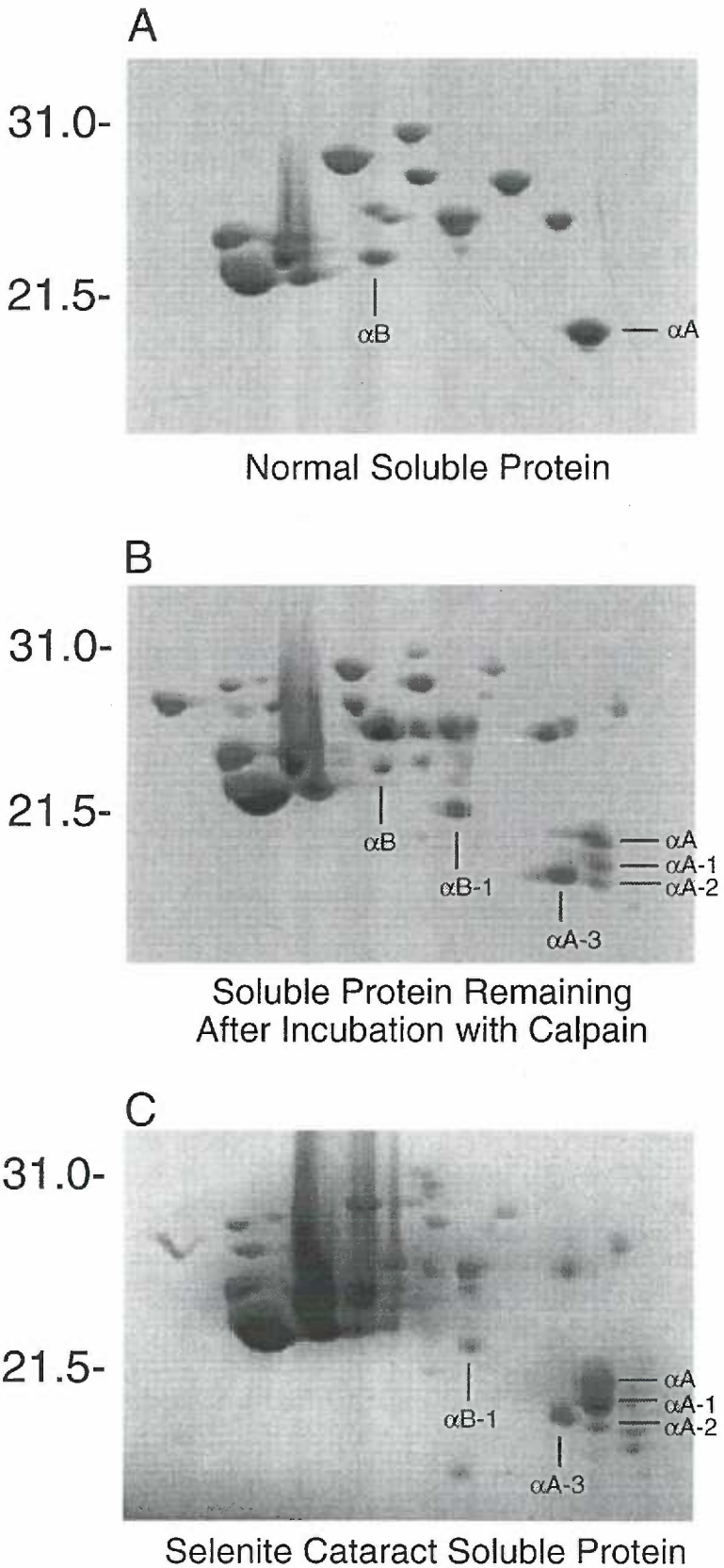
A
31.0-
21.5-
αB
αA
Normal Soluble Protein
B
31.0-
21.5-
αB
αB-1
αA-3
αA
αA-1
αA-2
Soluble Protein Remaining
After Incubation with Calpain
C
31.0-
21.5-
αB-1
αA-3
αA
αA-1
αA-2
Selenite Cataract Soluble Protein

excised, subjected to in situ trypsinization on the membrane surface, and tryptic fragments were separated by HPLC (Fig. 6). The HPLC elution profiles of the putative fragments resembled the profiles of their respective parent subunits, verifying the previous identifications (Fig. 5).

Sequence Analysis of Peaks from Tryptic Mapping.

Sequence analysis of two of the peaks resulting from tryptic digestion of α-crystallin confirmed the identity of these polypeptides as αA and αB. A peak eluting at 48 min from the αA digest (Fig. 6, αA) was subjected to 8 cycles of amino acid sequence analysis. The peak contained two polypeptides with the sequences ALGPFYPS and XFSPQDLT, which matched published (44) sequences from rat αA crystallin. These residues were 13-20 and 79-86, respectively. Histidine (at the position marked X) is difficult to detect at low concentrations during PTH analysis, thus the identification of the residue at this position was not possible. A peak eluting at 56 min from the αB digest (Fig. 6, αB) contained a fragment with the sequence APSXIDTGLS. This sequence corresponded to residues 57-66 of hamster αB (123). The presence of tryptophan precluded identification of the residue at the position marked X in this sequence. The intact αA and αB subunits and all of their four fragments were N-terminally blocked, as determined by N-terminal sequence analysis.

Mass spectroscopy of Tryptic Fragments.

Mass spectroscopy (118) (conducted by Dr. Jean Smith) gave masses of 1006.5 and 1171.5, which were almost identical to the predicted masses of residues 13-20 and 79-86 of αA, differing only by 0.0 and 0.9 atomic mass units, respectively.

Fig. 6: HPLC separation of tryptic fragments of αA- and αB-crystallins and their partial degradation products produced by calpain. Polypeptides marked αA and αB in panel A, Fig. 5, and αA-1, αA-2, αA-3, and αB-1 in panel B, Fig. 5, were transferred to PVDF membrane. The polypeptide spots were excised, trypsinized on the membrane surface, and the resulting fragments were separated by HPLC. Intact αA and αB polypeptides were identified by partial amino acid sequence of the indicated tryptic fragments. Fragments with the sequence ALGPFYPS and XFSPQDLT corresponding to residues 13-20 and 79-86 of αA (44), were both present in the peak eluting at 48 min. The residue indicated by X could not be detected because of the presence of histidine at this position. The sequence APSXIDTGLS corresponding to residues 57-66 of hamster αB (123), was present in the peak eluting at 56 min. The residue indicated by X could not be detected because of the presence of tryptophan at this position. The polypeptides αA-1, αA-2, and αA-3 were identified as partially degraded αA based on the similarity of their tryptic maps (compare αA with αA-1, αA-2, and αA-3). The polypeptide αB-1 was identified as a partially degraded αB (compare αB with αB-1). *-Denotes the trypsin peak, and the numbers on the right side of each chromatogram are the absorbance values of the largest peak, excluding the trypsin peak.

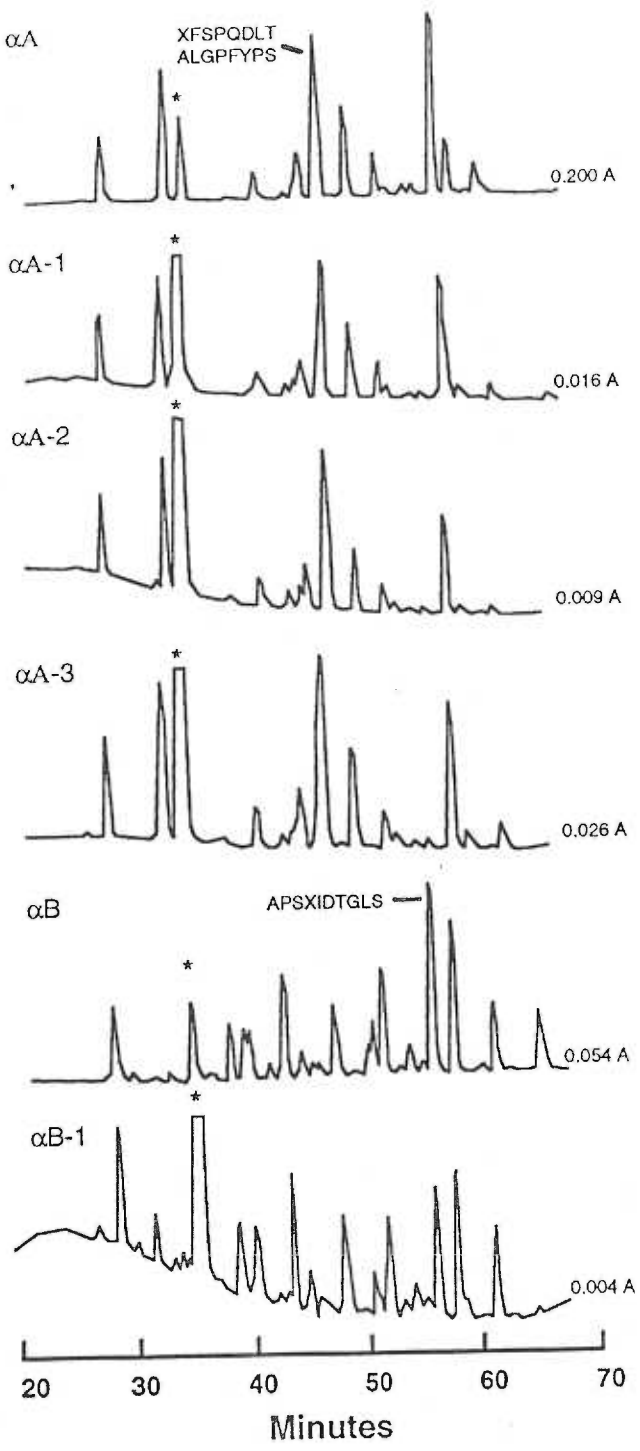
αA
XFSPQDLT
ALGPFYPS
*
0.200 A
αA-1
*
0.016 A
αA-2
*
0.009 A
αA-3
*
0.026 A
αB
APSXIDTGLS
*
0.054 A
αB-1
*
0.004 A
20
30
40
50
60
70
Minutes

Isolation and Purification of Bovine Lens Crystallins.

Bovine lenses were used in subsequent experiments because they contain large quantities of crystallins, and the majority of studies on α-crystallin chaperone function have been conducted on bovine lenses. In addition, the sequences of the crystallins are well-conserved, and differences between rat and bovine are few.

High-molecular weight α-crystallin (HMW), α-crystallin, βH-crystallin, βL-crystallin, and γ-crystallin peaks were isolated from the soluble protein fraction of fetal calf lenses (3-8 months *in utero*) by gel filtration. Fetal calf lenses were used because only small amounts of protein degradation and denaturation are present *in vivo*, as well as to avoid the possible aggregations between crystallins found in adult bovine lenses. Typical examples of gel filtration purification of crystallins from fetal calf lens are shown. Fetal calf lens cortex from 8 calves was chromatographed (Fig. 7A) but the resolution was not optimal (Fig.8A). To improve the purity of the crystallins, the pooled protein peaks were rechromatographed on the same column, as shown for α-crystallin (Fig. 7B) and βH-crystallin (Fig. 7C). This two-step process resulted in purification of α-crystallin, which was then devoid of detectable contamination by other crystallins on SDS-PAGE (Fig. 8B, lanes 3-11). The same procedure was followed to purify other crystallins (Figs.8C). Fetal calf lens nucleus (Fig. 9A) from three animals was also chromatographed on the same column and did not require further purification. The Mr standards (Fig. 9B) for gel filtration chromatography (Bio-Rad) are shown, and were run prior to chromatography of the crystallins to establish molecular weight ranges for the purifications.

Fig. 7A: Gel Filtration Chromatography During Purification of Fetal Calf Lens Cortex. The crystallin fractions from fetal calf lens cortex were isolated on Sephacryl HR-300, pooled, dialyzed against buffer I (pH=6.8). "HMW" represents high molecular weight α-crystallin, "A" represents α-crystallin, "BH" represents βH-crystallin, "βL" represents βL-crystallin, and "G" represents γ-crystallin.

Fig. 7B: Rechromatography of α-Crystallin Fraction from Fetal Calf Lens Cortex. "A" represents α-crystallin, "BH" represents βH-crystallin, and "βL" represents βL-crystallin.

Fig. 7C: Rechromatography of βH-Crystallin Fraction from Fetal Calf Lens Cortex. The major peak contains βH-crystallin.

Fig. 7D: Typical Chromatographic Profile from Previous Studies Showing Crystallin Peak Assignments.

"HMW" represents HMW alpha, "A" represents α-crystallin, "BH" represents βH-crystallin, "BL" represents βL-crystallin, "G_s" gamma-s-crystallin, "G_1" represents peak 1 of gamma-crystallin, and "G_2" represents peak 2 of gamma-crystallin.

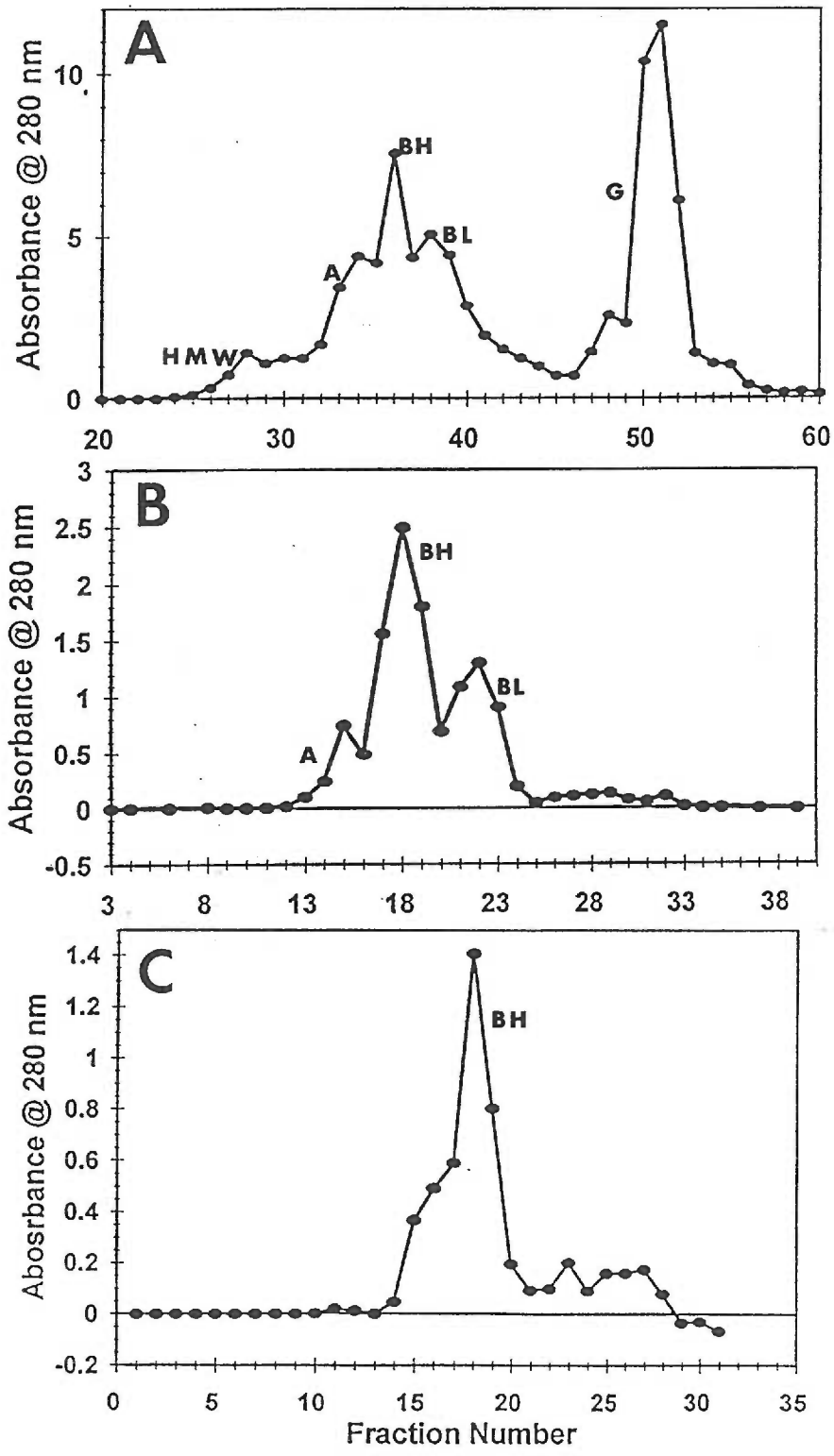
A
Absorbance @ 280 nm
10
5
0
HMW
A
BH
BL
G
20
30
40
50
60
B
Absorbance @ 280 nm
3
2.5
2
1.5
1
0.5
0
-0.5
A
BH
BL
3
8
13
18
23
28
33
38
C
Absorbance @ 280 nm
1.4
1.2
1
0.8
0.6
0.4
0.2
0
-0.2
BH
0
5
10
15
20
25
30
35
Fraction Number

D

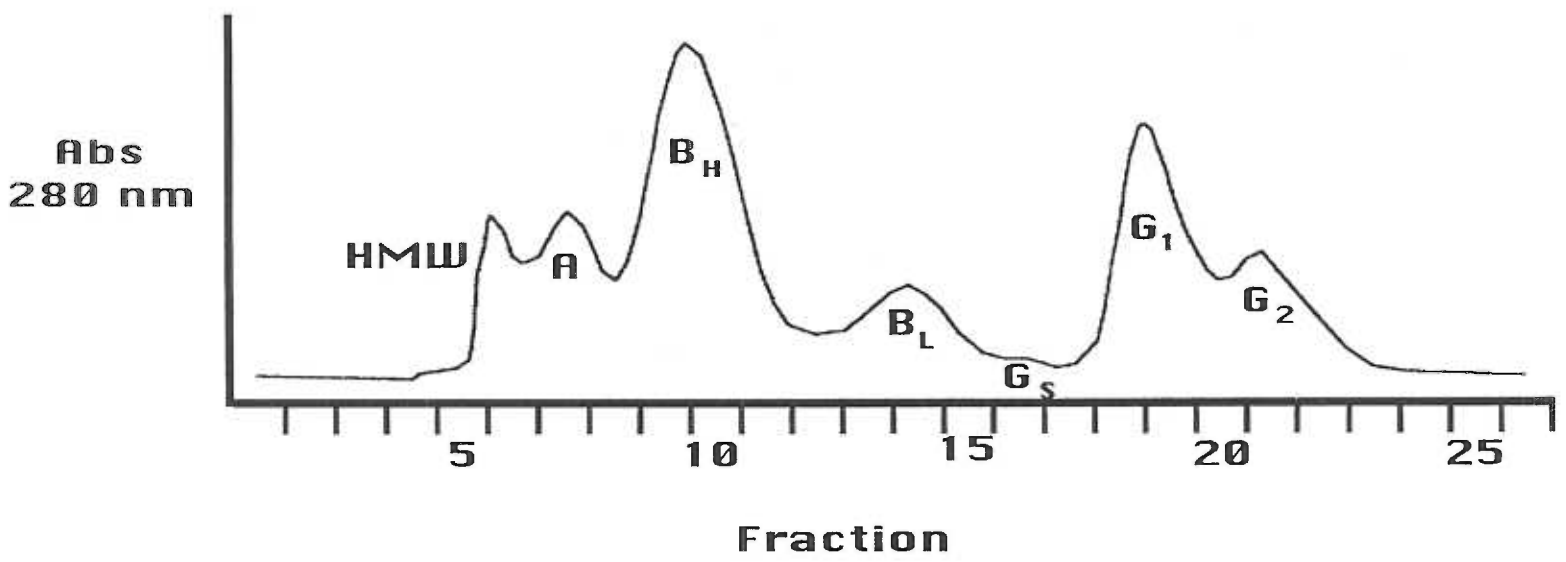

Fig. 8A: SDS-PAGE of Bovine Fetal Calf Lens Cortex. The protein peaks from the Sephacryl HR-300 gel filtration column were identified by 12% SDS-PAGE gel electrophoresis. Pooled, dialyzed protein fractions were added in the amount of 9 μg/lane, and the results show the presence of impurities, particularly in the α- and βH-crystallin fractions. These fractions were then rechromatographed on the same column, but in smaller quantities. Low molecular weight markers (Lanes 1 and 13); α-crystallin with βH-crystallin (Lanes 2-5); βH-crystallin plus βL-crystallin (Lane 6); βL-crystallin (Lanes 7-8); βs-crystallin (Lane 9); γ-crystallin (Lanes 10-12). The arrow designates the upper subunit of α-crystallin, αB, and αA is directly below it.

Fig. 8B: SDS-PAGE of Rechromatographed α-Crystallin. The rechromatographed α-crystallin from bovine fetal lens cortex (lanes 3-11) shows pure α-crystallin fractions, which were then used in the experiments with bovine crystallins. The arrow designates the upper subunit of α-crystallin, αB.

Fig. 8C: SDS-PAGE of Rechromatographed βH-Crystallin. The rechromatographed βH-crystallin from fetal lens cortex shows improved resolution, and most of the bands appear quite free of contamination. Low molecular weight marker (Lane 1); α-crystallin (Lane 3); βH-crystallin plus α-crystallin (Lane 4); βH-crystallin (Lane 5); βL-crystallin (Lanes 6-8). The arrow designates the upper subunit of α-crystallin, αB.

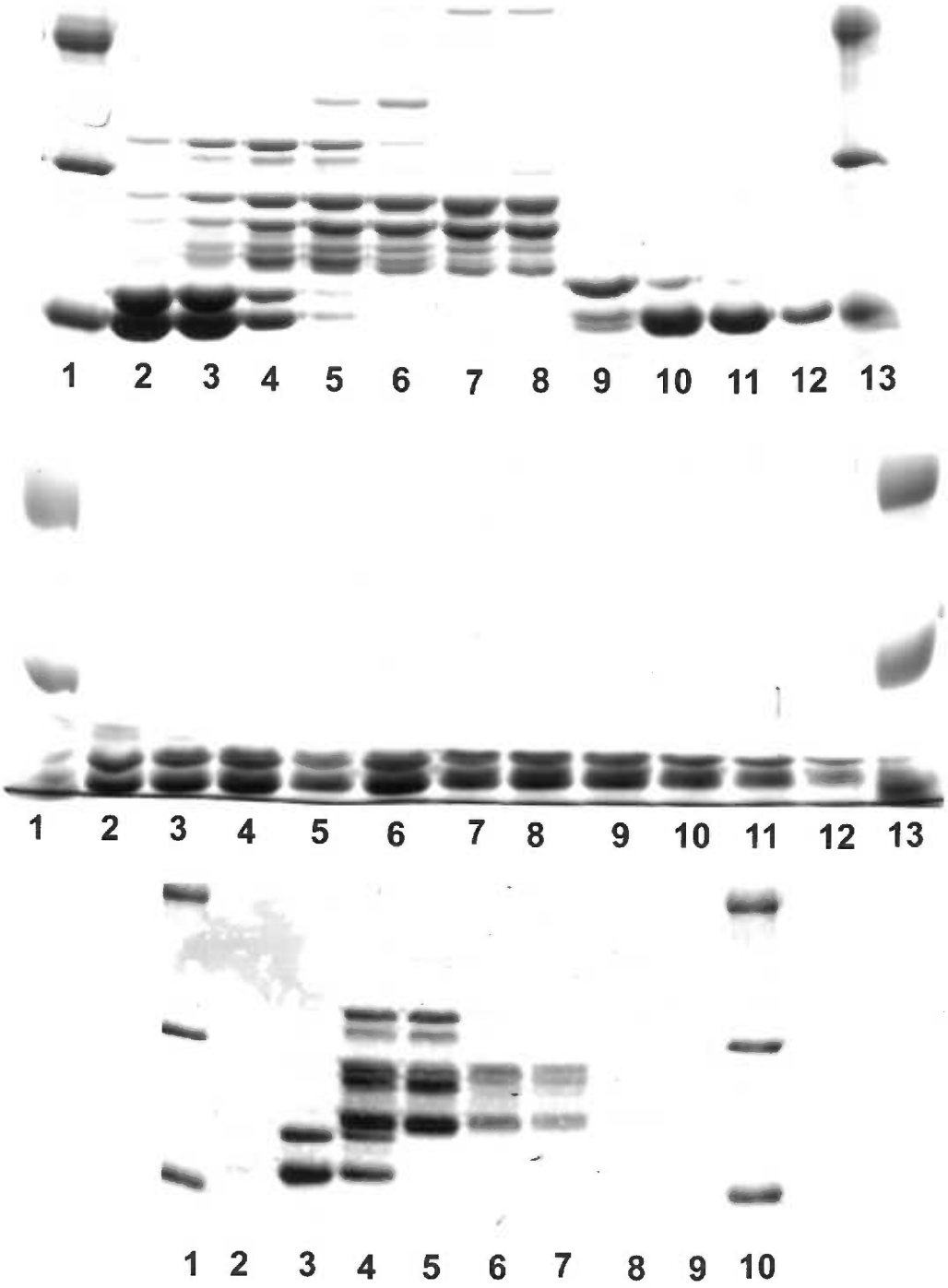
1 2 3 4 5 6 7 8 9 10 11 12 13
1 2 3 4 5 6 7 8 9 10 11 12 13
1 2 3 4 5 6 7 8 9 10

Fig. 9A: Gel Filtration Chromatography of Bovine Fetal Calf Lens Nucleus. Bovine fetal lens nucleus was purified on a Sephacryl HR-300 gel filtration column to isolate the crystallin fractions. "HMW" represents high molecular weight α-crystallin, "A" represents α-crystallin, "BH" represents βH-crystallin, "βL" represents βL-crystallin, and "G_1" represents peak 1 of γ-crystallin, and "G_2" represents peak 2 of γ-crystallin.

Fig. 9B: Standard Curve of Sephacryl HR-300 Column. This figure shows the Mr standards used to calibrate the column prior to chromatography of bovine fetal calf lens crystallins. The Mr standards were from Bio-Rad.

Figure 9C: SDS-PAGE of Bovine Fetal Lens Nucleus Purification. The protein peaks of bovine fetal calf lens nucleus were identified on 12% SDS-PAGE gel electrophoresis. The lanes were: Low molecular weight marker (Lane 1); α-crystallin (Lanes 2-3); α-crystallin plus βH-crystallin (Lane 4); βH-crystallin (Lane 5); βL-crystallin (Lane 6-7); βs-crystallin (Lane 8); γ-crystallin (Lanes 9-10). Although the resolution is better than cortex in many of the fractions, there are a few impurities in some fractions. Only the crystallin fractions from lanes free of contaminants were used.

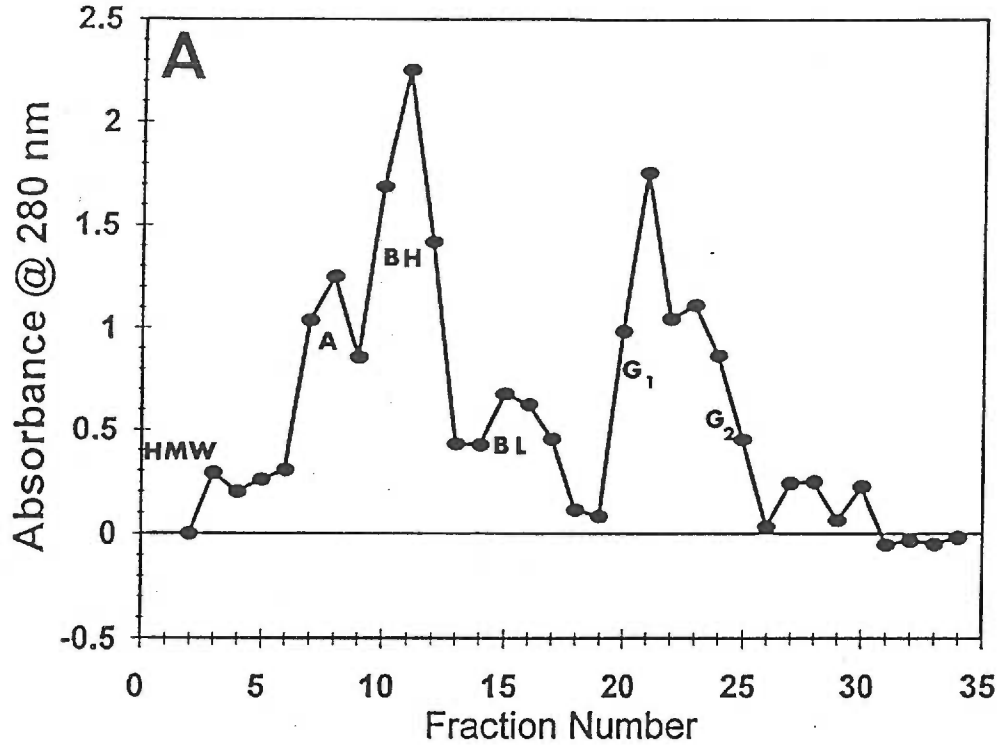
A
Absorbance @ 280 nm
Fraction Number
HMW
A
BH
BL
G1
G2
2.5
2
1.5
1
0.5
0
-0.5
0
5
10
15
20
25
30
35

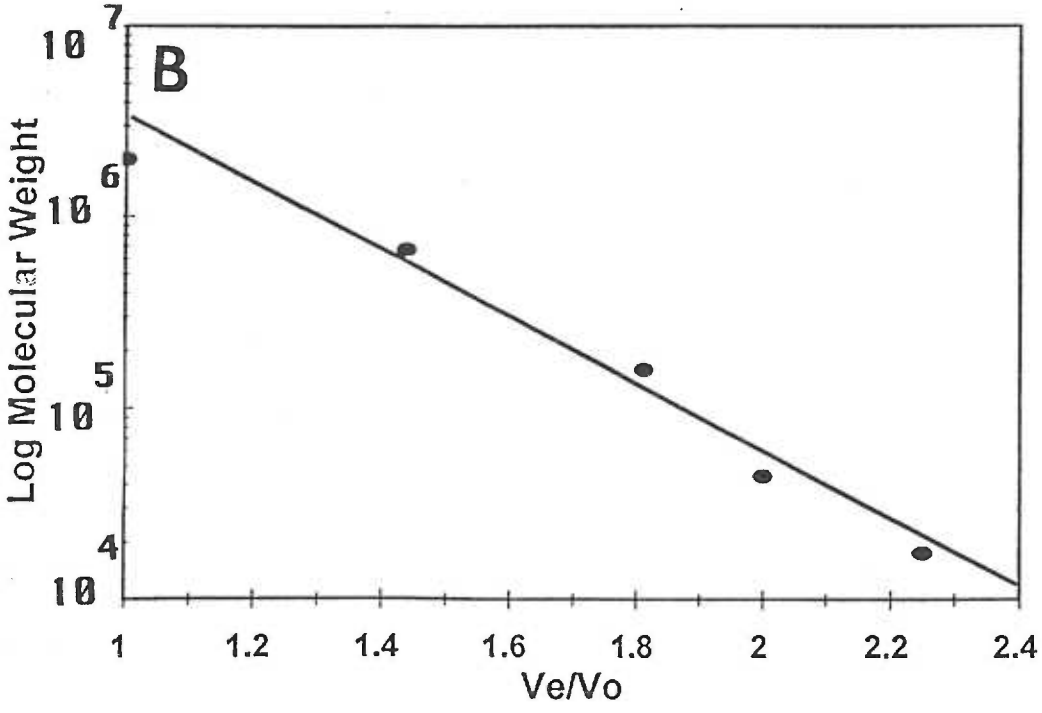
B
Log Molecular Weight
Ve/Vo
10 7
10 6
10 5
10 4
1
1.2
1.4
1.6
1.8
2
2.2
2.4

C

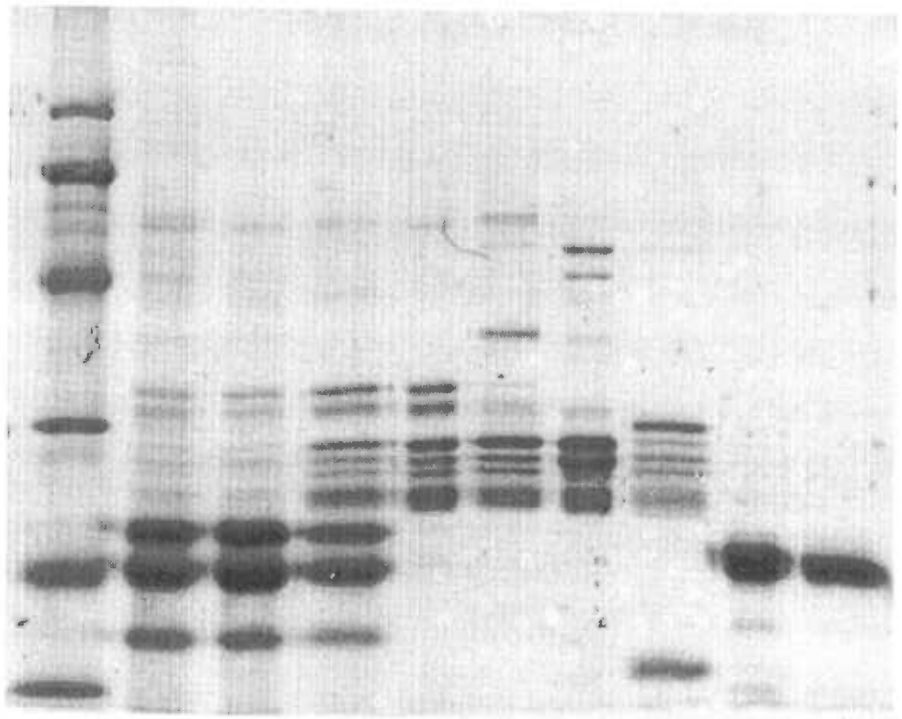

A 12% SDS-PAGE gel was used to identify the bovine fetal calf lens components for the nucleus (Fig. 9C).

Chaperone Concentration Dependence and Time Courses.

To initiate studies utilizing bovine rather than rat crystallins, the basic parameters of the heat aggregation assay were determined. Comparisons of βH from the nuclear and cortical regions and of βH and βL were then conducted.

In the first study, a time course of increased turbidity at increasing concentrations of nuclear βH-crystallin (Fig. 10), shows that mOD (turbidity) is directly proportional to βH concentration. Analysis of the chaperone activity of bovine α-crystallin added to βH-crystallin from the lens nucleus (Fig. 11) showed that at 30 min a ratio of 2:1 (α:β) produced efficient chaperone activity, while at 45 min a ratio of 3:1 or even 4:1 was necessary.

Comparison of α-Crystallin Chaperone Activity with βH-Crystallin from Lens Cortex or Nucleus and with Cortical βH- and βL-Crystallins.

The chaperone activity curve of βHCC (Fig. 12) shows that at 30 min βH-crystallin from the cortex only required α-crystallin ratio of 1:1 (α:β) for efficient chaperone activity, while at 45 min a ratio of 3:2 was necessary. Thus, nuclear βH-crystallin requires more α-crystallin for protection from heat aggregation than does cortical βH-crystallin (Figs. 11 and 12).

The chaperone ability of α-crystallin against heat denaturation of cortical βH- and βL-crystallins was also compared. The chaperone curve for βLCC (Fig. 13) shows that α-crystallin chaperone activity with βL-crystallin (βLCC) was very efficient. At 30 min,

a 1:2 (α:β) ratio provided effective protection, while at 45 min a 1:1 ratio was effective.

Fig. 10: Time Course of Turbidity for βH-Crystallin from the Fetal Calf Lens Nucleus.

Various concentrations of βH-crystallin from the nuclear region of normal fetal calf lenses (βHCN) were heated at 64° C for 45 minutes. The mOD increase (turbidity) is approximately proportional to the concentrations of βH-crystallin. In this experiment, n=3, and the error bars represent the standard deviation.

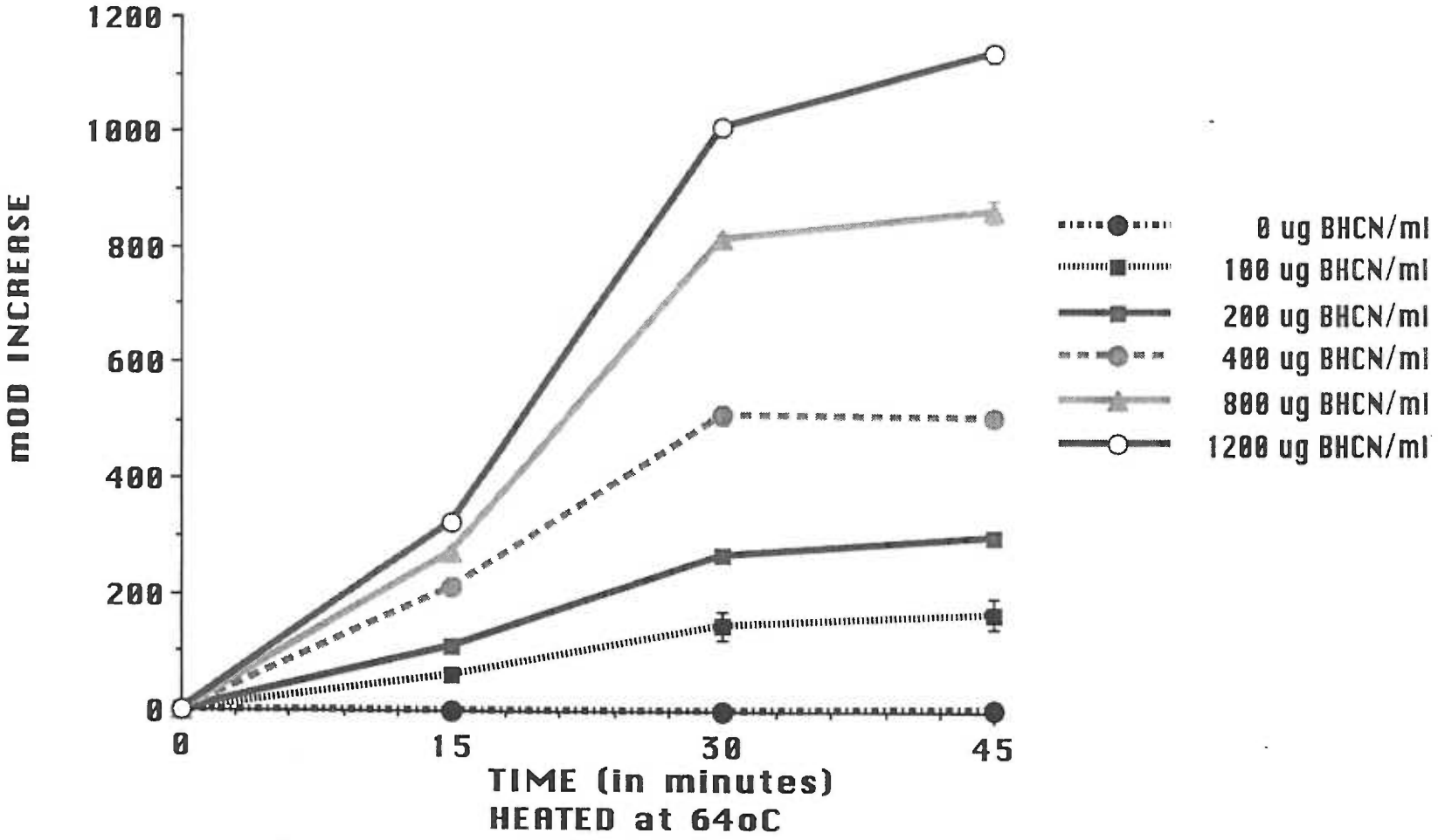
1200
1000
800
600
400
200
0
mOD INCREASE
0
15
30
45
TIME (in minutes)
HEATED at 64oC
0 ug BHCN/ml
100 ug BHCN/ml
200 ug BHCN/ml
400 ug BHCN/ml
800 ug BHCN/ml
1200 ug BHCN/ml

Fig.11: Effect of Increasing Concentrations of α-Crystallin on Heat Aggregation of βH-Crystallin from Fetal Calf Lens Nucleus.

Alpha-crystallin from control cortex was used in increasing concentrations as a chaperone against precipitation of βH-crystallin (100 μg/ml) from fetal lens nucleus (βHCN) heated at 64° C for the times (min) indicated. In this experiment, n=4, and the error bars represent the standard deviation.

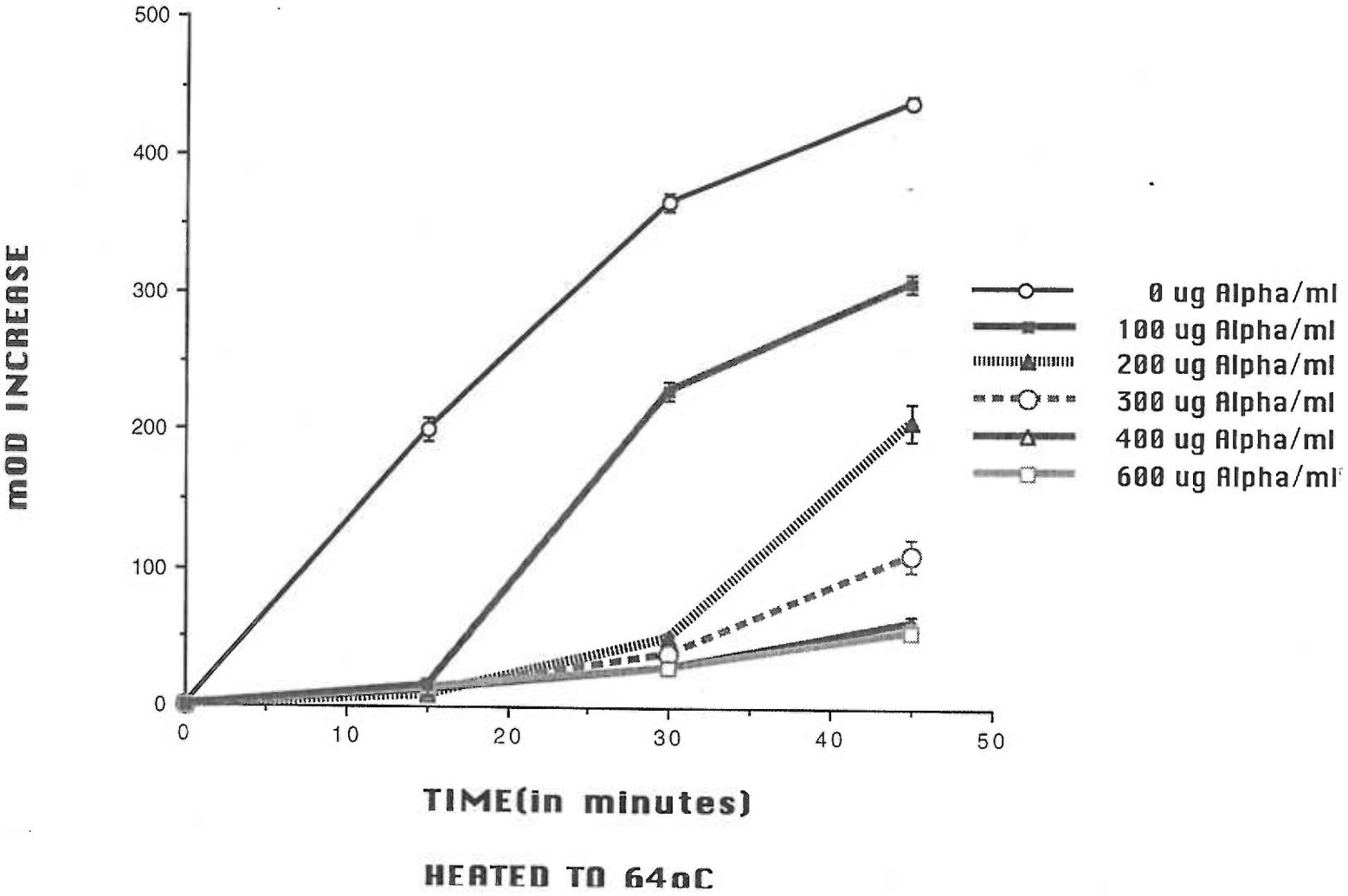

HEATED TO 64oC

Fig. 12: Effect of Increasing Concentrations of α-Crystallin on Heat Aggregation of βH-Crystallin from Fetal Calf Lens Cortex.

Alpha-crystallin from control cortex was used in increasing concentrations as a chaperone for βH-crystallin (200 μg/ml) from fetal lens cortex (βHCC) heated at 64° C for the times (min) indicated. The error bars represent the standard deviation (n=3).

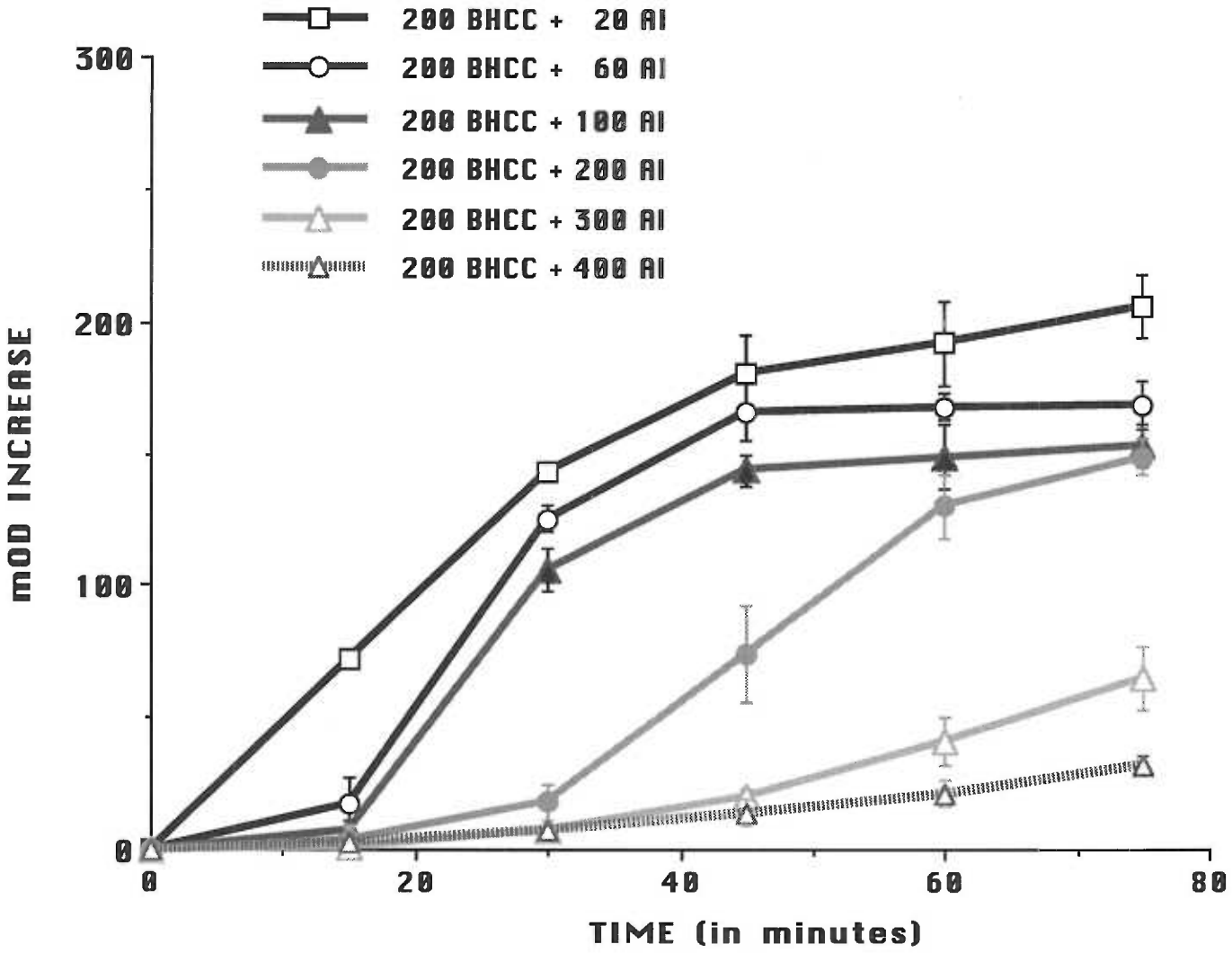
200 BHCC + 20 AI
200 BHCC + 60 AI
200 BHCC + 100 AI
200 BHCC + 200 AI
200 BHCC + 300 AI
200 BHCC + 400 AI
mOD INCREASE
300
200
100
0
0
20
40
60
80
TIME (in minutes)

Fig. 13: Effect of Increasing Concentrations of α-Crystallin on Heat Aggregation of βL-Crystallin from Fetal Calf Lens Cortex.

Alpha-crystallin from control cortex was used in increasing concentrations as a chaperone for βL-crystallin (200 μg/ml) from fetal lens cortex (βLCC) heated at 64° C for the times (min) indicated. The error bars represent the standard deviation (n=3).

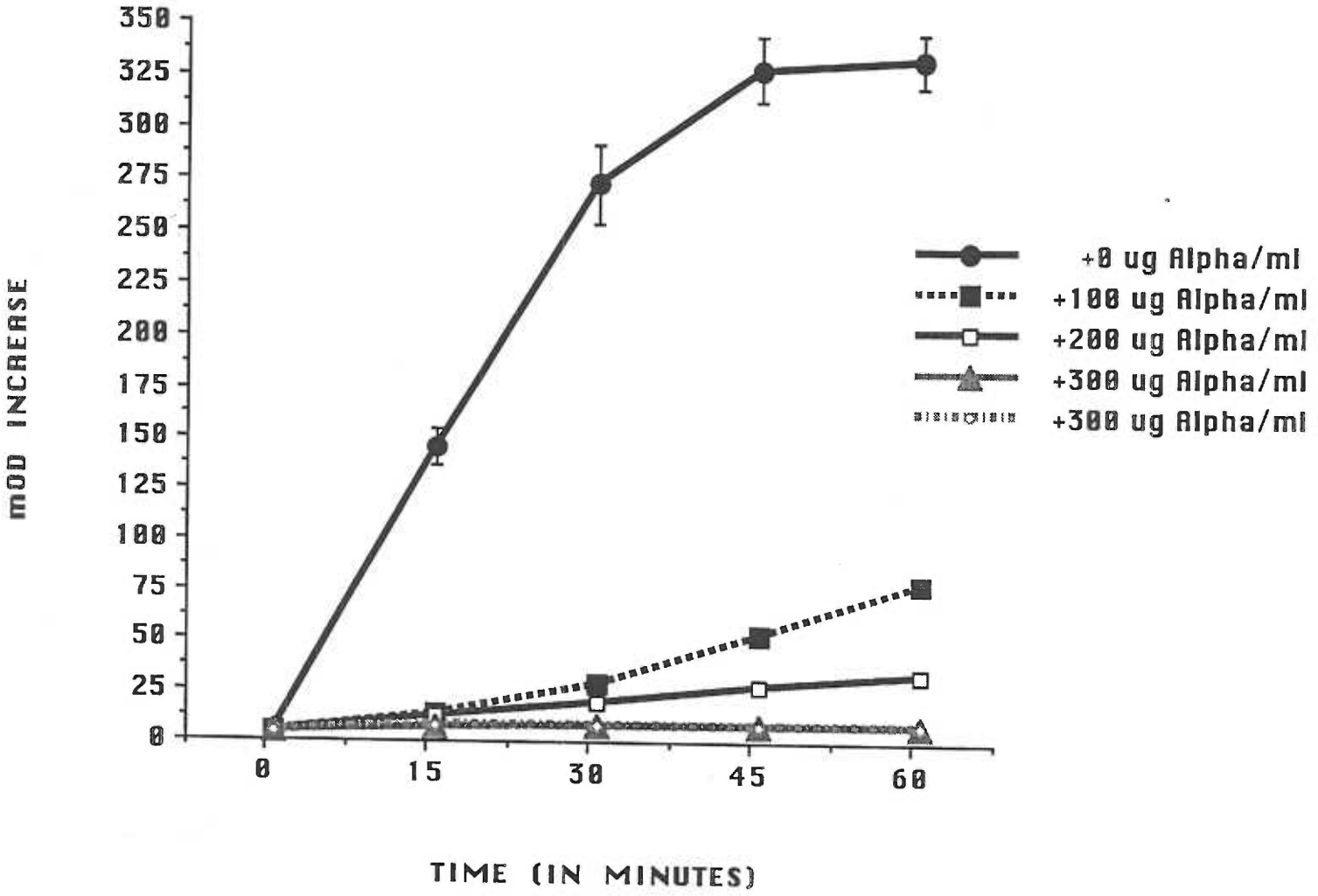
mOD INCREASE
350
325
300
275
250
225
200
175
150
125
100
75
50
25
0
0
15
30
45
60
TIME (IN MINUTES)
+0 ug Alpha/ml
+100 ug Alpha/ml
+200 ug Alpha/ml
+300 ug Alpha/ml
+300 ug Alpha/ml

Therefore βL-crystallin required less α-crystallin to prevent precipitation than did βH-crystallin. It was thus of interest to determine how long βL-crystallin was protected by α-crystallin, when subjected to a continued heat stress. Beta-crystallin (Fig. 14) was protected from appreciable heat-induced aggregation and precipitation for 7.5 hrs by a 1:1 (α:β) ratio and completely protected by a 3:2 ratio. Interestingly, a very similar profile was obtained when a βL-crystallin sample, which had been stored at 4° C for 4 months, was used in the same assay (data not shown).

Relative Chaperone Efficacy of Cortical and Nuclear α-Crystallins.

The comparisons of nuclear and cortical βH-crystallins showed clear differences in their chaperone requirements during the heat aggregation assay. Differences in the chaperone capability of α-crystallin from the cortex and the nucleus (Fig. 15, A-D) were also observed. In general, α-crystallin from the cortex is a much more effective chaperone (on a μg basis) of cortical βL-crystallin than is α-crystallin from the nucleus (note the differences in y-axis scales on Fig. 15B and D).

For comparison, a similar concentration curve of α-crystallin chaperone activity using both α- and β-crystallins from the control rat cortex is shown (Fig. 16). Effective chaperone activity is achieved at a 1:2 (α:β) ratio with the rat crystallins and with the fetal calf cortical crystallins (Fig. 15B). Thus, the α-crystallins from these two species exhibit similar chaperone behavior with their respective β-crystallins. These concentration curves and time courses established parameters for working with the bovine crystallins. They affirmed that bovine β-crystallin precipitated upon heating and that bovine α-crystallin acts as an effective chaperone.

Fig. 14: Chaperone Activity of α-Crystallin with βL-Crystallin in a 7.5 Hour Heat Aggregation Assay.

βL-Crystallin (200 μg/ml) from normal control cortex (βLCC) was protected from heat-induced aggregation by the indicated concentrations of α-crystallins (A) for 450 minutes (7.5 hours) at 64° C. The error bars represent the standard deviation (n=3).

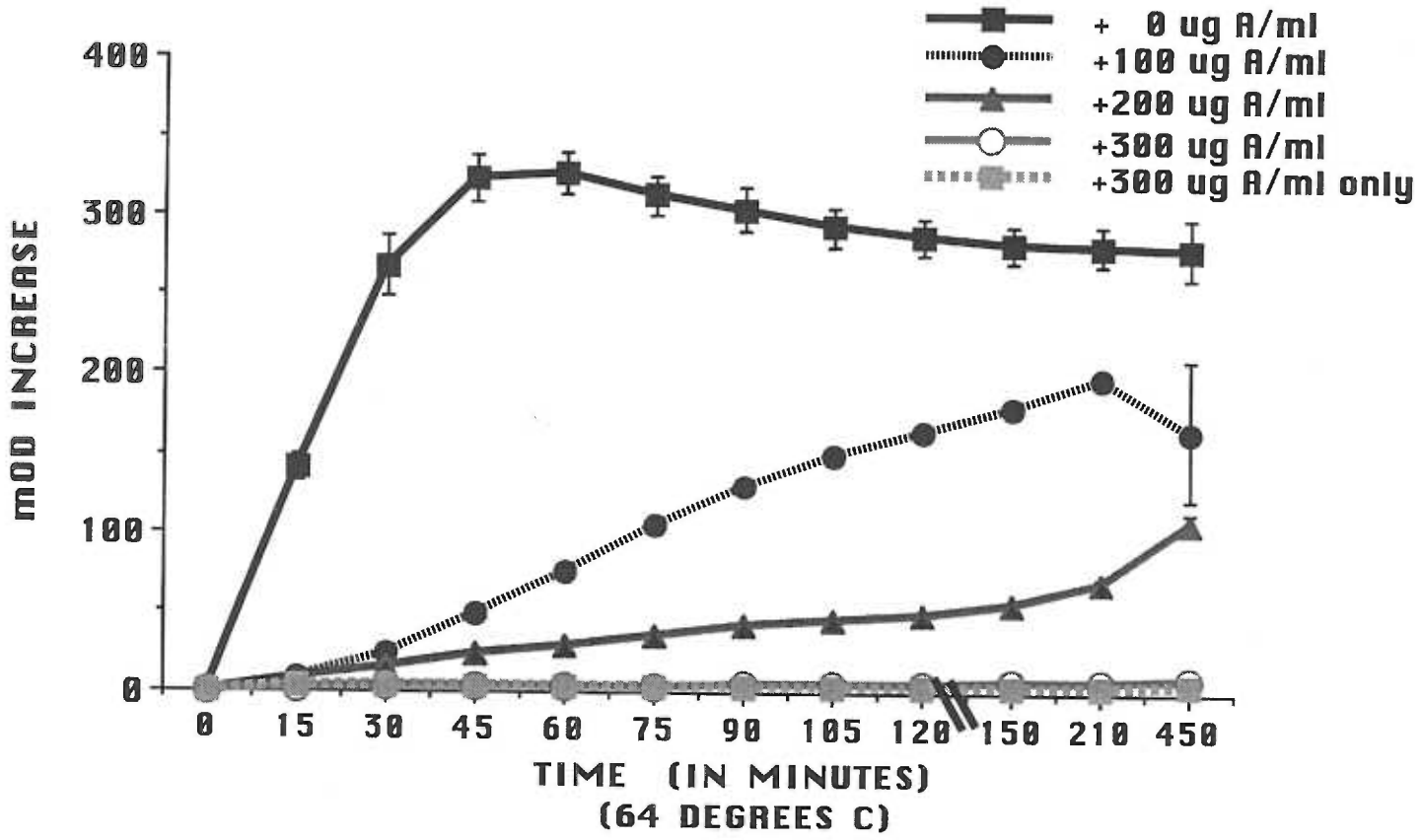
+ 0 ug A/ml
+100 ug A/ml
+200 ug A/ml
+300 ug A/ml
+300 ug A/ml only
400
300
200
100
0
mOD INCREASE
0
15
30
45
60
75
90
105
120
150
210
450
TIME (IN MINUTES)
(64 DEGREES C)

Fig. 15: Comparison of α-Crystallin from the Cortex and Nucleus As Chaperones of βL-crystallin.

Alpha-crystallin from fetal calf lens cortex (A and B) or nucleus (C and D) was used as a chaperone of βL-crystallin (80 μg/ml) from the cortex in the standard heat aggregation assay at 64° C. Time courses (A and C) and α-crystallin concentration curves (B and D) at 30 min are shown. The experiment was performed in triplicate, and the error bars are the standard deviation (n=3).

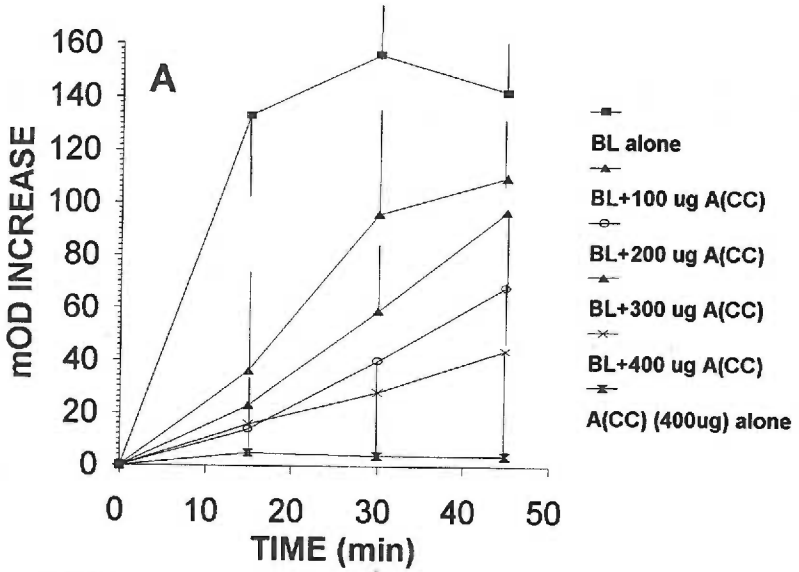
A
mOD INCREASE
160
140
120
100
80
60
40
20
0
0
10
20
30
40
50
TIME (min)
BL alone
BL+100 ug A(CC)
BL+200 ug A(CC)
BL+300 ug A(CC)
BL+400 ug A(CC)
A(CC) (400ug) alone

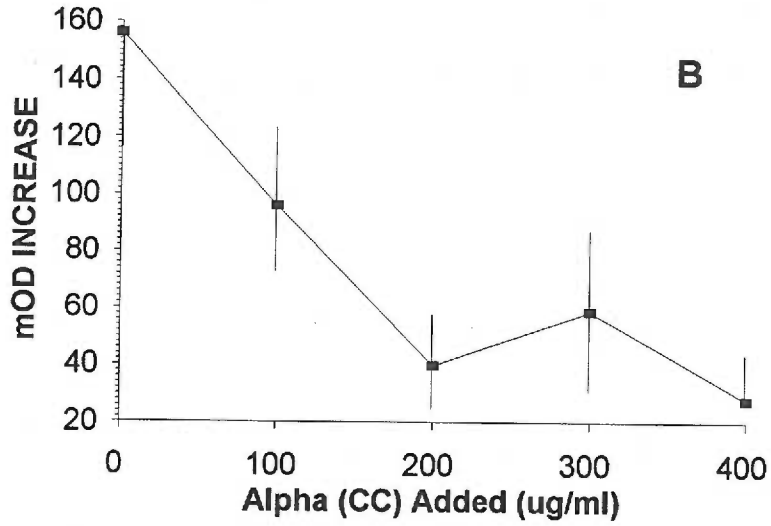
B
mOD INCREASE
160
140
120
100
80
60
40
20
0
100
200
300
400
Alpha (CC) Added (ug/ml)

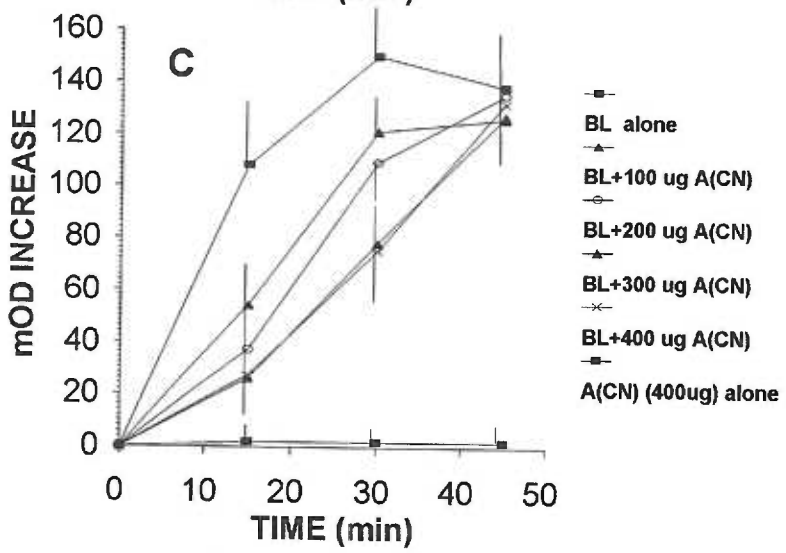
C
mOD INCREASE
160
140
120
100
80
60
40
20
0
0
10
20
30
40
50
TIME (min)
BL alone
BL+100 ug A(CN)
BL+200 ug A(CN)
BL+300 ug A(CN)
BL+400 ug A(CN)
A(CN) (400ug) alone

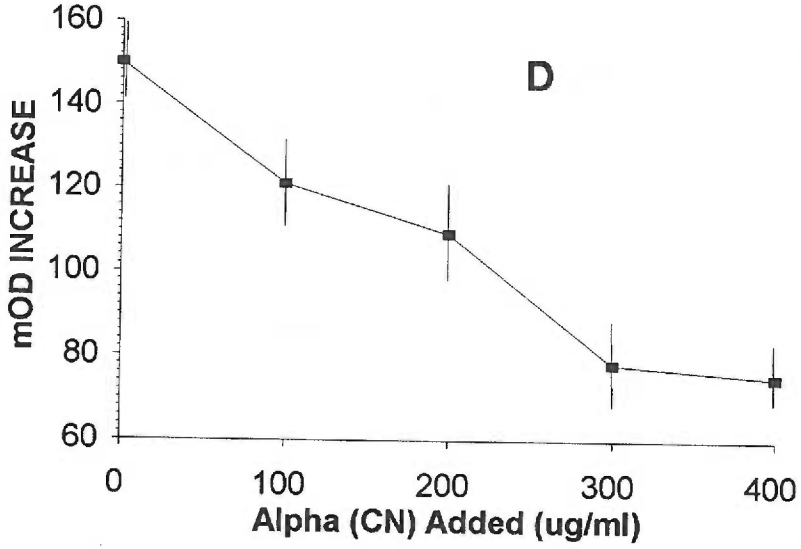
D
mOD INCREASE
160
140
120
100
80
60
0
100
200
300
400
Alpha (CN) Added (ug/ml)

Fig. 16: Concentration Curve of Rat α-Crystallin Acting as a Chaperone for Rat βL-crystallin.

Control cortical rat α-crystallin was use at the concentrations indicated in the standard heat aggregation assay to chaperone control cortical rat βL-crystallin (202 μg/ml) for 47 min. This experiment was performed with duplicates several times with different concentrations, but the pattern was the same for all the experiments. This graph shows a repeatable, typical example, and the bars represent the range.

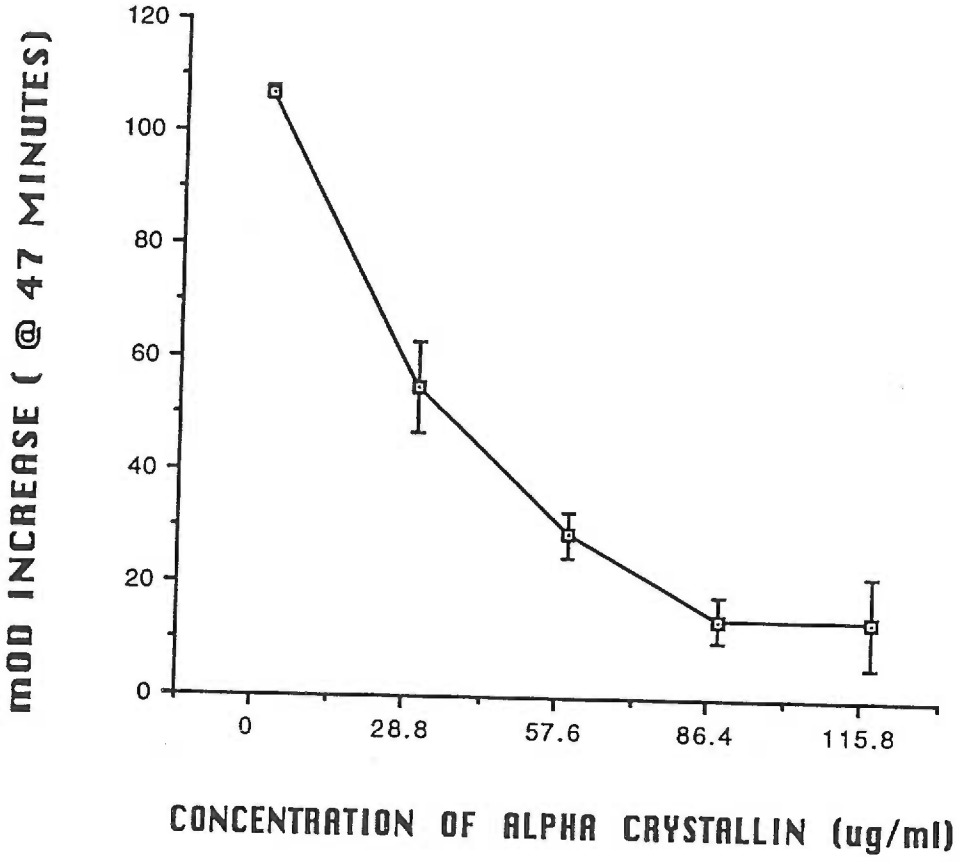
mOD INCREASE (@ 47 MINUTES)
120
100
80
60
40
20
0
0
28.8
57.6
86.4
115.8
CONCENTRATION OF ALPHA CRYSTALLIN (ug/ml)

The purpose of the next group of studies was to evaluate the β-crystallins, which become insoluble and precipitated when heated at 64° C for 30 minutes. Since insolubilization of crystallins is thought to play an important role in cataractogenesis, these studies were performed to determine: 1) how much protein precipitated upon heating, 2) what subunits of β-crystallin precipitated, and 3) how α-crystallin chaperone activity influences β-crystallin insolubilization.

Quantitation of β-crystallins Insolubilized with Heat.

For the quantitation studies, the groups included: 1) 75 μg βL-crystallin / ml only (control), 2) 25 μg α-crystallin / ml plus 75 μg βL-crystallin / ml, and 3) 50 μg α-crystallin / ml plus 50 μg βL-crystallin / ml.

βL-Crystallin Precipitation with Heat: Control studies showed that without heat (Fig. 17A), no βL-crystallin precipitated. In contrast, a relatively large amount, 12%, of soluble βL-crystallin precipitated when heated. As shown earlier, addition of α-crystallin to βL-crystallin in the ratios of 1:3 or 1:1 (α:βL) prevented protein precipitation during heating.

βH-Crystallin Precipitation With Heat: Similarly, βH-crystallin did not precipitate in the absence of heat (Fig. 17B). Upon heating βH-crystallin, 28.7% precipitated. Addition of α-crystallin to βH-crystallin in the ratio of 1:1 (α:βH) also prevented protein precipitation. However, at 1:3 (α:βH) 15% of the βH precipitated. Thus, βH-crystallin in more susceptible than βL-crystallin to heat precipitation.

Two-Dimensional Gels of β-Crystallins.

The studies above showed that heating of β-crystallins caused unspecified protein

Fig. 17A: Analysis of Protein Levels in Pellets of βL-Crystallin Precipitated by Heat.

Beta Light-Crystallin precipitates were analyzed for protein levels after heating for 64° C for 30 minutes with and without added α-crystallin. "A" represents α and "BL" represents βL; the numbers are the μg of each, respectively, added to the assay. "NoH" represents not heated, while "H" represents heated. For these studies, the groups included: 1) 75 μg βL-crystallin / ml only (control), 2) 25 μg α-crystallin / ml plus 75 μg βL-crystallin / ml (1α:3β ratio), and 3) 50 μg α-crystallin / ml plus 50 μg βL-crystallin / ml (1α:1β ratio). This was a preliminary experiment prior to 2-D gel electrophoresis. The study was performed with single samples a total of three times, however, the methodology differed between experiments, so statistics could not be performed. The pattern was the same for all of the experiments and this graph shows a typical example of the effects of heat and α-crystallin upon βL-crystallin.

Fig. 17B: Analysis of Protein Levels in Pellets of βH-Crystallin Precipitated by Heat.

Beta Heavy-Crystallin precipitates were analyzed for protein levels after heating for 64° C for 30 minutes with and without added α-crystallin. "A" represents α-crystallin added and "BH" represents βH-crystallin; the numbers are the μg of each, respectively, added to the assay. "NoH" represents not heated, while "H" represents heated. For these studies, the groups included: 1) 75 μg βH-crystallin / ml only (control), 2) 25 μg α-crystallin / ml plus 75 μg βH-crystallin / ml (1α:3β ratio), and 3) 50 μg α-crystallin /

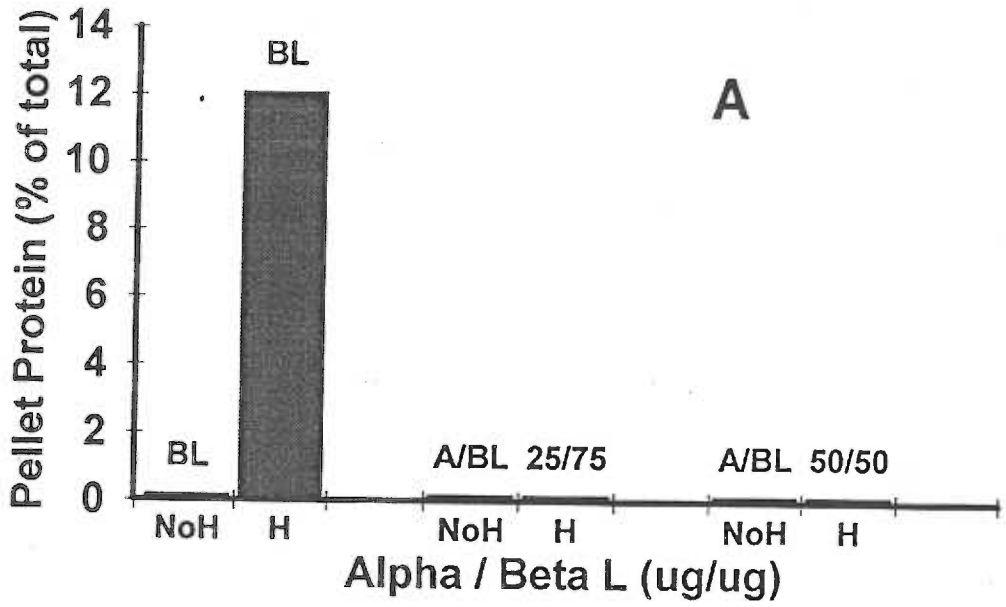
A
Pellet Protein (% of total)
14
12
10
8
6
4
2
0
BL
BL
A/BL 25/75
A/BL 50/50
NoH
H
NoH
H
NoH
H
Alpha / Beta L (ug/ug)

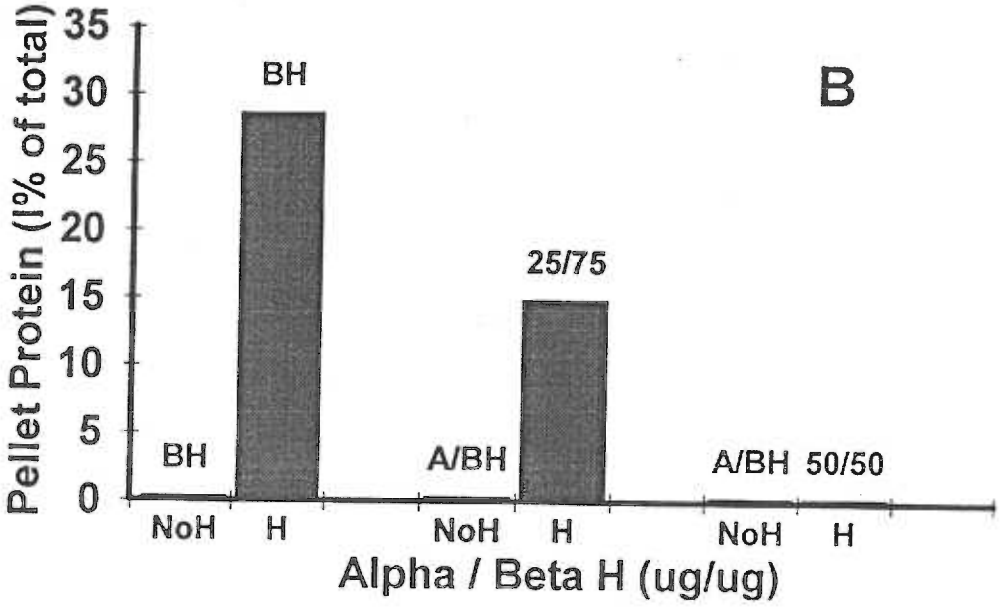
B
Pellet Protein (I% of total)
35
30
25
20
15
10
5
0
BH
25/75
BH
A/BH
A/BH 50/50
NoH
H
NoH
H
NoH
H
Alpha / Beta H (ug/ug)

ml plus 50 μg βH-crystallin / ml (1α:1β ratio). The study was performed with single samples a total of three times, however, the methodology differed between experiments, so statistics could not be performed. The pattern was the same for all of the experiments and this graph shows a typical example of the effects of heat and α-crystallin upon βH-crystallin.

subunits of βL-and βH-crystallin to precipitate. Which specific subunits, (or all of them) precipitated, was unknown. To determine which subunits precipitated, two-dimensional gel electrophoresis of heated supernatants and pellets and of unheated supernatants were performed.

Two-Dimensional Gels of β-crystallins Following Heat Treatment: Differential precipitation of certain polypeptides in βH-crystallin occurred after heating (Figs. 18, 19 and 20). βB1a and βB1b were enriched in the pellet, while βB2, βB3, βA1, βA3, and βA4 remained fairly soluble, and thus were at similar levels in both heated and unheated supernatants. It is apparent, however, that a portion of each subunit does precipitate and can be observed on gel of the heated pellet, albeit in lower relative amounts.

Parallel analysis of βL-crystallin also showed differential precipitation of subunits in response to heating (Fig. 21, 22 and 23). βB2 and βB3 were enriched in the pellet after heating, while βA1, βA2, βA3 and βA4 were at similar levels in both heated and unheated supernatants. The βA1 and βA3 are particularly unrepresented in the pellet relative to the others.

βL-crystallin does not contain βB1a or βB1b. However, both βL- and βH-crystallins contain βB2 and βB3, although these subunits are only enriched in the pellet of heated βL-crystallin. Thus, the individual polypeptides of βH-and βL-crystallin show different susceptibilities to heat precipitation. The subunits were identified by visual comparison with published photographs of gels of adult and calf bovine and fetal human β-crystallin subunits. These assignments were verified by an expert in two-dimensional gel analysis of β-crystallins, Dr. Christine Slingsby (University of London, England).

Fig. 18: Unheated βH-Crystallin Supernatant.

Two-dimensional gel electrophoresis of the supernatant from unheated βH-crystallin. βB1a, βB1b, βB2, βB3, are basic subunits, while βA1, βA2, βA3, and βA4 are acidic subunits of βH-crystallin.

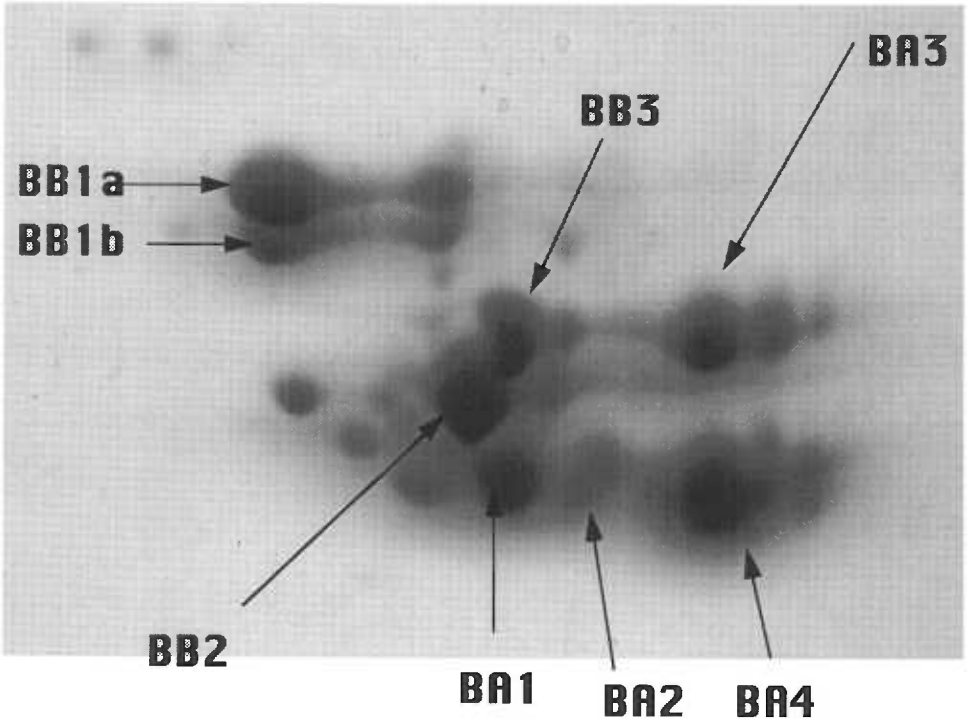
BA3
BB3
BB1a
BB1b
BB2
BA1
BA2
BA4

Fig. 19: Heated βH-Crystallin Supernatant.

Two-dimensional gel electrophoresis of the supernatant from βH-crystallin, which had been heated at 64° C for 30 minutes. βB1a, βB1b, βB2, βB3, are basic subunits, while βA1, βA2, βA3, and βA4 are acidic subunits of βH-crystallin.

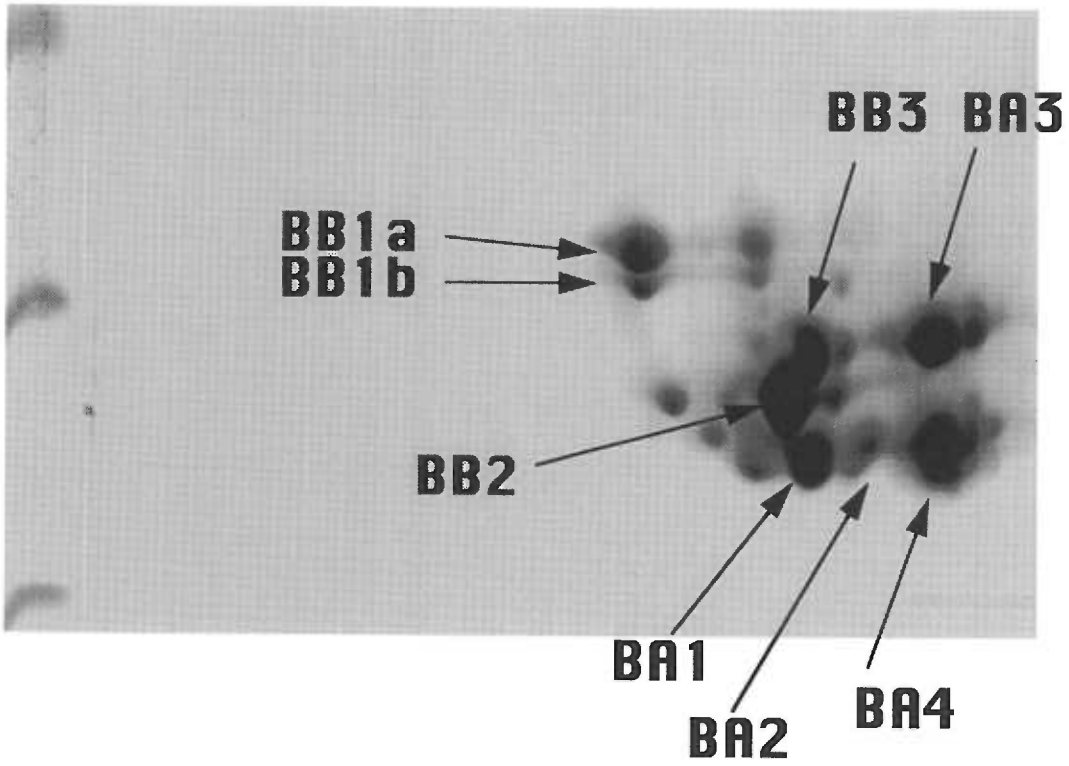
BB3
BA3
BB1a
BB1b
BB2
BA1
BA2
BA4

Fig. 20: Heated βH-Crystallin Pellet.

Two-dimensional gel electrophoresis of the pellet of βH-crystallin, which had been heated at 64° C for 30 minutes. βB1a, βB1b, βB2, βB3, are basic subunits, while βA1, βA2, βA3, and βA4 are acidic subunits of βH-crystallin.

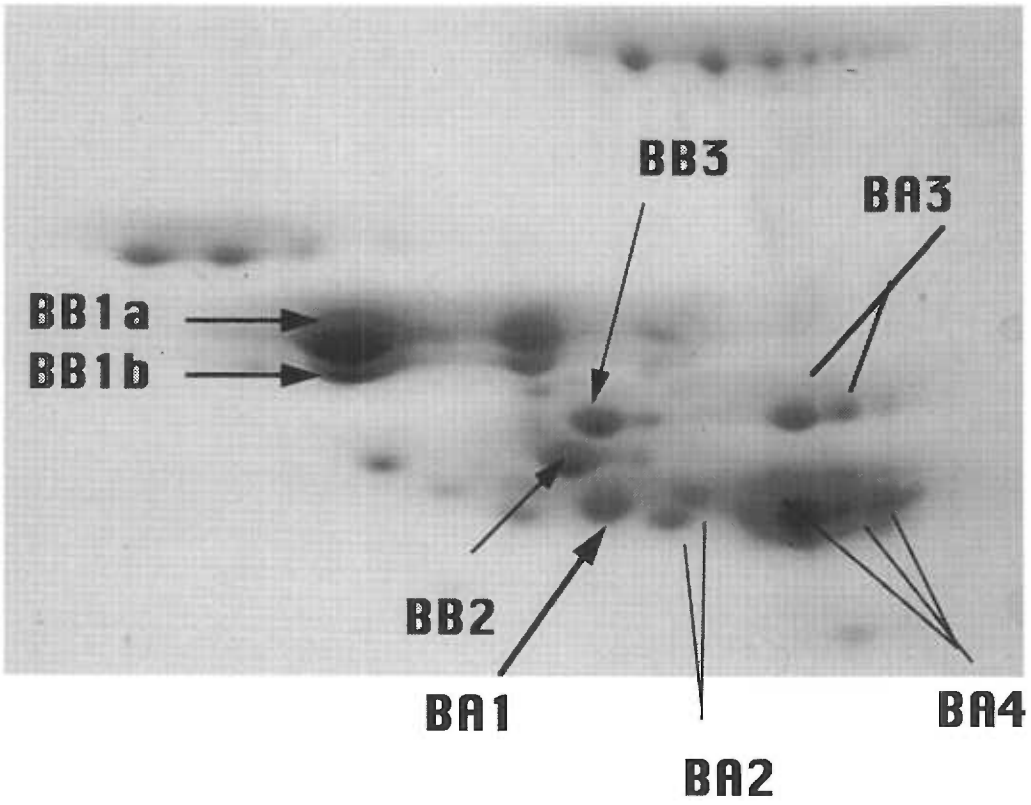
BB3
BA3
BB1a
BB1b
BB2
BA1
BA2
BA4

Fig.21: Unheated βL-Crystallin Supernatant.

Two-dimensional gel electrophoresis of the supernatant from βH-crystallin, which had not been heated. βB2, βB3, are basic subunits, while βA1, βA2, βA3, and βA4 are acidic subunits of βL-crystallin.

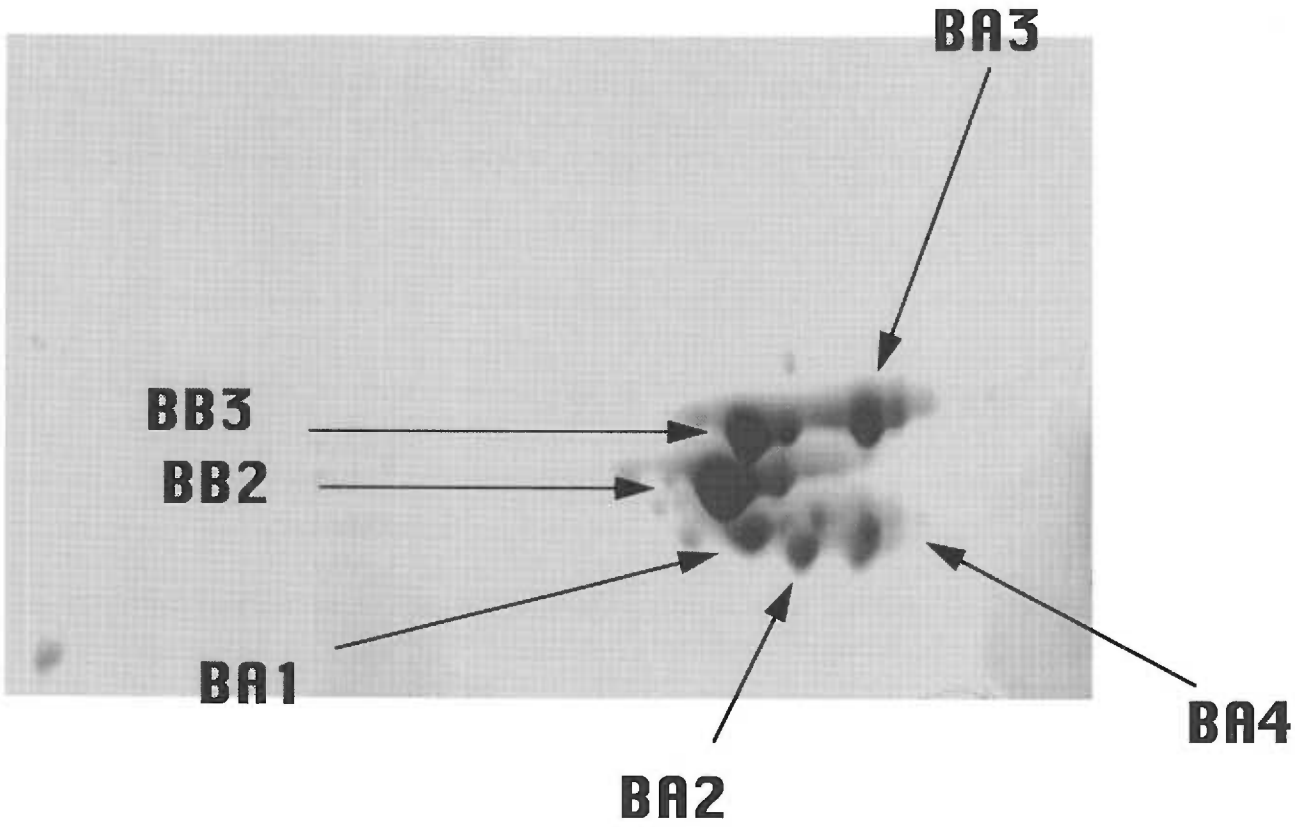
BA3
BB3
BB2
BA1
BA2
BA4

Fig. 22: Heated βL-Crystallin Supernatant.

Two-dimensional gel electrophoresis of the supernatant from βH-crystallin, which had been heated at 64° C for 30 minutes. βB2, βB3, are basic subunits, while βA1, βA2, βA3, and βA4 are acidic subunits of βL-crystallin.

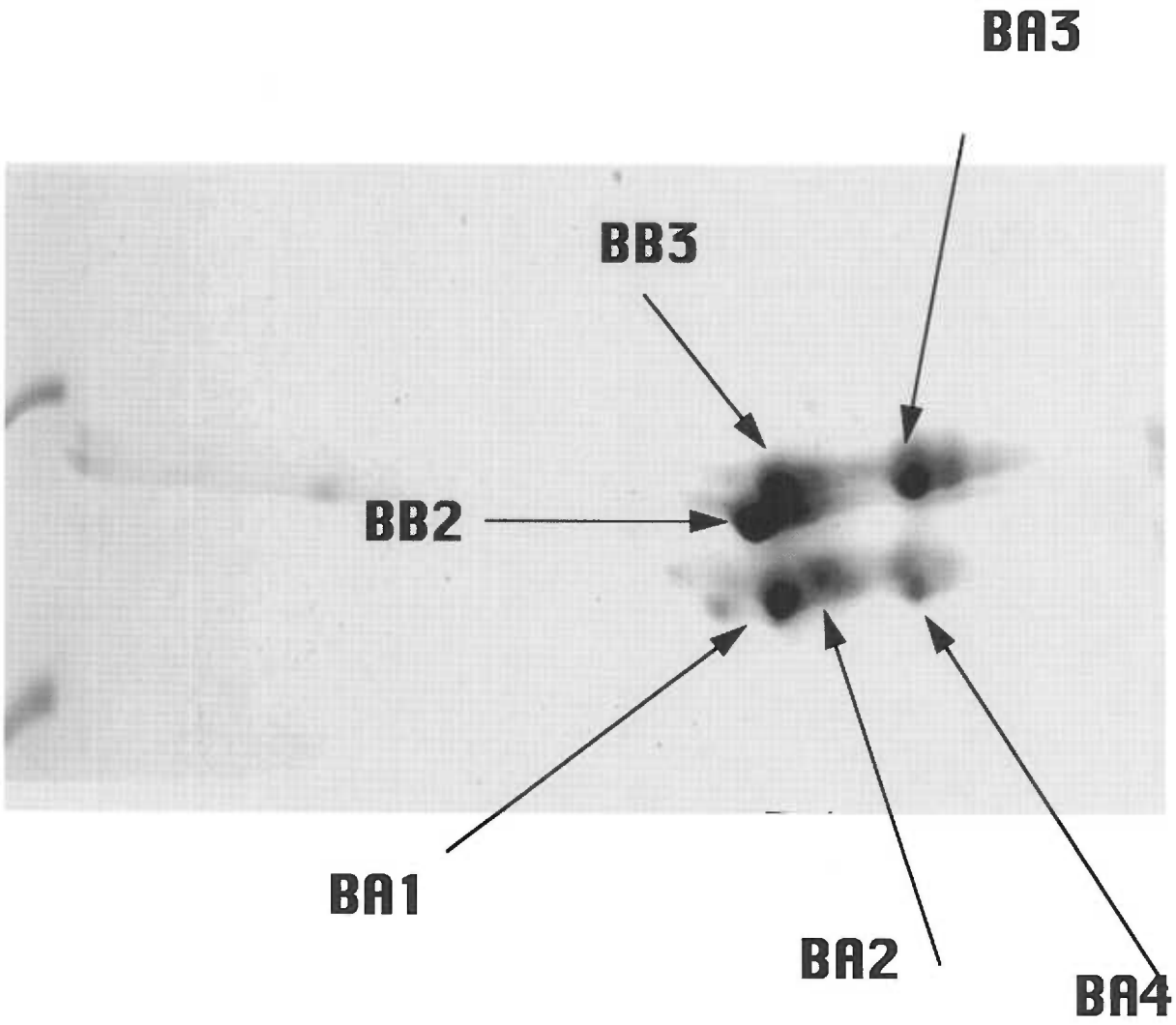
BA3
BB3
BB2
BA1
BA2
BA4

Fig. 23: Heated βL-Crystallin Pellet.

Two-dimensional gel electrophoresis of the pellet of βL-crystallin, which had been heated at 64° C for 30 minutes. βB2, βB3, are basic subunits, while βA2, βA3, and βA4 are acidic subunits of βL-crystallin.

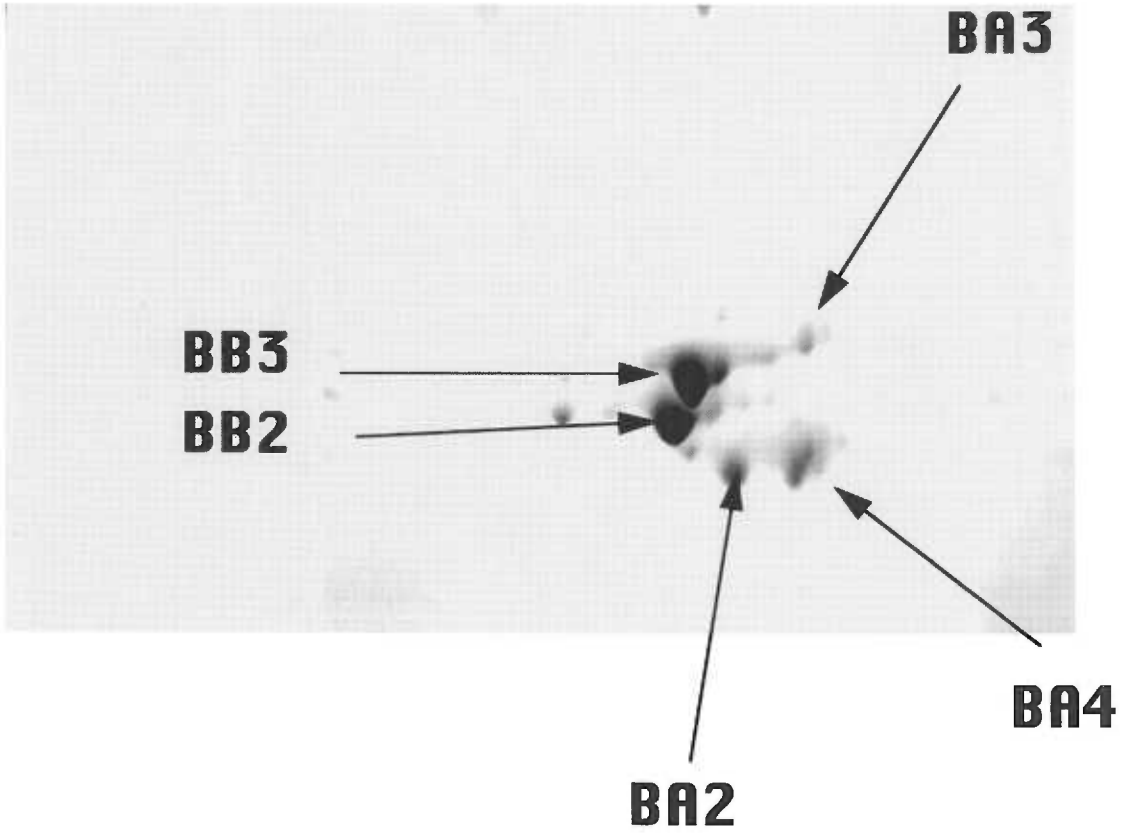
BA3
BB3
BB2
BA4
BA2

Densitometric Scanning of Two-Dimensional Gels: Semi-quantitative analysis of the β-crystallin gels by densitometric scanning was used to confirm the visual observations presented above. The density of each protein spot was expressed as a percentage of the total density of proteins on the gel (Table I). Most notable was the predominance of βB1a (20%) and βB1b (6.5%) in the pellet from the heat precipitated βH-crystallin gel and βB2 (25.3%) and βB3 (22.5%) in the pellet from the heat-precipitated βL-crystallin gel. Thus, βB1a and βB1b fragments of βH-crystallin are thermodynamically unstable and readily precipitate. This was interesting because the intact parent crystallin, βB1, is a good substrate for calpain. The results also suggested that the presence of βB1 subunits in βH-crystallin account for the greater requirement of this crystallin for α-crystallin to prevent heat-induced aggregation of βH-crystallin. In the absence of βB1, the βB2 and βB3 polypeptides of βL-crystallin appear to be more susceptible to precipitation than when present in βH-crystallin.

Comparison of HMW and α-Crystallin as Chaperones.

HMW α-crystallin has the same subunits as native α-crystallin, however, the aggregates of HMW α-crystallin (> 1 million kDa) are larger than the native α-crystallin (800 kDa). Recent reports have implicated HMW α-crystallin as binding partially denatured β-and γ-crystallins and thereby preventing further denaturation (62). Therefore, the purpose of the next study was to determine if HMW α-crystallin is as effective a chaperone as the normal LMW form of α-crystallin in protecting βL-crystallins against heat denaturation.

Table I. : Densitometric Analysis of Two-Dimensional Gels of β-Crystallins.

CRYSTALLIN	SUBUNIT	HEATED PELLET	HEATED SUPERNATANT	UNHEATED SUPERNATANT
βH	βB1a	20	5.45	8.3
βH	βB1b	6.5	2.36	3.3
βL	βB2	25.3	14.3	16.5
βL	βB3	22.5	12.6	14.6

Values are the density of several subunit spots each expressed as a percentage of the total density of all the spots on the respective gel. In each case, the values presented are for the same gels that are shown in the respective figures, but are in close agreement with parallel analysis of from one to four separate gels subjected to identical treatment.

Bovine HMW α-crystallin and normal LMW α-crystallin were incubated separately with βL-crystallin (Fig. 24). βL-crystallin (200 μg/ml) and 100 μg/ml of either α-crystallin or HMW α-crystallin from fetal calf lenses were heated to 60° C for 135 minutes. βL-crystallin + HMW α-crystallin group showed an increased turbidity of approximately 70 mOD upon heating, while the native LMW α-crystallin + βL-crystallin group increased only 15 mOD. The inset shows a dose-response curve of LMW α-crystallin or HMW α-crystallin chaperone activity. Thus, at the concentrations tested, LMW α-crystallin was a more effective chaperone than HMW α-crystallin in protecting βL-crystallin from heat-induced denaturation.

Alpha-Crystallin Preheating Studies.

A control (data not shown or see Fig. 25C below) used in many of the previous experiments was to heat α-crystallin alone; essentially no precipitation is observed in these controls. However, we next evaluated whether the chaperone activity of α-crystallin was diminished by heating, even though α-crystallin did not precipitate. The eventual precipitation of β-crystallins (after long periods of heating), with α-crystallin may partially the result of damage to α-crystallin. To test this, rat α-crystallin was preheated prior to incubation with βL-crystallin. Alpha-crystallin, at 61 μg/ml in buffer I, was preheated at 60° C for time periods of 0, 10, 30, 60, and 90 minutes. These preheated α-crystallins were then tested as chaperones in the βL-crystallin heat aggregation assay. Progressively increasing the time of preheating reduced the ability of α-crystallin to prevent precipitation of βL-crystallin (Fig. 25A and 25B). Thus, prior thermal denaturation may diminish chaperone activity. This may explain why chaperone

activity is lost at the longer time periods.

Fig. 24: Comparison of HMW α and LMW α-Crystallins as Chaperones.

HMW α- and normal (LMW) α-crystallin were compared to each other as chaperones of βL-crystallin from fetal calf lens cortex (βLCC). The inset shows dose-response curves for LMW α-crystallin or HMW α-crystallin chaperone activities. The error bars represent the standard deviation (n=3).

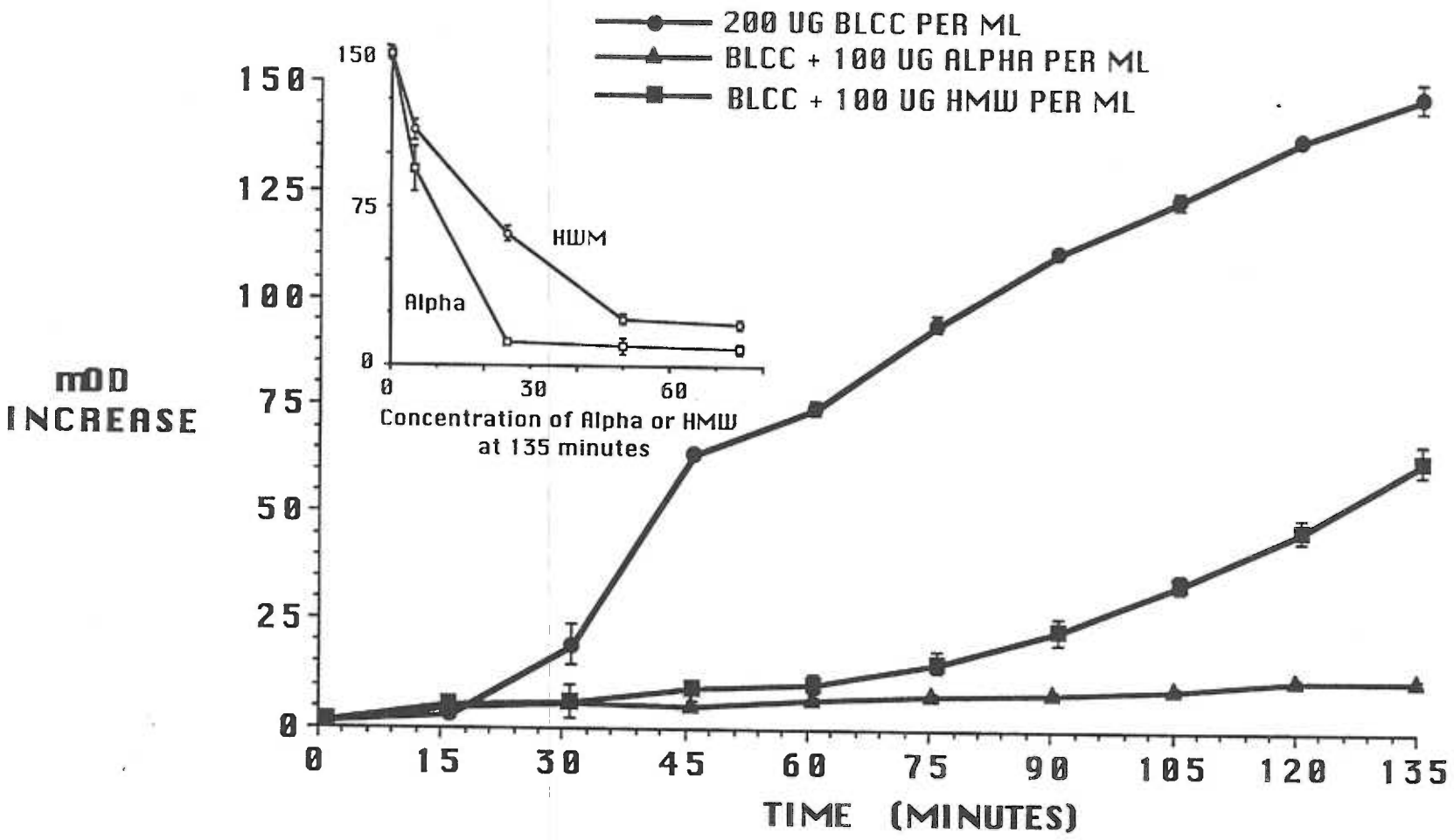
200 UG BLCC PER ML
BLCC + 100 UG ALPHA PER ML
BLCC + 100 UG HMW PER ML
mOD INCREASE
150
125
100
75
50
25
0
0
15
30
45
60
75
90
105
120
135
TIME (MINUTES)
150
75
0
HWM
Alpha
0
30
60
Concentration of Alpha or HMW at 135 minutes

Fig. 25A: Alpha-Crystallin Preheating Studies.

Alpha-crystallin was preheated at 60° C for 0, 10, 30, 60, or 90 minutes, cooled and then used (at 61 μg/ml) in the standard heat aggregation assays to chaperone βL-crystallin (at 100 μg/ml). The time course for the chaperone assay using α-crystallins which had been preheated for the times indicated in the legend is shown. The determinations were in duplicate, and the error bars represent the range. Other values obtained in a variation of this experiment showed the same pattern, and this graph is presented as a typical, repeatable example.

Fig. 25 B: Effects of Preheating of α-Crystallin on its Chaperone Activity.

The preheating time of α-crystallin is shown on the x-axis and the mOD increase which was measured at 75 min in the chaperone assay (Fig. 25A) is shown on the y-axis. The determinations were in duplicate, and the error bars represent the range. A variation of this experiment resulted in the same pattern. This graph shows a typical, repeatable example.

Fig. 25 C: Controls for Fig. 25A.

Parallel control wells for the standard heat aggregation assay shown above (Fig. 25A). Preheated α-crystallin samples (as in A above) incubated alone in the chaperone assay show no effect of preheating on their solubility.

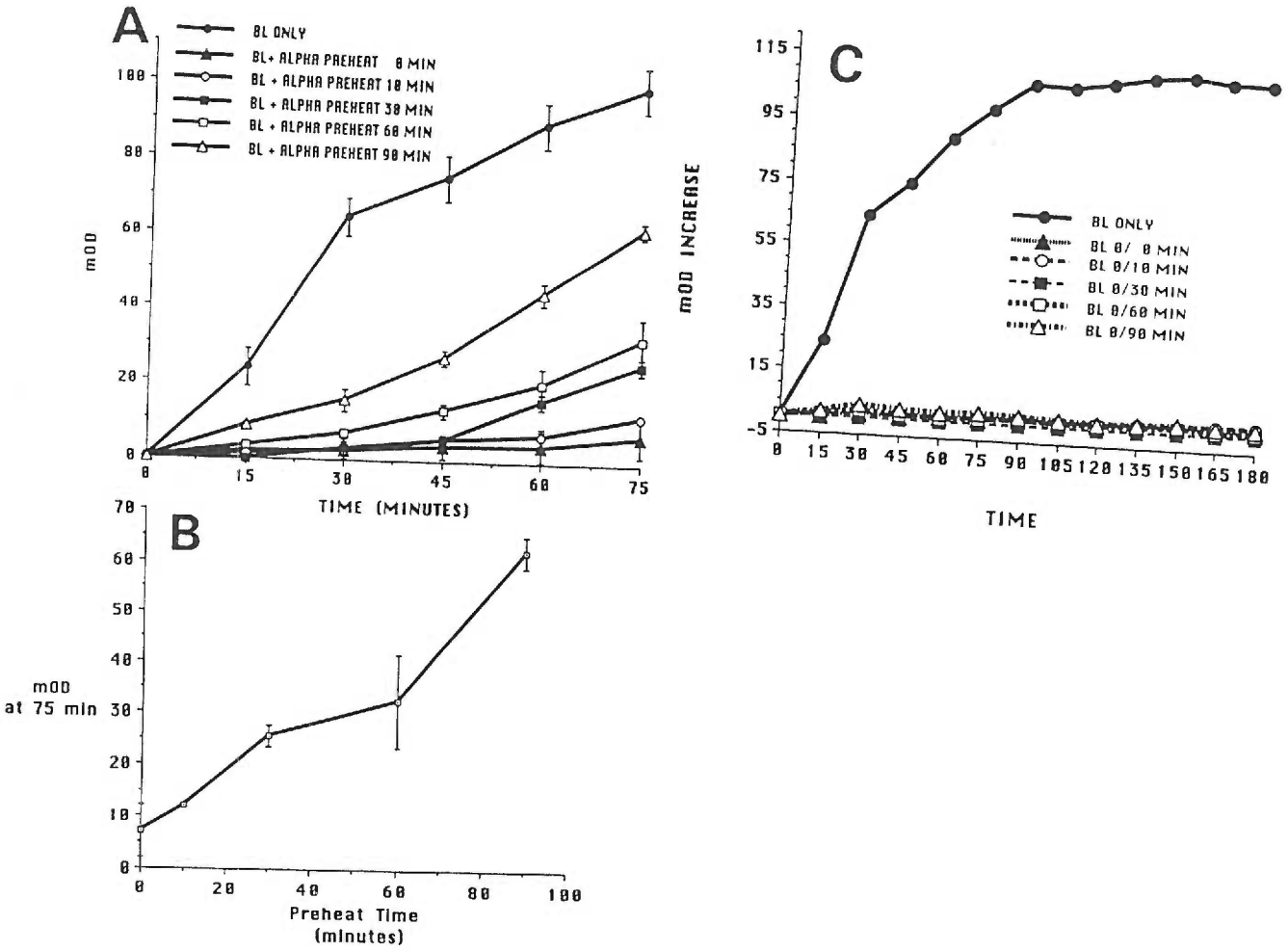
A
BL ONLY
BL+ ALPHA PREHEAT 0 MIN
BL + ALPHA PREHEAT 10 MIN
BL + ALPHA PREHEAT 30 MIN
BL + ALPHA PREHEAT 60 MIN
BL + ALPHA PREHEAT 90 MIN
mOD
TIME (MINUTES)
B
mOD at 75 min
Preheat Time (minutes)
C
mOD INCREASE
BL ONLY
BL 0/ 0 MIN
BL 0/10 MIN
BL 0/30 MIN
BL 0/60 MIN
BL 0/90 MIN
TIME

Chaperone Activity of Alpha-Crystallin Subunits.

Another factor that could play a role in the effectiveness of α-crystallin as a chaperone is the relative proportions of individual subunit chains in the native α-crystallin aggregate. Normal (LMW) α-crystallin exhibits a wide-range of molecular weights, from 300,000 to 800,000 (13,63,64). This heterogenity may be caused by differences in the relative proportion of αA and αB subunits and in the total number of subunits present (13,63,64). There are no extensive data determining if α-crystallin aggregates, composed of only one type of subunit, will function independently as a chaperone, or if both αA and αB subunits are required (147). Since differences in chain composition imply differences in charge, secondary and tertiary structure, and other factors, it is probable that the α-crystallins are not equivalent in acting as chaperones. Therefore, the purpose of the next experiment was to determine if the subunit chains function as molecular chaperones individually, or if both subunit chains are necessary for α-crystallin to act as a chaperone.

Effects of Urea Treatment on α-crystallin Chaperone Activity: Since urea is normally used in the separation of the α-crystallin subunits, a preliminary experiment was conducted to determine if native α-crystallin was damaged by incubation with 6 M urea. Following incubation with urea for 1 hour at room temperature, α-crystallin was dialyzed extensively with buffer I and was tested for chaperone activity in protecting βL-crystallin from heat denaturation (Fig. 26A). Interestingly, the chaperone activity of urea-treated α-crystallins was modestly enhanced, rather than diminished. βL-crystallin incubated with untreated α-crystallin showed slightly greater turbidity than did β-

crystallin incubated with urea-treated α-crystallins (Fig. 26B). This was true at all concentrations of urea-treated α-crystallin examined, and may indicate that partial denaturation of the α-crystallin molecule allows better binding to β-crystallin. Figures 27A and 27B are concentration curves of untreated α-crystallin and urea-treated α-crystallin at 30 and 60 minutes, respectively. Figure 27C shows controls of βL-crystallin only, untreated α-crystallin, and urea-treated α-crystallin.

Separation of Rat α-crystallin Subunits: Since the chaperone activity of native α-crystallin was not negatively affected by urea exposure, rat α-crystallin subunits were separated in urea by ion exchange using an HPLC. Three subunits were resolved: αA, αB, and αAInsert. The latter is an αA polypeptide with a 23-amino acid peptide insert found only in rodents (Fig. 28). There was an insufficient amount of αAInsert for detailed chaperone assays. The αA and αB subunit fractions were collected, individually dialyzed against buffer I to allow reaggregation, and identified by SDS-PAGE (Fig. 29). These two subunits and intact unfractionated α-crystallin (αt) were added individually to βL-crystallin and their respective chaperone activities were measured in the heat aggregation assay (Fig. 30 A,B,C,D). At high concentrations, αA had greater chaperone activity than αt, which in turn had greater chaperone activity than αB (Fig. 30C).

Greater dilutions of the α-crystallin subunits exhibited a different pattern of intermolecular interactions (Fig. 30A and B). At these lower concentrations of α-crystallin, the two subunits lost chaperone capability, and αA became the least effective chaperone. At the 15 and 25 μg/ml concentrations, the chaperone ability of the subunit chains was similar. At both concentrations, the αt became the most efficient chaperone.

Fig. 26A: Chaperone Activity of Urea-Treated α-Crystallin.

Alpha-crystallin was denatured with 6 M urea, dialyzed to allow renaturation, and subsequently used in the heat aggregation assay to test for ability to chaperone βL-crystallin. This experiment was performed once at each alpha concentration. Since this was a only a pilot experiment to determine if chaperone activity was present after urea treatment, no statistical analysis was conducted.

Fig. 26B: Chaperone Activity of Normal Untreated α-Crystallin.

As a comparison, the same preparation of normal α-crystallin, which had not been exposed to urea, was used in parallel heat aggregation assays. This experiment was performed once at each concentration. A statistical analysis was not performed, since this was a only a pilot experiment to determine if chaperone activity was present after urea treatment.

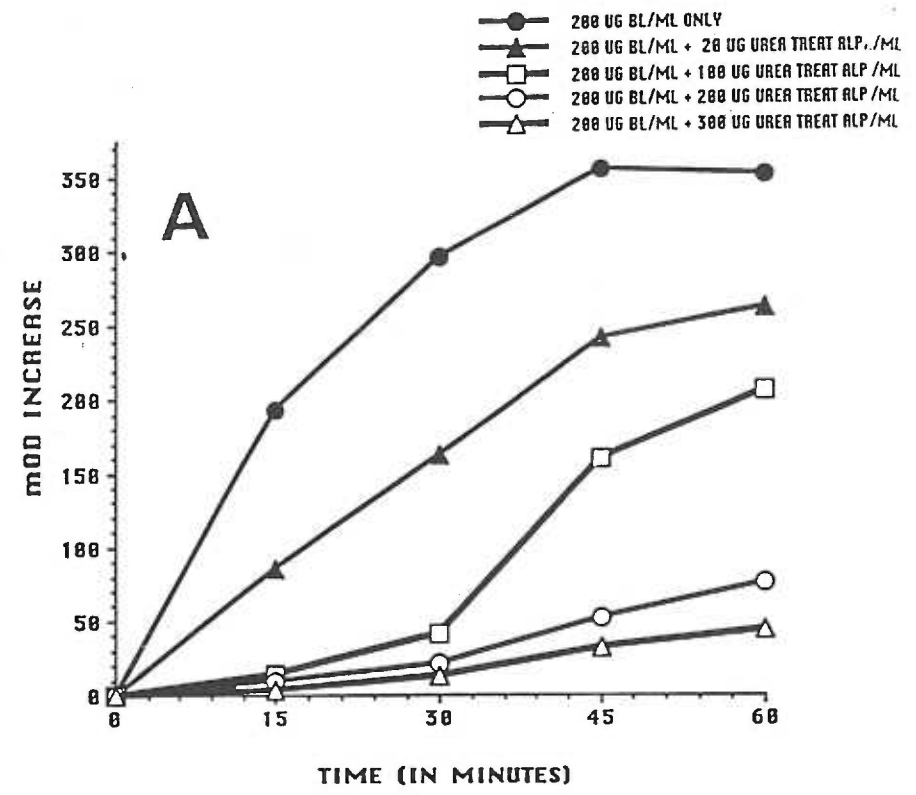
200 UG BL/ML ONLY
200 UG BL/ML + 20 UG UREA TREAT ALP /ML
200 UG BL/ML + 100 UG UREA TREAT ALP /ML
200 UG BL/ML + 200 UG UREA TREAT ALP /ML
200 UG BL/ML + 300 UG UREA TREAT ALP/ML
A
mOD INCREASE
350
300
250
200
150
100
50
0
0
15
30
45
60
TIME (IN MINUTES)

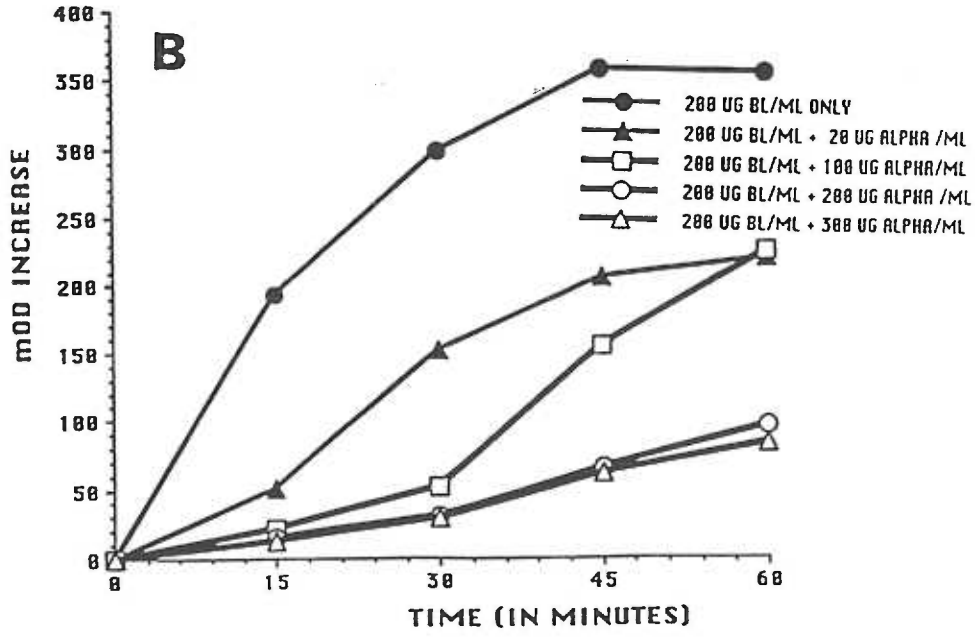
B
400
350
300
250
200
150
100
50
0
mOD INCREASE
200 UG BL/ML ONLY
200 UG BL/ML + 20 UG ALPHA /ML
200 UG BL/ML + 100 UG ALPHA/ML
200 UG BL/ML + 200 UG ALPHA /ML
200 UG BL/ML + 300 UG ALPHA/ML
0
15
30
45
60
TIME (IN MINUTES)

Fig. 27A: Concentration Curve of Untreated and Urea-Treated α-Crystallins used as Chaperones of βL-Crystallin at 30 Minutes.

Both α-crystallins (untreated and urea-treated) show excellent chaperone ability with βL-crystallin (200 μg/ml) at 30 minutes, from a concentration of 25 to 75 ug α-crystallin/ml. This experiment was performed once at each concentration. Since this was only a pilot experiment to determine if chaperone activity was present after urea treatment, it was not feasible to perform a statistical analysis.

Fig. 27B: Concentration Curve of Untreated and Urea-Treated α-Crystallins as Chaperones of βL-Crystallin at 60 Minutes.

Both α-crystallins (untreated and urea-treated) show excellent chaperone ability with βL-crystallin (200 μg/ml) at 60 minutes, from a concentration of 25 to 75 ug α-crystallin/ml. This experiment was performed once at each concentration. Since this was only a pilot experiment to determine if chaperone activity was present after urea treatment, it was not feasible to perform a statistical analysis.

Fig. 27C: Controls for Untreated and Urea-Treated α-Crystallins Chaperone Activity.

βL-Crystallin only, untreated α-crystallin only, and urea-treated α-crystallin only in the standard heat denaturation assay.

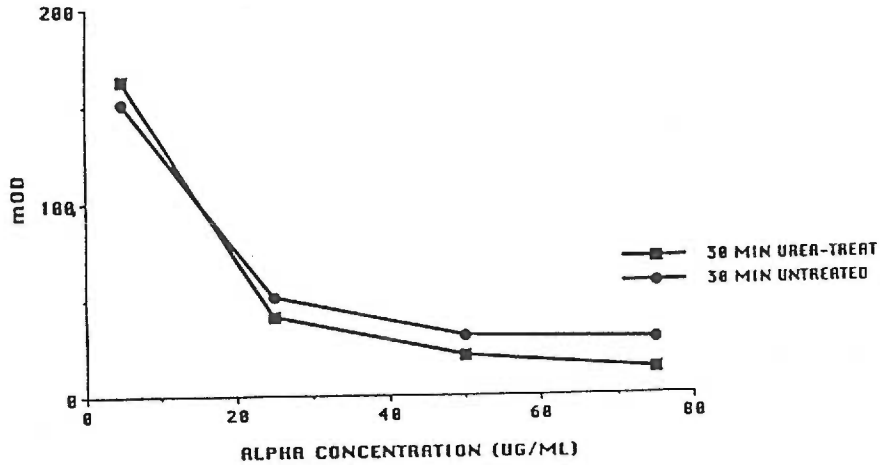
200
100
0
mOD
0
20
40
60
80
ALPHA CONCENTRATION (UG/ML)
30 MIN UREA-TREAT
30 MIN UNTREATED

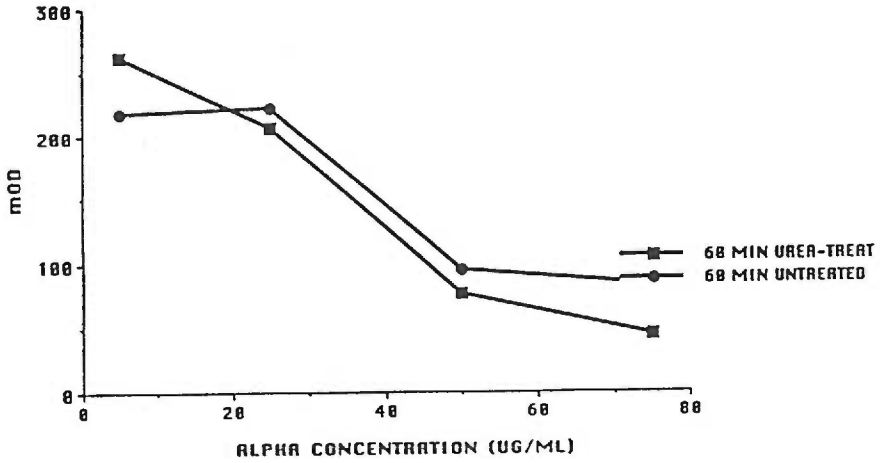
300
200
100
0
mOD
0
20
40
60
80
ALPHA CONCENTRATION (UG/ML)
60 MIN UREA-TREAT
60 MIN UNTREATED

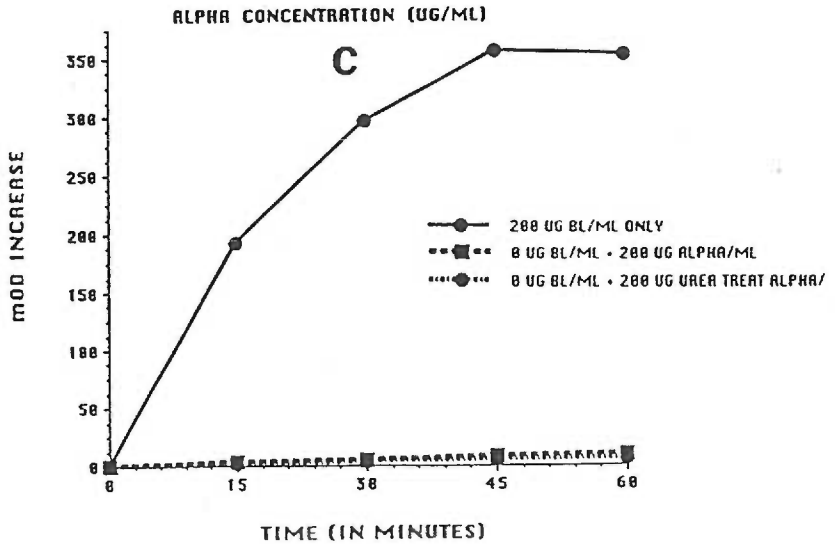
ALPHA CONCENTRATION (UG/ML)
C
350
300
250
200
150
100
50
0
mOD INCREASE
0
15
30
45
60
TIME (IN MINUTES)
200 UG BL/ML ONLY
0 UG BL/ML + 200 UG ALPHA/ML
0 UG BL/ML + 200 UG UREA TREAT ALPHA/

Fig.28: Chromatograph of Separated Rat α-Crystallin Subunits on HPLC.

Rat α-crystallin subunits were separated by an ion exchange chromatography column. The two major peaks are αB and αA, respectively. The salt gradient (100 mM) and absorbance curves are shown.

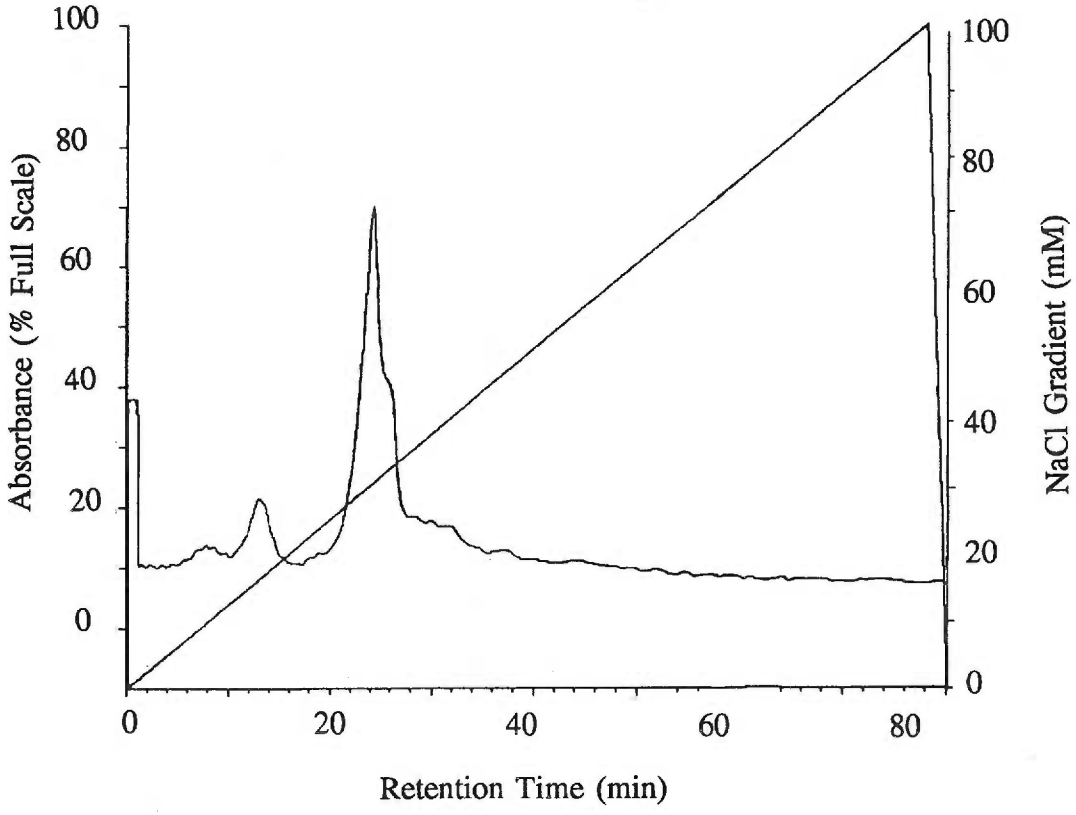
Absorbance (% Full Scale)
100
80
60
40
20
0
0
20
40
60
80
Retention Time (min)
NaCl Gradient (mM)
100
80
60
40
20
0

Fig. 29: One-Dimensional Gel Electrophoresis of α-Crystallin Subunits Separated by Ion Exchange Chromatography.

Composite photograph of lanes from several gels showing individual fractions of α-crystallin subunits from whole rat lenses. After separation on ion exchange HPLC, each fraction was dialyzed without pooling, and the individual fractions were analyzed on 12% SDS-PAGE gel electrophoresis. The lanes on the gel were : low molecular weight standards, lane 1; αA-crystallin, lane 2; αB-crystallin, lane 3; αA insert, lane 4; αt-crystallin (unfractionated), lane 5. A composite photograph was made because of the large number of gels required for analysis of individual fractions.

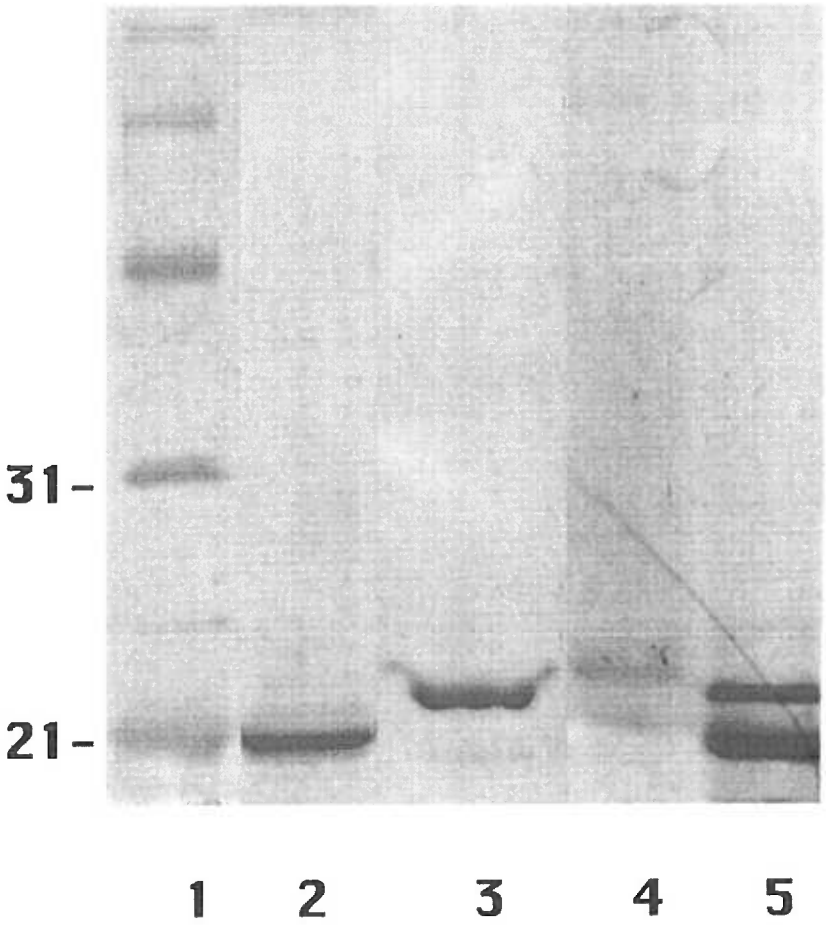
31-
21-
1
2
3
4
5

Fig. 30A: Chaperone Activity Assay of α-Crystallin Subunits (15 μg α-crystallin/ml) with βL-Crystallin.

Heat aggregation assay of 167 μg βL-crystallin/ml protected by α-crystallin subunits and unfractionated αt at 15 μg α-crystallin/ml. The error bars represent the standard deviation (n=3).

Fig. 30B: Chaperone Activity Assay of α-Crystallin Subunits (25 μg α-crystallin/ml) with βL-Crystallin.

Heat aggregation assay using 25 μg of the respective α-crystallins / ml. The error bars represent the standard deviation (n=3).

Fig. 30C: Chaperone Activity Assay of α-Crystallin Subunits (50 μg α-crystallin/ml) with βL-Crystallin.

Heat aggregation assay using 50 μg of the respective α-crystallins / ml. The error bars represent the standard deviation (n=3).

Fig. 30D: Concentration Curves of α-Crystallin Subunit Chaperone Activity.

Alpha A, αB, and αt at varying concentrations (15, 25, or 30 μg/ml) acting as a chaperone for 167 μg βL-crystallin/ml at 75 minutes in the heat aggregation assay. The error bars represent the standard deviation (n=3).

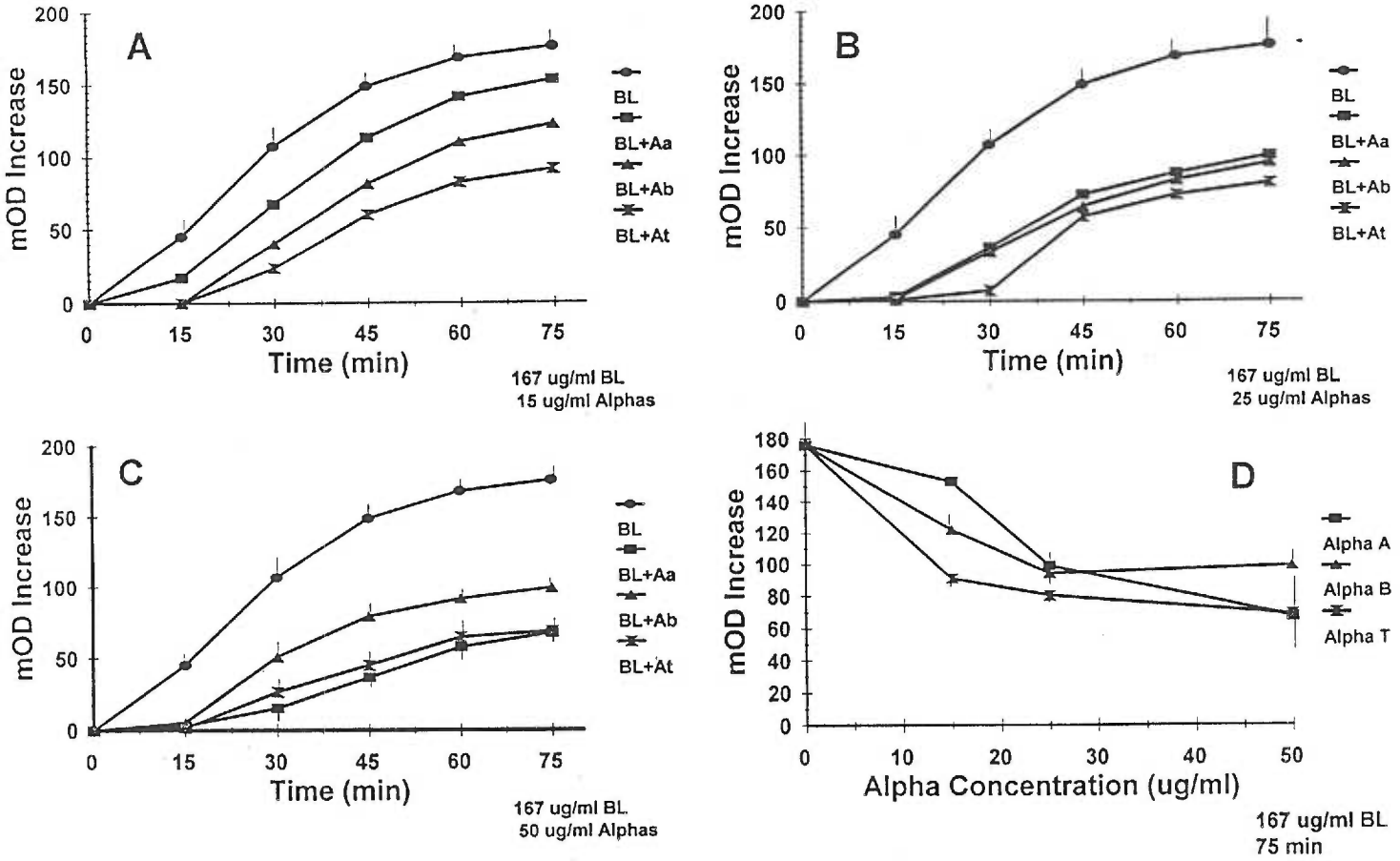
A
mOD Increase
Time (min)
BL
BL+Aa
BL+Ab
BL+At
167 ug/ml BL
15 ug/ml Alphas
B
mOD Increase
Time (min)
BL
BL+Aa
BL+Ab
BL+At
167 ug/ml BL
25 ug/ml Alphas
C
mOD Increase
Time (min)
BL
BL+Aa
BL+Ab
BL+At
167 ug/ml BL
50 ug/ml Alphas
D
mOD Increase
Alpha Concentration (ug/ml)
Alpha A
Alpha B
Alpha T
167 ug/ml BL
75 min

A concentration curve of the α-crystallin subunits chaperone activity summarizes the effects of the three concentrations (Fig. 30D). Thus, concentration effects may play a pivotal role in the chaperone ability of α-crystallin subunits. All subunits responded to changes in concentration, but the chaperone activity of αA was most adversely affected by dilution and αt was least affected. More dilute solutions can have different intermolecular actions between the α-crystallin subunits and β-crystallins (95). These data suggested that chaperone activity for both subunit species is higher at higher concentrations. This is perhaps fortuitous, since the α-crystallin concentration *in vivo* is quite high, i.e. in the range of approximately 30 mg/ml.

Separation of Bovine α-crystallin Subunits: The results above with rat crystallins were confirmed by similar studies with bovine crystallins. Bovine α-crystallin was separated into three subunit peaks (Fig. 31) using the same procedure as for the rat crystallins. The three peaks produced were: αA, αB, and αA modified. Note that bovine lens does not contain αAInsert. The αA modified may be αA with post-translational changes. SDS-PAGE confirmed the identification of the α-crystallin subunits (Fig. 32).

Comparison of the Chaperone Activity of Bovine α-crystallin Subunits: The chaperone ability of bovine αA- and αB-crystallin subunits were compared to each other and to the unseparated α-crystallin, αt (Fig. 33). The chaperone capabilities of the bovine α-crystallin subunits demonstrated the same pattern as observed at high α concentrations in the rat. At 30 min, αA was the optimum chaperone, followed by αt, and αB had little chaperone activity. By 75 min, all had lost considerable chaperone

Fig. 31: Chromatograph of the Separation of Fetal Calf Lens α-Crystallin Subunits. Alpha-crystallin subunits αA, αB, and αA modified were separated by ion exchange chromatography on HPLC as in Fig. 28. The chromatograph shows three major peaks, which are, respectively, αB, αA and αA modified.

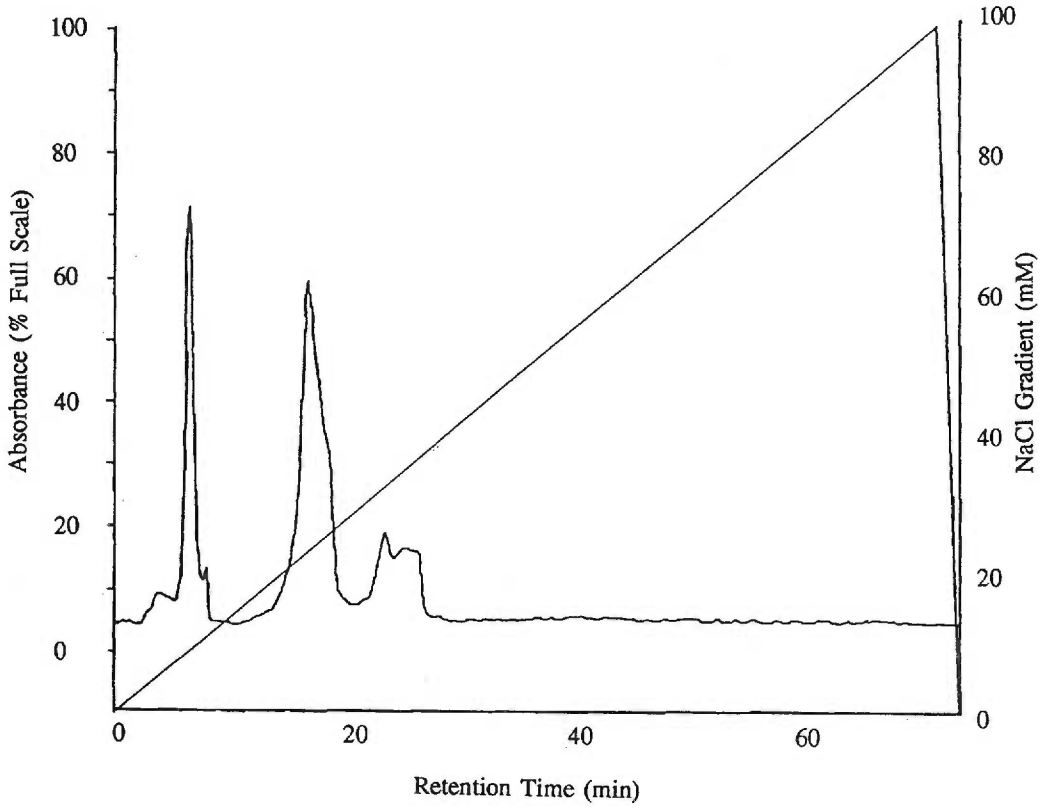
100
80
60
40
20
0
Absorbance (% Full Scale)
0
20
40
60
Retention Time (min)
100
80
60
40
20
0
NaCl Gradient (mM)

Fig. 32: One-Dimensional SDS-PAGE Gel Electrophoresis of Separated Fetal Calf Lens α-Crystallin Subunits for Chaperone Assay.

Composite photograph of lanes from several gels for identification of individual subunits of fetal calf lens α-crystallins used in the standard heat aggregation assay. The lanes were low molecular weight markers, lane 1; αB-crystallin, lane 2; αA-crystallin, lane 3; and αA modified crystallin, lane 4.

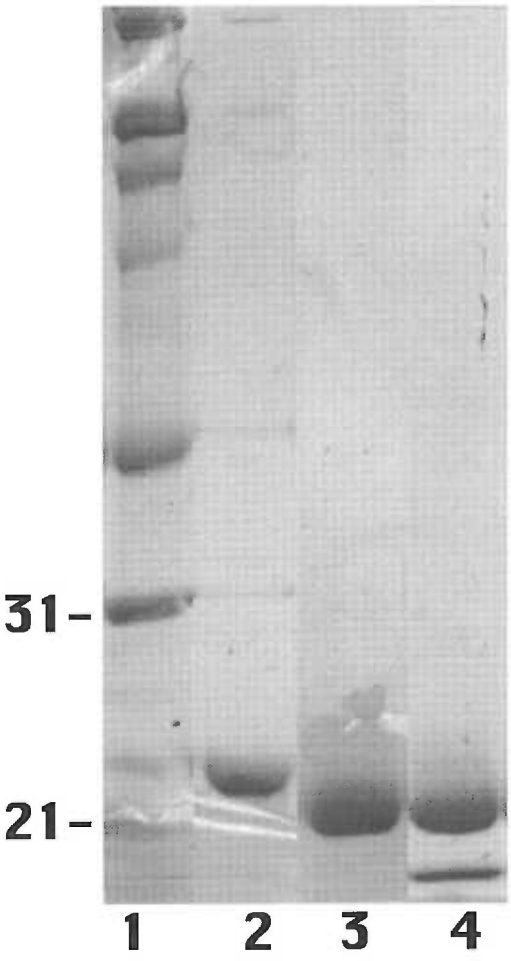
31-
21-
1
2
3
4

activity but their relative activities were similar. To understand the interaction between α- and βL-crystallins, lower concentrations of βL-crystallin (200 μg/ml) were used in the standard heat aggregation assay with 100 μg of the individual α-crystallins / ml (Fig. 34). At these concentrations, αt showed the best chaperone activity, αA modified was nearly as competent, and αA and αB were the least effective as chaperones. Thus, with the bovine α-crystallin, as with the rat previously, the ratio of αA to αB may be more important in dilute solutions. Where αt is at 2:1 (αA:αB), more efficient chaperone activity is observed, than with αA alone. Since altering the αA:αB ratio changed the effectiveness of the α-crystallin chaperone activity, we examined which ratios of α- and β-crystallins would be most effective as chaperones.

Optimum Ratios of Alpha-Crystallin Subunits for Chaperone Activity.

The purpose of this experiment was to determine the optimum ratio of α-crystallin subunits for chaperone activity. The ratios of bovine αA to αB tested were: 1:1, 1:2, and 2:1, respectively. Chaperone activity was tested in the βL-crystallin (200 μg/ml) heat aggregation assay at 60° C for 135 minutes. The 1:1 ratio was least effective (Fig. 35). Intriguingly, both the 2:1 and the 1:2 ratios were significantly more effective than the 1:1 ratio. Thus, the optimal ratio of αA:αB for chaperone activity was concentration-dependent. However, the 2:1 ratio was very effective. This is significant because the native α-crystallin ratio *in vivo* is at least 2:1.

Effect of Calpain Proteolysis upon the Chaperone Capability of Alpha-Crystallin Subunits.

The purpose of this experiment was to determine the influence of proteolysis on

Fig. 33: Comparison of the Chaperone Activity of α-Crystallin Subunits from Fetal Calf Lens at High Concentrations of α- and βL-Crystallins.

Thirty and 75 minute time points are shown for the alpha subunits and αt (88 μg/ml) used to chaperone βL-crystallin (668 μg/ml) in the standard heat aggregation assay. The error bars represent the standard deviation (n=3).

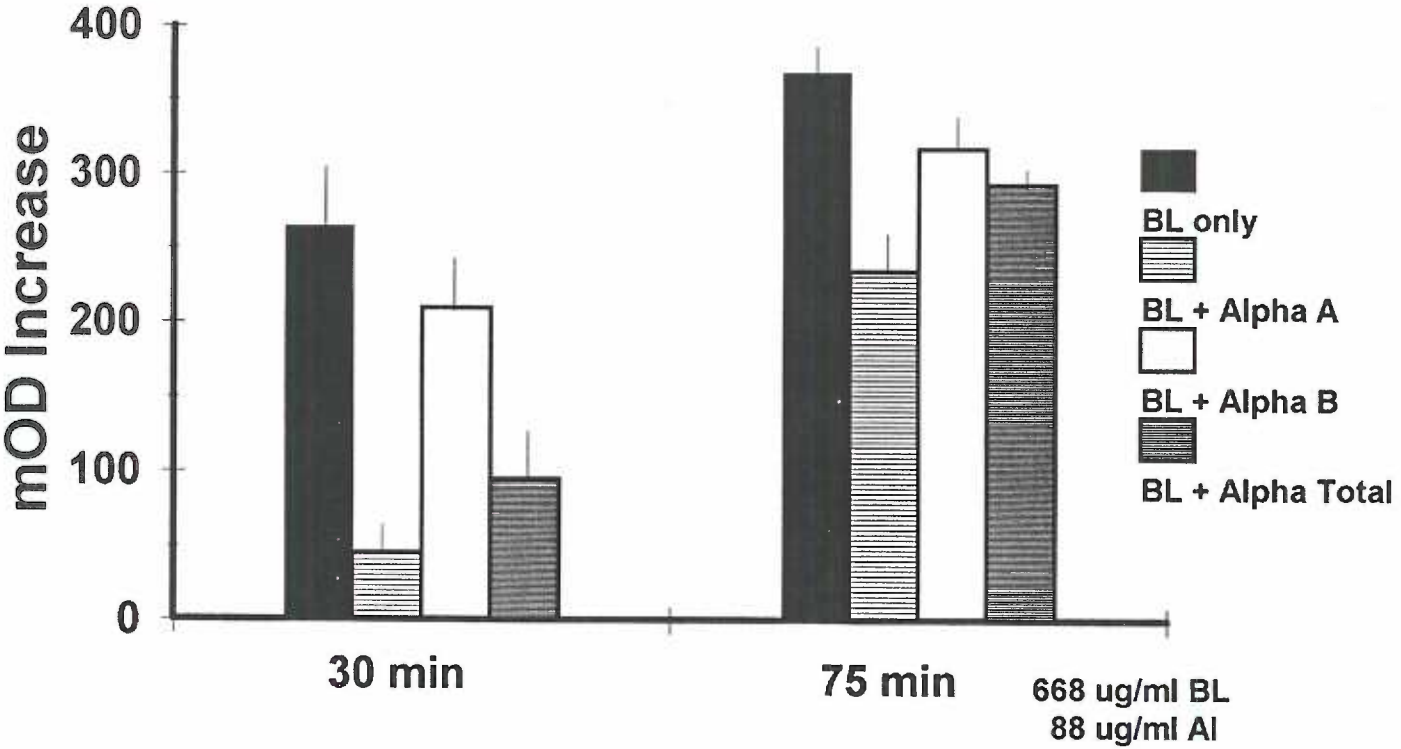
400
300
200
100
0
mOD Increase
30 min
75 min
BL only
BL + Alpha A
BL + Alpha B
BL + Alpha Total
668 ug/ml BL
88 ug/ml Al

Fig. 34: Comparison of the Chaperone Activity of Fetal Calf α-Crystallin Subunits against βL-Crystallin at High α- and Low βL-Crystallin Concentrations.

Standard heat aggregation assay was used to indicate α-crystallin subunits (100 μg/ml, relatively high concentration) for chaperone activity against βL-crystallin (200 μg/ml, relatively low concentration). The error bars are the standard deviations (n=3).

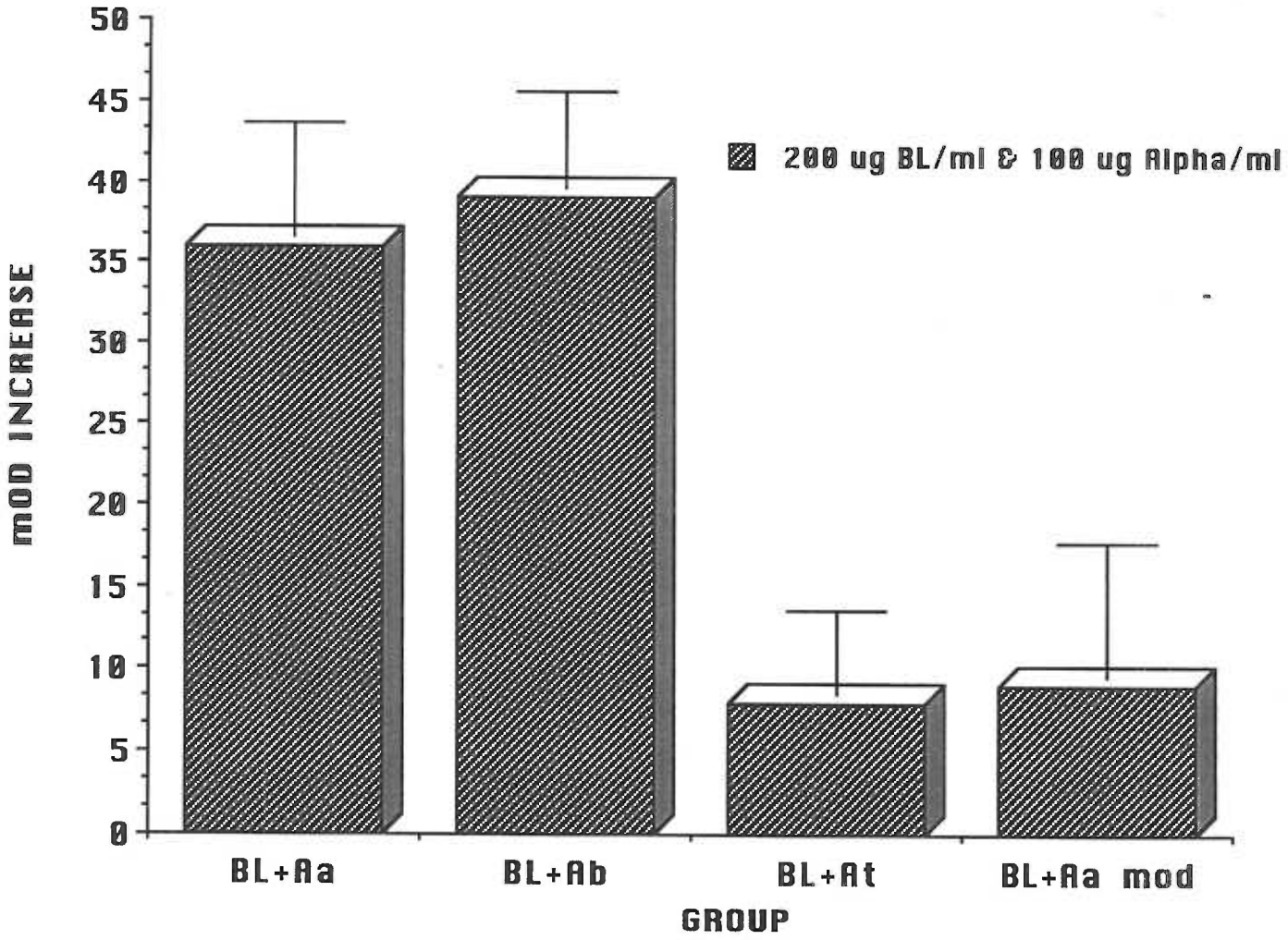
50
45
40
35
30
25
20
15
10
5
0
mOD INCREASE
200 ug BL/ml & 100 ug Alpha/ml
BL+Aa
BL+Ab
BL+At
BL+Aa mod
GROUP

Fig. 35: Optimum Ratios of Bovine Alpha-Crystallin Subunits for Chaperone Activity.

Standard heat aggregation assay using bovine βL-crystallin (200 μg/ml) was performed with the ratios of αA and αB indicated (designated Aa and Ab in the figure).

The error bars are the standard deviations (n=3).

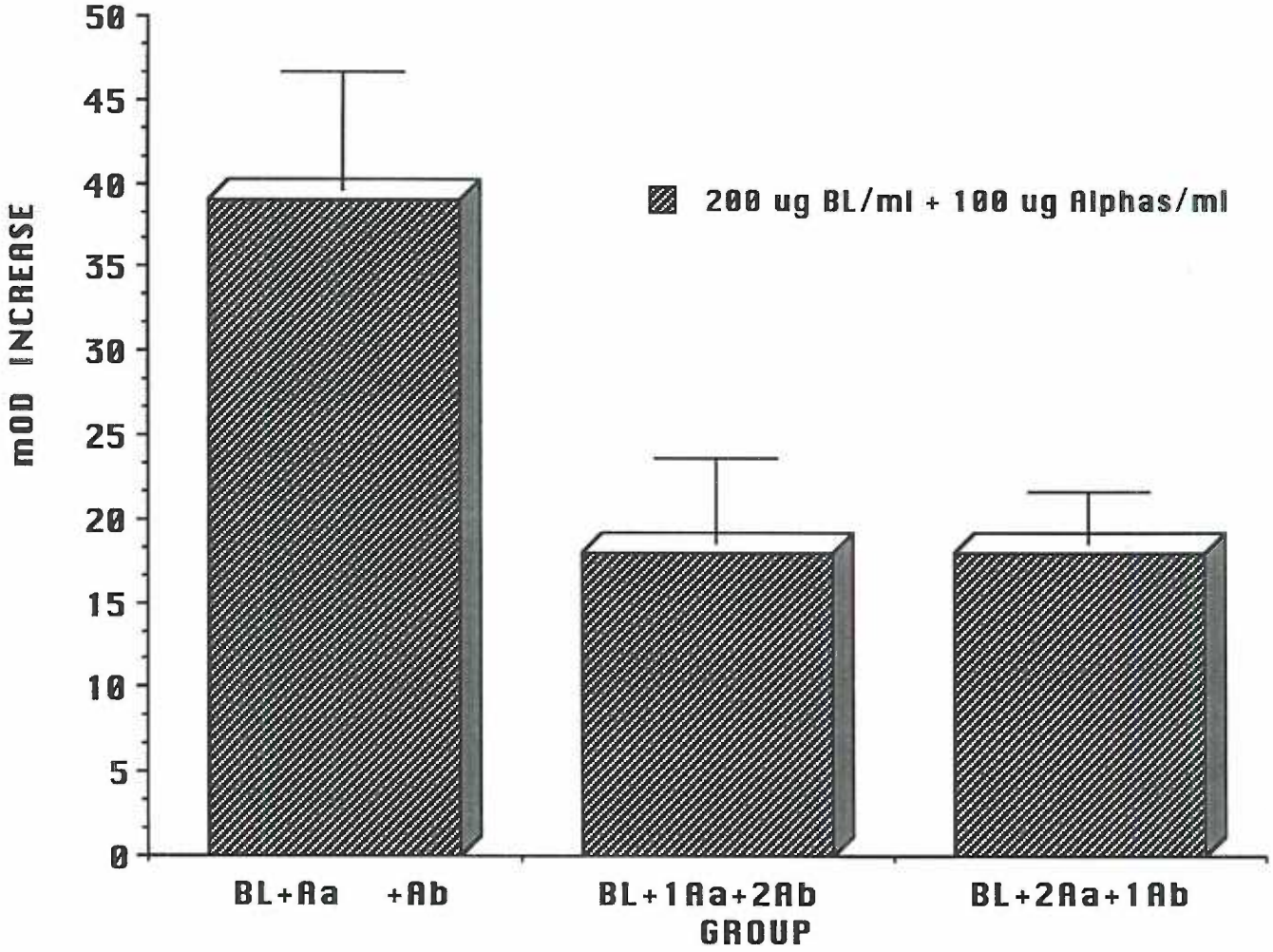
50
45
40
35
30
25
20
15
10
5
0
mOD INCREASE
200 ug BL/ml + 100 ug Alphas/ml
BL+Aa +Ab
BL+1Aa+2Ab
BL+2Aa+1Ab
GROUP

the chaperone activity of αA-and αB-crystallin subunits. The studies presented earlier using intact α-crystallin aggregates showed that proteolysis of the C-terminus by calpain caused a reduction in chaperone activity of α-crystallin (92). Whether this reduction was caused by cleavage of the αA-, αB-, or both subunits was unclear. Consequently, we examined the influence of calpain proteolysis on chaperone activity of the individual α-crystallin subunits.

The three groups tested were αA, αB, and αtotal (Fig. 36). Each group was subdivided into untreated controls (Fig. 36A); calpain-treated (Fig. 36B); and calpain-treated in the presence of inhibitory levels of E64 (Fig. 36C). All α-crystallin groups were utilized at a concentration of 88 μg/ml, and the βL-crystallin concentration for the heat denaturation assay was 668 μg/ml. The effect of calpain treatment on the α-crystallins was demonstrated by SDS-PAGE (Fig. 37). Alpha total (αt), αA, and αB (lanes 2, 5, and 8, respectively) are untreated, (lanes 3, 6, and 9) are calpain-treated, and (lanes 4, 7, and 10) are E64 inhibited calpain treated. Calpain-treatment caused limited proteolysis of αt and its subunits, αA and αB, indicating that both subunits are substrates for calpain. Addition of E64 inhibited proteolysis, indicating that the proteolysis was caused by calpain, not simply the incubation procedure.

The most efficient chaperone was untreated αA, which showed a turbidity increase of only about 160 mOD at 45 minutes (Fig. 36A). When αA was subjected to calpain treatment (Fig. 36B), the mOD was 285 at 45 minutes, demonstrating a severe loss of chaperone activity. Loss of chaperone activity was prevented by the cysteine

protease inhibitor of calpain, E64 (Fig. 36C). Visual inspection of the graph shows that calpain treatment also caused a severe loss of chaperone activity upon proteolysis of αt; E64 again prevented this loss of chaperone activity. The least efficient chaperone of all, αB, showed a smaller effect upon proteolysis by calpain. Addition of E64 actually improved chaperone activity of αB to levels slightly better than the untreated αB. The control groups in this experiment were: βL-crystallin only, αA only, αB only, and αt only. The α-groups showed negligible changes in turbidity upon heating. These data confirmed that loss of chaperone activity because of calpain was the result of proteolysis of both of the individual α-subunits. The effect on the αA subunit is the most influential in reducing chaperone activity.

Fig. 36A: Untreated αA, αB, and αt Acting as Chaperones in Protecting βL-Crystallin.

Untreated αA, αB, and αt were compared as chaperones for βL-crystallin by the standard heat aggregation assay. The error bars represent the standard deviation (n=3).

Fig. 36B: Calpain-Treated αA, αB, and αt Acting as Chaperones in Protecting βL-Crystallin.

Calpain-treated αA, αB, and αt were compared as chaperones for βL-crystallin by the standard heat aggregation assay. The error bars represent the standard deviation (n=3).

Fig. 36C: Calpain-Inhibited αA, αB, and αt Acting as Chaperones in Protecting βL-Crystallin.

Alpha A, αB, and αt were treated with calpain inhibited by E64, a cysteine protease inhibitor and used in the standard heat aggregation assay. The error bars represent the standard deviation (n=3).

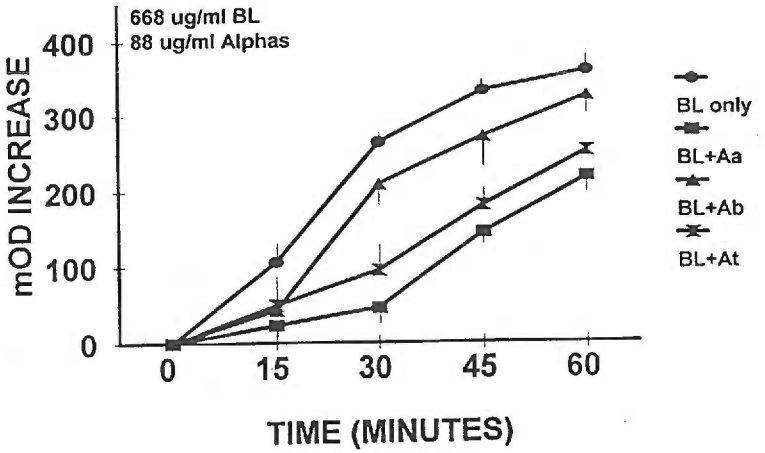
668 ug/ml BL
88 ug/ml Alphas
mOD INCREASE
400
300
200
100
0
0
15
30
45
60
TIME (MINUTES)
BL only
BL+Aa
BL+Ab
BL+At

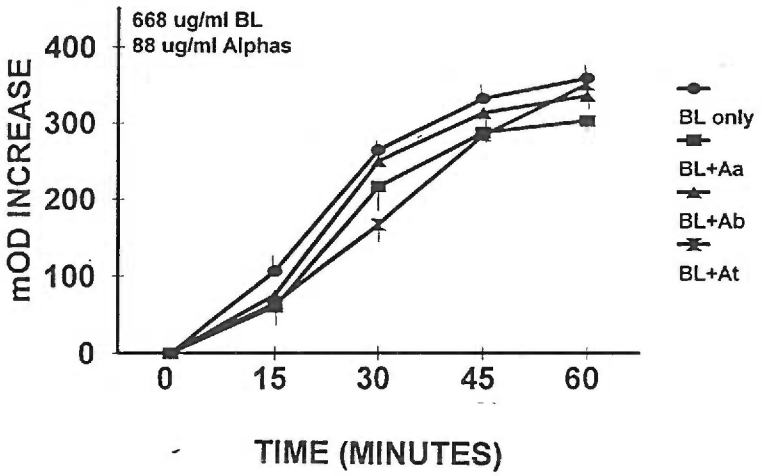
668 ug/ml BL
88 ug/ml Alphas
mOD INCREASE
400
300
200
100
0
0
15
30
45
60
TIME (MINUTES)
BL only
BL+Aa
BL+Ab
BL+At

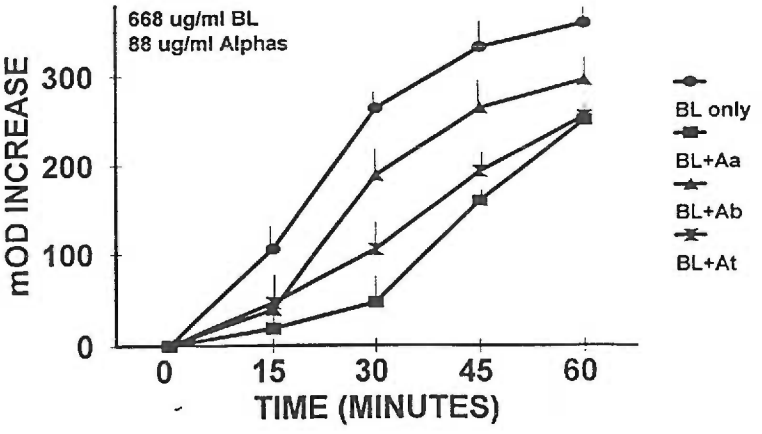
668 ug/ml BL
88 ug/ml Alphas
mOD INCREASE
300
200
100
0
0
15
30
45
60
TIME (MINUTES)
BL only
BL+Aa
BL+Ab
BL+At

Fig. 37: One-Dimensional SDS-PAGE Gel Electrophoresis of α-Crystallin Subunits that were Untreated, Calpain-Treated, Calpain-Inhibited.

Alpha total (At), alpha A (Aa), and alpha B (Ab) (Lanes 2, 5, and 8, respectively) were untreated; (Lanes 3, 6, and 9) were calpain-treated At, Aa, and Ab respectively; and (Lanes 4, 7, and 10) were E64 inhibited At, Aa, and Ab respectively. Beta-crystallins are also shown: βH-crystallin (BH), and βL-crystallin (BL).

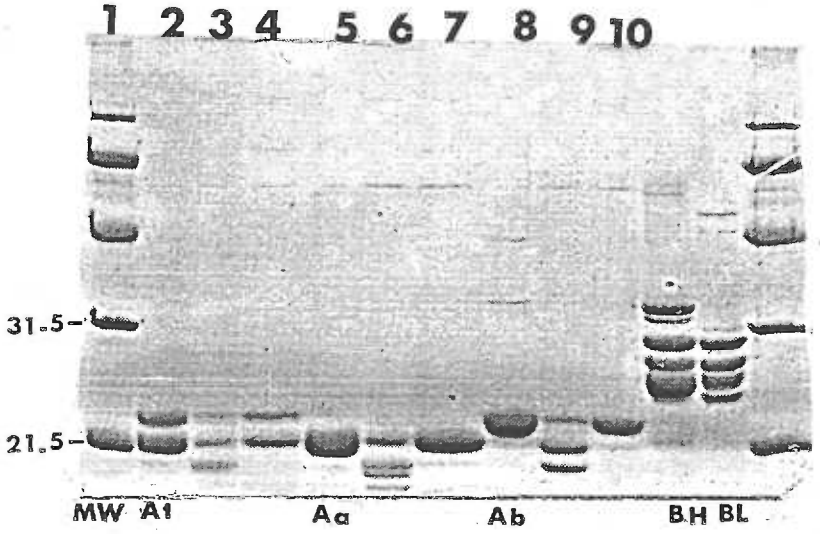
1 2 3 4 5 6 7 8 9 10
31.5
21.5
MW A1 Aα Ab BH BL

Effect of Calpain Proteolysis upon the Chaperone Activity of HMW Alpha-Crystallin.

Since α-crystallin has greater chaperone activity than HMW α-crystallin, we next tested the basis for this greater chaperone activity. Both α-crystallin and HMW α are composed of the same subunits, although the ratios of αA:αB subunits and the total number of subunits are different.

We hypothesized that HMW α-crystallin might be more easily cleaved by calpain than the normal LMW α-crystallin. The effect of calpain proteolysis on HMW α-crystallin was therefore investigated to determine if proteolyzed HMW α-crystallin protected βL-crystallin from heat denaturation differently than intact HMW α-crystallin. HMW α-crystallin from fetal calf lens was proteolyzed by calpain. The cleavage sites for calpain on the α-crystallins are known (171). Both proteolyzed and unproteolyzed HMW α-crystallin (88 μg/ml) was tested against heat denaturation of 668 ug βL-crystallin/ml at 60°C. Calpain had little effect upon the chaperone activity of HMW α-crystallin (Fig.38). The basis for this lack of effect was that calpain did not cause detectable cleavage of HMW α, as shown on the SDS-PAGE gel (Fig. 39). The controls in this experiment were HMW α-crystallin only, calpain-treated HMW α-crystallin only, and calpain-inhibited HMW α-crystallin only. None of these controls showed any precipitation, when examined under the same conditions as the experimental groups. Thus, HMW α was not a good substrate for calpain. One could speculate that the calpain proteolysis process *in vivo* may affect only native α-crystallin, not the HMW aggregate.

Fig. 38A: Effect of Calpain upon the Chaperone Activity of HMW α-Crystallin.

Untreated, calpain-treated and calpain-inhibited HMW α-crystallin were used to chaperone βL-crystallin in the standard heat aggregation assay. The error bars represent the standard deviation (n=3).

Fig. 38B: Controls for the Effect of Calpain upon the Chaperone Activity of HMW α-Crystallin.

Untreated, calpain-treated, and calpain-inhibited HMW α-crystallin controls (no βL-crystallin added to HMW) showed all of the HMW α-crystallin had low mOD. The error bars represent the standard deviation (n=3).

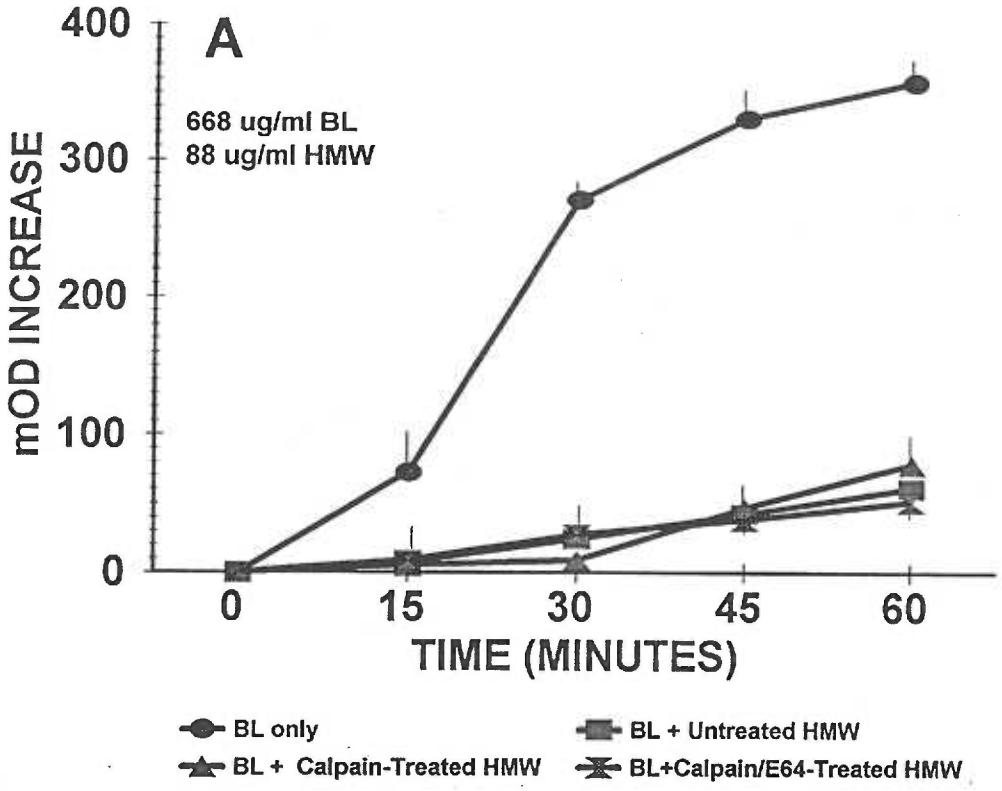
A
668 ug/ml BL
88 ug/ml HMW
mOD INCREASE
400
300
200
100
0
0
15
30
45
60
TIME (MINUTES)
BL only
BL + Untreated HMW
BL + Calpain-Treated HMW
BL+Calpain/E64-Treated HMW

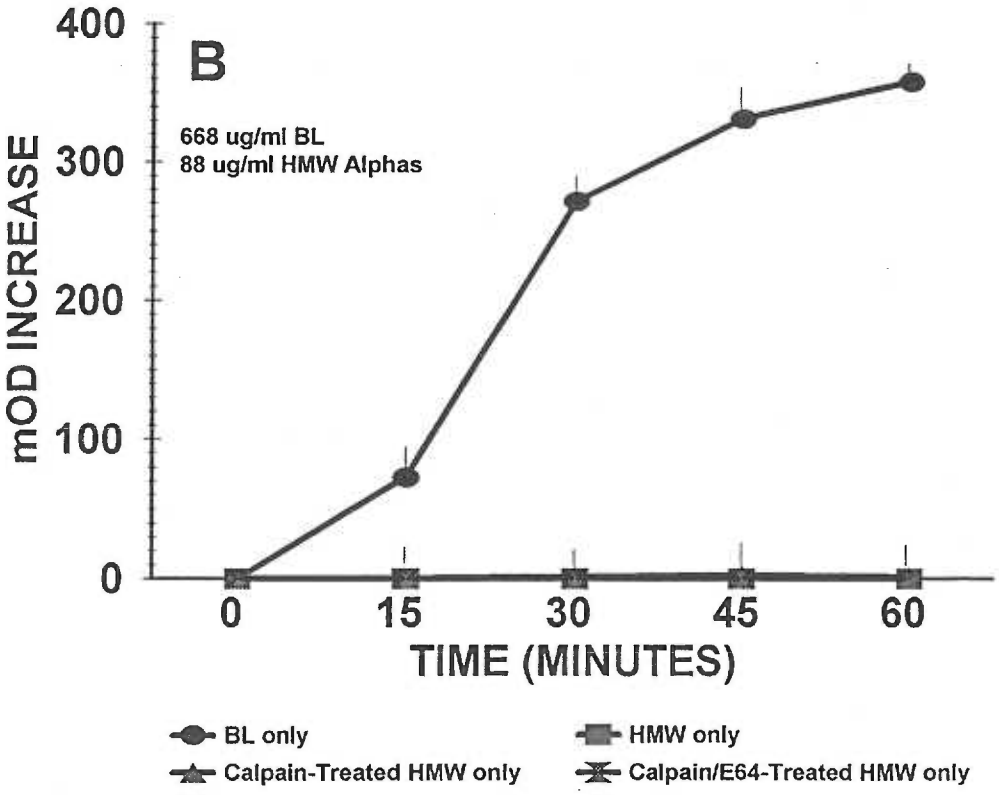
B
668 ug/ml BL
88 ug/ml HMW Alphas
mOD INCREASE
400
300
200
100
0
0
15
30
45
60
TIME (MINUTES)
BL only
HMW only
Calpain-Treated HMW only
Calpain/E64-Treated HMW only

Fig. 39: One-Dimensional SDS-PAGE Gel Electrophoresis of Untreated, Calpain-Treated, and Calpain-Inhibited HMW α-Crystallin.

SDS-PAGE gel showing low molecular weight standards, lane 1; untreated (native) α-crystallin from fetal calf lens, composed of an upper αB band and a lower αA band at 21 kDa, lane 2; calpain-treated HMW α-crystallin shows no proteolysis, lane 3; and calpain-inhibited HMW α-crystallin shows no change; lane 4.

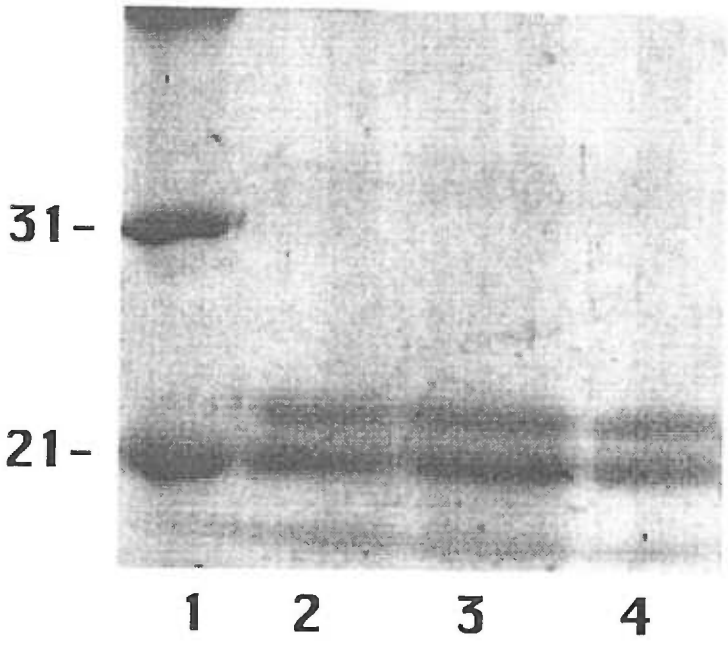
31-
21-
1
2
3
4

BSA as a Chaperone.

The purpose of this experiment was to determine if the chaperone activity of α-crystallin is unique, or would any protein show chaperone activity against βL-crystallin heat denaturation. BSA was tested to determine if it prevented heat denaturation of βL-crystallin (Fig. 40). Bovine α-crystallin from fetal lens cortex was incubated with βL-crystallin at 64° C for 120 minutes and compared with 5, 25, 50, 75, and 100 μg BSA/ml incubated with 200 μg βL-crystallin /ml. The control groups were: 75 μg α-crystallin/ml only, 75 μg BSA/ml only, and 200 μg βL-crystallin/ml only, incubated under the same conditions. BSA did not function as a chaperone at any of the concentrations of BSA used. In contrast, addition of 75 μg α-crystallin/ml totally prevented βL-crystallin precipitation. The results of this control experiment suggest that α-crystallin is a specific chaperone protein. This experiment adds justification to the preceding experiments and supports dual functions for α-crystallin in the lens, where it is a major structural protein as well as a chaperone protein.

Fig. 40: BSA as a Chaperone.

BSA was tested to determine if it prevented heat denaturation of βL-crystallin from fetal calf lens in the standard heat aggregation assay. The error bars represent the standard deviation (n=3).

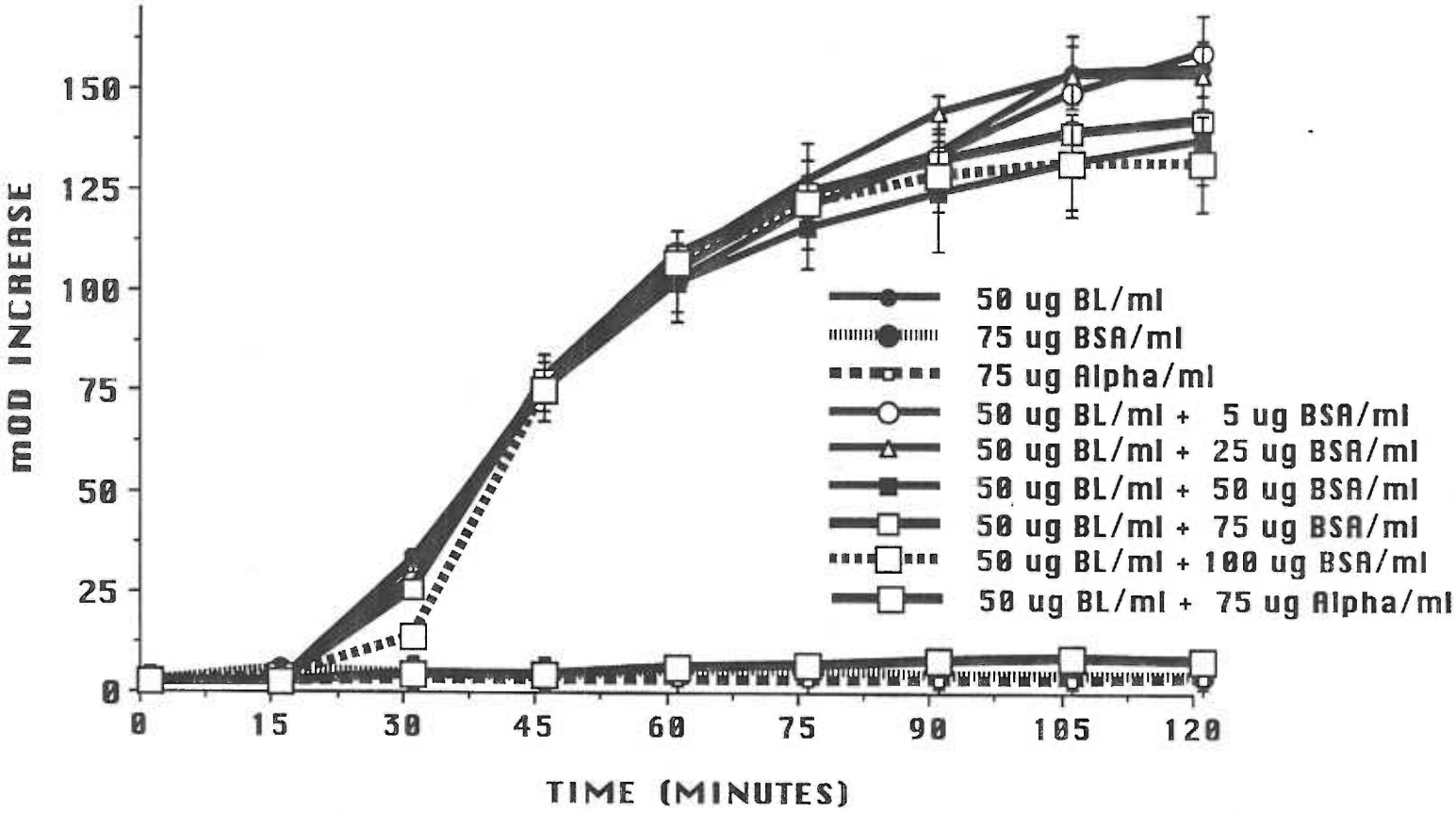
mOD INCREASE
150
125
100
75
50
25
0
0
15
30
45
60
75
90
105
120
TIME (MINUTES)
50 ug BL/ml
75 ug BSA/ml
75 ug Alpha/ml
50 ug BL/ml + 5 ug BSA/ml
50 ug BL/ml + 25 ug BSA/ml
50 ug BL/ml + 50 ug BSA/ml
50 ug BL/ml + 75 ug BSA/ml
50 ug BL/ml + 100 ug BSA/ml
50 ug BL/ml + 75 ug Alpha/ml

DISCUSSION

Major Findings of These Studies.

The working hypothesis tested is that α-crystallin stabilizes and prevents precipitation of β-crystallin in the lens, and thereby prevents cataract. Several pieces of information obtained support the hypothesis. First, when α-crystallin was incubated with calpain II *in vitro*, the C-terminus was lost and chaperone activity was reduced. Second, the chaperone activity of α-crystallin from selenite cataract was diminished *in vivo,* probably by action of calpain on α-crystallin. This is the first evidence that chaperone function is diminished in a cataract model, and the data implicate a specific enzyme found in the lens, calpain II, as causing removal of the C-terminus of α-crystallin. Our *in vitro* data demonstrate that intact α-crystallin, cleaved by calpain II, was proteolyzed in a manner similar to that of *in vivo* α-crystallin isolated from the lens of animals with selenite nuclear cataract. Consequently, a better understanding of selenite cataract formation and of the role of α-crystallins as chaperones in this process has been obtained.

Other new supporting data provided by these studies defined the interactions between α-and β-crystallins. In the absence of α-crystallin, βH-crystallins precipitated more readily than do βL-crystallins, when exposed to heat. More α-crystallin was required to prevent heat-induced protein precipitation of βH-crystallins than of βL-crystallins. Two-dimensional gel analysis showed that precipitates of heated βH-crystallin contained an increased proportion of subunits βB1a and βB1b, while precipitates of heated βL-crystallin contained an increased proportion of βB2 and βB3.

We also studied the interaction between α- and β-crystallins. Preheating α-crystallin reduced its ability to serve as a chaperone of βL-crystallin. Comparisons between HMW and LMW α-crystallins show that LMW α-crystallins are more efficient chaperones. Alpha-crystallin subunit studies exhibited a concentration dependence for optimal chaperone activity, with αA serving as the most efficient chaperone at higher concentrations, and native intact αt serving as the efficient chaperone at lower concentrations. The optimum subunit ratio of α-crystallins for chaperone activity with βL-crystallin was found to be 2:1 (αA:αB). The αA chaperone activity was most severely decreased by calpain proteolysis. Calpain did not cleave HMW α-crystallin and had little effect upon chaperone activity. Alpha-crystallin was shown to act as a chaperone against heat denaturation of γ-crystallins. In the lens of the eye, crystallin proteins must resist the photooxidative, chemical and physical insults that disrupt and denature proteins. Since some lens crystallins are synthesized before birth and persist without protein turnover throughout the lifetime of the individual, possibly some 70-100 years, it follows that stability must be a key feature in these proteins' repertoire. Our studies have helped to clarify how α-crystallin may assist in preserving the stability of lens crystallins.

Relation of These Studies To Previous Work.

Factors Affecting Stability of Proteins.

Factors which determine the half-life of a protein and intracellular turnover rate are: size; surface charge; hydrophobicity; the oxidation state of histidine, cystine, and methionine; the aggregation state of multimeric systems; the presence of blocked amino

acid terminals; and the presence or absence of PEST sequences (areas rich in proline (P), glutamic acid (E), serine (S), and threonine (T) (13,134). The consequence of reduced stability is the denaturation or degradation of the protein, as occurs during aging or cataract (63,64,134a).

Denaturation, Degradation of Lens Proteins and Aging.

There are numerous reports in the literature associating the processes listed above with aging. For example, the nuclear region of the adult bovine lens contains degraded polypeptides, suggesting that a specific, limited degradation of α-crystallin subunits increases with age (158). Increased high molecular weight aggregates are also associated with aging (141) and the highest concentration of degraded polypeptides are found in these aggregates (13). Cleavage products of α- and γ-crystallins have been detected in HMW protein aggregates in cataractous human lenses (132). Many factors may be involved in degradation and denaturation of lens proteins. During aging, the crystallins undergo extensive post-translational changes, such as super-aggregation, deamidation, C-terminal degradation, insolublization, and formation of disulfide and non-disulfide cross-links (63). Another common intracellular cause of degradation and denaturation of lens crystallins is proteolysis (134a).

Proteolysis of Lens Crystallins.

During cataractogenesis, definite proteolysis has been observed with marked loss of lens proteins as well as a corresponding increase in free amino acids (10). Most of the soluble proteins of the lens are crystallins, which exist at extremely high concentrations (30%) and which play important structural roles in the lens. Proteolysis

can thus have severely deleterious effects on transparency of the lens. Proteolysis of crystallins may change the tertiary structure of the molecule so that more hydrophobic areas are exposed. These hydrophobic areas are subject to interaction with hydrophobic areas of other similarly unfolded proteins, causing aggregation (67). Aggregation and subsequent precipitation of proteolyzed crystallins eventually leads to opacification of the lens (78,147).

Chaperone Activity of Rat Lens α-crystallins from Selenite Cataract.

Previous work has shown that α-crystallin chaperone activity diminishes upon aging of bovine lenses (79). In the current investigations, opacities appearing in lenses from young rats with selenite cataract showed a more rapid loss of chaperone activity. Five days after an injection of selenite, the lens nucleus showed both opacity and loss of α-crystallin chaperone activity. In contrast, the chaperone activity of α-crystallins from the clear cortex of lenses from rats injected with selenite was only slightly reduced. The significance of this finding is that α-crystallin is implicated directly as an important factor in maintaining lens clarity. Opacification of the lens triggered by selenite was correlated with improper functioning of α-crystallin, demonstrating the crucial role of α-crystallin in the lens.

Chaperone Activity of α-crystallin Incubated with Calpain II.

Former investigations have examined the C-terminal end of α-crystallin in regard to proteolysis and chaperone activity. Yoshida et al.(171) found that calpain II caused limited degradation of bovine α-crystallins by cleaving αA on the carboxyl side of residues 162 and 163, and αB on the carboxyl side of residues 163 and 170. In a

separate study, removal of 16 and 12 residues from the C-terminus of αA and αB, respectively, by limited trypsin digestion caused loss of chaperone activity (147). Since αA is 173 amino acids, and αB is 175 amino acids in length, this suggested that the proteolytic cleavage of only a few residues at the C-terminus of αA and αB would decrease chaperone activity. However, trypsin is not a major lens proteinase *in vivo*. Calpain is a major lens proteinase.

Several pieces of evidence from the present investigation support the hypothesis that calpain II is responsible for α-crystallin proteolysis and the loss of chaperone activity in selenite cataract. First, incubation of intact α-crystallin with calpain markedly reduced chaperone function; the addition of E64, a calpain inhibitor, blocked this effect (Fig. 4B). Second, the pattern of fragmentation from limited proteolysis of α-crystallins isolated from *in vivo* selenite cataract was similar to that produced by incubation of calpain with α-crystallin *in vitro*. In both cases, the proteolysis was characterized by decreases in intact αA and αB crystallin polypeptides, and appearance of three fragments of αA, and one fragment of αB that migrated similarly during parallel two-dimensional gel electrophoresis (Fig. 5). Calpain appears to decrease chaperone activity in a manner similar to that occurring with aging, by removal of a portion of the C-terminus of α-crystallins (54,145). The three partially degraded αA and one partially degraded αB fragments remained N-terminally blocked following calpain proteolysis. To obtain fragments of these sizes, a 1-2 kDa decrease in molecular weight must have occurred by removal of a portion of the C-terminus.

The reason why removal of such a limited number of residues causes loss of

chaperone function is unknown. It is possible that removal of the C-terminus decreases chaperone activity by destabilizing α-crystallin aggregates. Alternatively, the C-terminus may be directly involved in the interaction of α-crystallins with destabilized or unfolded β-crystallins. A recently proposed model of α-crystallin may explain how destabilization of α-crystallin aggregates affects the chaperone activity (161). A micellar subunit assembly has been proposed as the quaternary structure of α-crystallin. The proposed model has a three-layer structure in which the inner layer is a micelle containing 12 αA subunits. Structural stability is provided by an apolar region directed inward and constituting a hydrophobic core. An intermediate layer with a structure similar to the first layer, is composed of six subunits with an apolar face directed toward the hydrophobic core. These two layers form a micellar-type structure with hydrophobic areas on the inside. A third layer adds more subunits and can accommodate 24 αA or αB in a cuboctahedron-type symmetrical structure. This three-layered structure has been proposed to be the 800 kDa fraction of α-crystallin and is unstable. Heating the three-layered structure separates the outer layer from the two inner micellar-type layers. The resulting two inner-layered structure is thought to be the 300 kDa fraction of α-crystallin, which is quite stable and resistant to heat (161).

Previous studies (62) using electron microscopy have shown that partially denatured crystallins bind to α-crystallins in the inner core. Truncation of the C-terminus of α-crystallins, as observed in the current *in vitro* and *in vivo* studies, may prevent interaction with the β-crystallins. Truncation of αA, which constitutes the inner micelle, may be especially deleterious to chaperone function. In the current studies,

calpain was found to truncate α-crystallin with a concomitant loss of chaperone activity. The data from the present animal studies provides a rationale for studies of human cataract formation.

Insolubilization with Heat.

In addition to the cleavage of α-crystallin, the destabilization of β-crystallins may be a determining factor contributing to cataract formation. Several studies have suggested that destabilization or unfolding of the β-crystallins is critical in formation of aggregates in the lens (73). A destabilized or unfolded β-crystallin is more susceptible to interaction and aggregation with other unfolded crystallins. Aggregated β-crystallins become insoluble in the lens and precipitate; these are long-recognized characteristics of aging and cataract (63,65). Recent improvements in measurements of water-insoluble crystallins by physicochemical methods have made it possible to show that insolubilization involves a partial unfolding and exposure of the internal hydrophobic groups resulting in a greater exposure of tryptophan residues to solvent. The conformational changes in these proteins result in a higher index of refraction than in soluble proteins; therefore the amount of light scattered is increased (13,102). Since partially denatured β-crystallins are implicated in cataract formation (127), we conducted insolubilization studies of β-crystallins with and without α-crystallin.

In the studies of βH-crystallin insolubilization, heat treatment precipitated approximately 29% of the total protein. Insolubilization of βL-crystallin following heat-treatment showed that only 12% precipitated. This indicated a difference in the susceptibility of β-crystallin to heat insolubilization. Addition of a small amount of α-

crystallin, in a ratio of 1:3 (α:β), was enough to totally prevent βL-crystallin precipitation; however, a 1:1 (α:β) ratio was needed to protect βH-crystallin from heat-induced aggregation. Therefore, βL-crystallin was more heat-tolerant than βH-crystallin, since more of the protein remained in the supernatant after heating. Furthermore, less α-crystallin was required as a chaperone to prevent precipitation of βL-crystallin, than of βH-crystallin. The amount of α-crystallin required to act as a chaperone may influence the amount of βH- or βL-crystallin that precipitates. These data imply that a shortage of intact α-crystallin favors precipitation of βH-crystallin more than of βL-crystallin. Pertinent to this, βH-crystallin is preferentially lost in selenite cataract (37). These differences are of significance because they suggest that heat stability and interaction with α-crystallin chaperone are related to specific polypeptides within the βH- and βL-crystallin aggregates.

Precipitation of β-crystallin subunits.

The previous experiments showed that more βH-crystallin precipitated with heat than βL-crystallin; this precipitation was diminished by the addition of α-crystallin. The two-dimensional gels showed that βB1a and βB1b were predominantly heat-precipitated from the βH-crystallin. For βL-crystallin, the βB2 and βB3 subunits were predominantly heat-precipitated. This differential precipitation is both marked and intriguing. The difference between the subunits is that βH-crystallin contains βB1a and βB1b, while βL-crystallin does not. Densitometric analysis of the 2-D gels reconfirmed the visual inspection by showing that heat preferentially precipitates βB2 and βB3 from βL-crystallin and BB1a and BB1b from βH-crystallin.

Preheating Alpha-Crystallin.

Previous studies have indicated that α-crystallin binds to partially denatured crystallins (62,127). However, it is not known if α-crystallin must be partially unfolded to act as a chaperone. Thus, we determined whether α-crystallin chaperone activity was influenced by preheating before it interacted with βL-crystallin. The results showed that progressively increasing the preheating time caused a dimunition of chaperone capability with βL-crystallin. Thus, extensive unfolding of α-crystallin by heating may have been responsible for this loss of chaperone activity.. It also indicates that the native tertiary, or perhaps more importantly the quaternary structure, of α-crystallin is critical for chaperone activity.

The function of α-crystallin in the eye, other than as a structural protein, is to interact with and prevent aggregation of the β-crystallins. Thus, α-crystallin aids in maintaining the structural integrity of the eye and visual transparency (142). The heat-damaged or partially degraded α-crystallin may still function as a chaperone, but with reduced efficacy. The implications of this for an individual with damage to α-crystallin are that changes in lens transparency, such as opacification, may occur sooner in life.

Concentration of Alpha-Crystallin Subunits in Chaperone Activity.

Another factor influencing the chaperone activity and the stability of α-crystallin is the concentrations of the individual αA and αB subunits. The separation of α-crystallin subunits was performed to determine whether either or both of the subunits were the functional chaperone for βL-crystallin. Another possibility explored was that the α-crystallin subunits acted only as a chaperone when present together. Urea was

used to separate the α-crystallin subunits. In terms of possible quaternary structure, urea may act the same way as heat in the micellar model of α-crystallin. The outer layer may dissociate from the two inner layers, thereby converting α-crystallin to the smaller, more thermodynamically stable, 300 kDa structure. In this smaller α-crystallin form, heat- as well as urea-induced denaturation is reversible (16,64). After separation of the subunits by urea (6 M) treatment, both rat and bovine α-crystallins should be monomeric. These separated subunits showed differences in the chaperone capability from native intact α-crystallin. In the rat, at 50 μg/ml of α-crystallin, αA was a more effective chaperone than αB. Native intact α-crystallin, αt, exhibits chaperone activity between αA and αB, although it is nearly as effective as αA. This is consistent with the fact that native α-crystallin, αt, is composed of a 2:1 ratio of αA:αB (106). At low concentrations of rat α-crystallin (15 and 25 μg/ml), αt was the most efficient chaperone, and αA and αB were equally ineffective.

Although the urea was easily removed by dialysis, the α-crystallin may not have renatured to the original putative three-layered, micellar quaternary structure. With the dissolution of the original quaternary structure, hydrophobic sites may be exposed which are available to bind unfolded βL-crystallin. Preliminary studies of α-crystallin demonstrated that after incubation in urea (with subsequent extensive dialysis), α-crystallin retained chaperone activity. In fact, it was a slightly more efficient chaperone than α-crystallin that was untreated with urea. Milder urea treatment has been shown (64,154,161) to dissociate the outer layer from the inner layers in trimers, which rapidly formed a similar two-layered structure. However, the pure subunit preparations may

well form other structures. Alpha-A may form the two-layer structure, with hydrophobic surfaces exposed, and so be able to act as a chaperone in a slightly more effective manner. Alpha-B, however, is not found on the inner layer and, upon dissociation to trimers, may or may not form a two-layer structure. What this would resemble in terms of hydrophobic interactions is unclear. The general inability of αB to serve as an effective chaperone in these studies, suggests that either it does not form a comparable structure or if it does form, that it is an ineffective structure.

Mammalian crystallins have unusual interactive properties, especially at high concentrations (95). Crystallin proteins begin general interactions with other proteins at a concentration of about 17%, while most proteins begin such intermolecular interactions at a concentration of 30% (95). The 15 μg α-crystallin/ml solution with βL-crystallin was 18%, a rather dilute solution for interaction, even for crystallins. Concentration differences displayed by α-crystallin may be a function of the total protein in the solution, but also may be related to more specific βL-crystallin interactions. βL-crystallin is an aggregate that interacts differently in different concentrations, possibly because of its unusual shape. Koenig et al. (95) investigated interactive properties of βL-crystallin by NMR at low, medium, and high concentrations to characterize interprotein interactions. βL-crystallin appears to resemble a barbell, with globular protein heads on each end connected in the middle by a long arm. It is not as compact as many proteins. One disadvantage of a less compact structure in solute is that the usual repulsive intermolecular interactions become larger at lower total protein concentration.

Optimum Ratios of Alpha-Crystallin Subunits.

Another important factor influencing chaperone activity is the overall ratio of αA to αB. There are several known combinations of native α-crystallin subunits *in vivo*. A previous study of purified αA and αB subunits of bovine α-crystallin *in vitro* presented evidence that at a ratio of lower than 2:1 (αA:αB), an abnormal aggregate termed α-neoprotein, was formed (13,106). This protein was different from native α-crystallin in quaternary structure, a property that led to its identification in lenses *in vivo* (106). Although it is not in the lenses of young rats or calves, it is found in the adult of both species. To mimic the α-neoprotein of α-crystallin, therefore, α-crystallin subunits from the lenses of young rats and calves were used herein to determine if the "pseudo-α-neoprotein" would act to chaperone βL-crystallin in the standard heat aggregation assay.

The most efficient ratio of αA and αB for chaperone activity for calf α-crystallin, was 2:1 (αA:αB). A 1:1 ratio, equivalent to the neoprotein, exhibited low chaperone activity. The 1:2 (αA:αB) ratio, was equally competent to the 2:1 (αA:αB) ratio as a chaperone. Thus, the ratio that occurs in native α-crystallin (2:1) acted as the most efficient chaperone *in vitro*. The 1:1 ratio, the "pseudo-neoprotein", was the least efficient chaperone. The significance of these experiments is that several combinations of αA and αB possess chaperone capability. However, the 2:1 (αA:αB) ratio found *in vivo* is the most common ratio, as well as the most efficient.

HMW α-Crystallin is a Less Efficient Chaperone.

HMW α-crystallin increases with age, and this increase has been associated with cataractogenesis (140,141). SDS-PAGE shows that the molecular weights of the

individual α-crystallin subunits remain the same; therefore, formation of HMW species must occur by noncovalent association of α- or α- plus other crystallins (17). To determine if HMW α would serve as a chaperone of βL-crystallin, its chaperone activity was compared with that of LMW α-crystallin. Both LMW and HMW α-crystallin are composed of αA and αB subunits. LMW has a MW of 300-800,000, while HMW has a MW of about 1 million. It was determined that partially denatured β-and γ-crystallins are found in the core of the HMW α-crystallin (62,127). Whether the HMW α-crystallin aggregate binds more βL-crystallin or if it prevents proper binding of βL-crystallin is unknown. Our studies show that HMW α-crystallin is not as efficient a chaperone for βL-crystallin as LMW α-crystallin. HMW α-crystallin was an equally competent chaperone initially during heat denaturation, but HMW α began losing chaperone activity before LMW α-crystallin.

The composition of HMW α-crystallin may explain this observation. HMW α-crystallin is composed of 1:2 (αA:αB) chains (12,63), while LMW α-crystallin is composed of 2:1 (αA:αB) ratios. Although in our earlier subunit ratio studies, 1:2 (αA:αB) was as effective as 2:1 (αA:βB), the reconstituted 1:2 structure may not be identical to the HMW α-crystallin aggregate.

Proteolysis of α-crystallin Subunits.

The chaperone activity of α-crystallin was diminished by calpain-treatment (92). Therefore, which subunit, αA or αB, was critical to α-crystallin chaperone activity was determined. The most effective chaperone at this concentration (88 ug/ml), αA, was the most adversely affected by calpain, and proteolysis was apparent on the gel. Alpha-B

crystallin also showed extensive proteolysis on the gel, but the chaperone activity was not significantly diminished. However, it was an ineffective chaperone initially. Alpha-total crystallin was rather severely diminished as a chaperone, as has been discussed previously (92). Thus αA is the most important of the subunits in terms of chaperone activity of native α-crystallin.

The αA and αB have sequences that are very similar in length and molecular weight, with approximately 60% amino acid sequence homology. Yoshida, et.al. (171) showed that calpain catalyzed a limited proteolysis of αA and αB chains *in vitro*. The sites of cleavage, on the C-terminal of both subunits were: 1) for the chain (Arg163-Glu164) and (Ser162-Arg163) and 2) for the αB chain (Arg163-Glu164) and (Thr170-Ala171). Our 1-dimensional gel of αA, αB, and αt-crystallins subjected to calpain showed proteolysis of all chains, but each showed a different pattern. However, while Yoshida's work states that calpain cleaves both subunits, and our one-dimensional gel of these crystallins subjected to calpain agrees with Yoshida, the minimal efficacy of αB as a chaperone limits our interpretation. Although, the differences in the C-terminal sequences of αA and αB may be central to the difference in their chaperone efficacy, this can not be definitively concluded from our data. Other portions of these two subunits may be critical to chaperone activity. An intact C-terminus is necessary for α-crystallin chaperone activity (92), but may not be sufficient by itself.

Proteolysis of HMW α-Crystallin.

LMW α-crystallin was a more efficient chaperone than HMW α-crystallin. The reason for this difference is unclear, since α-crystallin subunits are the basis for both

chaperones. Since the effect of calpain on LMW α-crystallin was previously examined with regard to chaperone activity, it was of interest to know if calpain inactivated HMW α-crystallin.

Calpain-treated bovine HMW α-crystallin shows no evidence of cleavage on an SDS-PAGE gel. Similarly, calpain-treated HMW α-crystallin shows nearly identical chaperone activity to HMW α-crystallin that has not been treated. This raises interesting speculation about the structural differences of HMW α-crystallins and LMW α-crystallins *in vivo*. The HMW α-crystallin is composed of α-crystallin subunits and therefore should be subject to proteolysis by calpain, unless the C-terminal ends (where calpain cleaves) are buried or otherwise protected from cleavage.

BSA as a Chaperone.

BSA was used as a control protein to examine the possibility that any protein could act as a chaperone of β-crystallin. BSA, in a wide range of concentrations generally used in incubating α-crystallin with βL-crystallin, showed no chaperone activity with βL-crystallin. Thus, the chaperone activity of α-crystallin is not a general property of all proteins.

SUMMARY

In summary, we have determined *in vitro* that incubation of α-crystallin with calpain II causes the C-terminal to be cleaved, and this cleavage was directly correlated with reduced chaperone activity. Subsequently, we implicated the lens enzyme calpain II as responsible for proteolysis of α-crystallin *in vivo* in an animal model of cataract. Alpha-crystallin from selenite nuclear cataract was proteolyzed and exhibited a reduced chaperone activity. We have established the first evidence of a specific enzyme involved in diminishing chaperone activity in a model of cataract.

In addition, we examined relationships between two of the crystallins, α and β. A differential response to heat was found with β-crystallins, with βH- precipitating more readily than βL-crystallin. The basis for this was found to be the precipitation of two subunits, βB1a and βB1b. A biochemically intriguing sidelight is that βB1 is a very good substrate for calpain, which under *in vivo* conditions could cause precipitation of βB1 in the lens. Alpha-crystallin was a more efficient chaperone for βL- than for βH-crystallin. We noted a possible relationship between βB1 and βB2 and βB3. When βB1 was not present, as in βL-crystallin, βB2 and βB3 were more likely to precipitate when exposed to heat stress.

Further factors were investigated in the maintenance of α-crystallin chaperone activity. Preheating reduced the ability of α-crystallin to serve as a chaperone. The low molecular weight α-crystallin form was a more efficient chaperone, particularly over extended time periods, than was the high molecular weight form. This may be pertinent since the proportion of α-crystallins in the HMW form increases with aging. However,

this could also serve a protective function, since HMW α-crystallin is less susceptible to calpain action.

When the subunits of α-crystallin were studied separately in terms of their chaperone activity, αA was more efficient overall than unfractionated α-crystallin, which was more efficient than αB. Intriguingly, at concentrations far below physiological levels, this order changed with αA becoming less effective as a chaperone. Calpain proteolyzed both of the individual subunits as well as the unfractionated α-crystallin. The chaperone activity was diminished by this proteolysis, with the most dramatic loss occurring for αA. The most effective αA to αB ratio was 2 to 1, which is the physiologic ratio of the LMW or predominant native form, and the 1 to 1 ratio of the "neo-protein" was least effective as a chaperone.

We have proved our hypothesis and shown that the chaperone activity of α-crystallin is a critical feature in the maintenance of normal lens clarity. Mechanisms of crystallin aggregation and precipitation resulting from compromised chaperone activity of α-crystallin are central to the formation of cataract. Since future treatments to ameliorate this phenomenon have the potential for significant humanitarian impact, a molecular understanding of the *in vivo* mechanism of a cataract model is of considerable biomedical importance.

REFERENCES:

1. Alcala J, Lieska N, Maisel H (1975) Exp Eye Res 21, 581-95.
2. Alcala J, Maisel H (1985) in *The Ocular Lens: Structure, Function, and Pathology.* (Maisel H, ed) Marcel Dekker, New York, pp. 169-222.
3. Andria G, Taniuchi H (1978) J Biol Chem 253, 2262-70.
4. Anfinsen CB (1973) Science 181, 223-30.
5. Anfinsen CB, Haber E, Sela M, White FH (1961) Proc Natl Acad Sci 47, 1309-14.
6. Aoyama A, Frohli E, Schafer R, Klemenz R (1993) Mol Cell Biol 13, 1824-35.
7. Azuma M, Shearer TR, Matsumoto T, David LL, Murachi T (1990) Exp Eye Res 51, 393-401.
8. Azuma M, Shearer T (1992) FEBS Lett 307, 313-317.
9. Baker D, Sohl JL, Agard DA (1992) Nature 356, 263-5.
10. Barber GW (1973) Exp Eye Res 16, 84-91.
11. Becker J, Craig EA (1994) Eur J Biochem 219, 11-23.
12. Benedek GB (1971) Appl Optics 10, 459-73.
13. Berman ER (1991) *Biochemistry of the Eye.* Plenum Press, New York.
14. Bhat SP, Nagineni CN, Horwitz J (1988) Invest Ophthalmol Vis Sci (Suppl) 29, 426.
15. Bhat SP, Magineni CN (1989) Biochem Biophys Res Commun 158, 319-25.
16. Bindels JG, Siezen RJ, Hoenders HJ (1979) Ophahalmol Res 11, 441-2.

17. Bloemendal H (ed) (1981) *Molecular and Cellular Biology of the Eye Lens.* Wiley & Sons, NY.

18. Bloemendal H, Vermorken AJM, Kibbelaar M, Dunia I, Benedetti EL (1977) Exp Eye Res 24, 413-5.

19. Blond S, Goldberg M (1987) Proc Natl Acad Sci 84, 1147-51.

20. Blundell T, Lindley P, Miller L, Moss D (1981) Nature 289, 771-7.

21. Boyle D, Takemoto L (1994) Exp Eye Res 58, 9-16.

22. Boyle D, Gopalakrishnan S, Takemoto L (1993) Biochem Biophys Res Commun 192, 1147-54.

23. Brakenhoff RH, Guests von Kessel AH, Oldenburg M (1990) Hum Genet 85, 237-40.

24. Broekhuyse RM, Kuhlmann ED (1974) Exp Eye Res 19, 297-302.

25. Bryan P (1992) Biochemistry 31, 4937-47.

26. Cheng MY, Hartl F-U, Martin J, Pollock RA, Kalousek F (1989) Nature 337, 620-5.

27. Chiesa R, McDermott MJ, Spector A (1989) Curr Eye Res 8, 151-8.

28. Christensen H, Pain RH (1991) Eur Biophys J 19, 221-9.

29. Cohen AI (1965) Invest Ophthalmol 4, 433.

30. Cohen LH, Westerhuis LW, DeJong WW, Bloemendal H (1978) Eur J Biochem 89, 259-66.

31. Cotlier E (1981) in *Alder's Physiology of the Eye* (Moses RA, ed) CV Mosby, St Louis, Mo, pp. 284-285.

32. Creighton TE (1990) Biochem J 270, 1-16.

33. Creighton TE (1991) Curr Biol 1, 8-10.

34. David LL, Shearer TR (1984) Invest Ophthalmol Vis Sci 25, 1275-1283.

35. David LL, Shearer TR (1986) Exp Eye Res 42, 227-238.

36. David LL, Shearer TR (1993) FEBS Lett 324, 265-70.

37. David LL, Shearer TR, Shih M (1992) J Biol Chem 268, 1937-1940.

38. David LL, Varnum MD, Lampi KJ, Shearer TR (1989) Invest Ophthalmol Vis Sci 30, 269-73.

39. David LL, Wright JW, Shearer TR (1992) Biochim Biophys Acta 1139, 210-216.

40. DeJong WW (1981) in *Molecular and Cellular Biology of the Lens.* (Bloemendal H, ed) Wiley & Sons, New York, pp.221-78.

41 DeJong WW, van Kleef FSM, Bloemendal H (1974) Eur J Biochem 48, 271-6.

42. DeJong WW, Leunissen JAM, Leenen PJM, Zweers A, Versteeg M (1988) J Biol Chem 263, 5141-5149.

43. DeJong WW, Leunissen JAM, Voorter CEM (1993) Mol Biol Evol 10, 103-26.

44. DeJong W, Van Der Ouderaa FJ, Versteeg M, Groenewoud G, Van Amelsvoort M, Bloemendal H (1975) Eur J Biochem 53, 237-242.

45. Delaye M, Tardieu A (1983) Nature 302, 415-7.

46. Dobson CM (1992) Curr Opin Struct Biol 2, 343-5.

47. Dobson CM, Evans PA, Radford SE (1994) TIBS 19, 31-7.

48. Driessen HPC, Herbrink P, Bloemendal H, DeJong W (1980) Exp Eye Res 31, 243-6.

49. Dubin RA, Wawrousek EF, Piatigorsky J (1989) Mol Cell Biol 9, 1083-91.

50. Eder J, Rheinnecker M, Fersht A (1993) Biochemistry 32, 18-26.

51. Ellis RJ (1987) Nature 328, 378-9.

52. Ellis RJ (1990) Science 250, 954-9.

53. Ellis RJ, van der Vies SM (1991) Annu Rev Biochem 60, 321-47.

54. Emmons T, Takemoto L (1992) Exp Eye Res 55, 551-554.

55. Fischer G, Schmid FX (1990) Biochemistry 29, 2205-12.

56. Fisher RF, Wakely J (1976) Trans Ophthalmol Soc UK 96, 278.

57. Flanagan JM, Kataoka M, Sortie D, Engelman DM (1991) Proc Natl Acad Sci 89, 748-52.

58. Freedman RB (1992) in *Protein Folding* (Creighton TE, ed), Freeman, New York, pp. 455-539.

59. Garland D, Zigler JS Jr, Kinoshita J (1986) Arch Biochem Biophys 251, 771-6.

60. Gething M-J, Sambrook J (1992) Nature 355, 33-45.

61. Georgopoulos C (1992) TIBS 17, 295-9.

62. Gopalakrishnan S, Boyle D, Takemoto L (1994) Invest Ophthalmol Vis Sci 35, 382-7.

63. Harding J (1981) in *Molecular and Cellular Biology of the Eye Lens* (Gloemendal H, ed) Wiley & Sons, NY, pp. 327-65.

64. Harding J (1991) *Cataract: Biochemistry, Epidemiology, and Pharmacology.* Chapman and Hall, London.

65. Harding JJ, Crabbe MJC (1984) in *The Eye* (Davson H, ed), 3rd ed, Acad Press,

Orlando, FL, pp. 207-492.

66. Harding JJ, Dilley KJ (1976) Exp Eye Res 22, 1-73.

67. Hartl F-U, Hlodan R, Langer T (1994) TIBS 19, 20-5.

68. Hartl F-U, Martin J, Neupert W (1992) Annu Rev Biophys Biomol Struct 21, 293-322.

69. Hartl F-U, Neupert W (1990) Science 247, 930-8.

70. Haynie DT, Freire E (1993) Proteins 16, 115-40.

71. Head MW, Goldman JE (1993) Invest Ophthalmol Vis Sci Suppl 34, 1340.

72. Hemmingsen SM, Woolford C, van der Vies SM, Tilly K, Dennis DT (1988) Nature 333, 330-4.

73. Hendrick JP, Hartl F-U (1993) Annu Rev Biochem 62, 349-84.

74. Hendriks W, Leunissen J, Nevo E, Bloemendal H, DeJong WW (1987) Proc Natl Acad Sci 84, 5320-4.

75. Hendrix RW (1979) J Mol Biol 129, 375-92.

76. Horwich AL, Neupert W, Hartl F-U (1990) Trends Biotechnol 8, 126-31.

77. Horwitz J (1992) Proc Natl Acad Sci USA 89, 10449-10453.

78. Horwitz J (1993) Invest Ophthalmol Vis Sci 34, 10-22.

79. Horwitz J, Emmons T, Takemoto L (1992) Current Eye Res 11, 817-822.

80. Horwitz J, Kabasawa I, Kinoshita JH (1977) Exp Eye Res 25, 199-208.

81. Horwitz J, McFall-Ngai M, Ding L-L, Yaron O (1986) in *The Lens: Transparency and Cataract* (Duncan G, ed) Eurage, Rijswijk, The Netherlands, pp. 227-40.

82. Huang Q-L, Russel P, Stone SH, Ziegler JS JR (1987) Curr Eye Res 6, 725-32.

83. Hutchison EB, Tichelaar W, Hofhaus G, Weiss H, Leonard KR (1989) EMBO J 8, 1485-90.

84. Ifeanyi F, Takemoto LJ (1990) Exp Eye Res 50, 113-6.

85. Ikemura H, Inouye M (1988) J Biol Chem 263, 12959-63.

86. Ingolia TD, Craig EA (1982) Proc Natl Acad Sci 79, 2360-4.

87. Inouye M (1991) Enzymes 45, 314-21.

88. Ireland M, Maisel H (1984) Curr Eye Res 3, 423-9.

89. Jakob U, Gaestel M, Engel K, Buchner J (1993) J Biol Chem 268, 1517-1520.

90. Kato K, Goto S, Hasegawa K, Shinohara H, Inaguma Y (1993) Biochim Biophys Acta 1175, 257-62.

91. Kato K, Shinohara H, Kurobe N, Goto S, Inaguma Y, Oshima K (1991) Biochim Biophys Acta 1080, 173-80.

92. Kelley MJ, David LL, Iwasaki N, Wright J, Shearer TR (1993) J Biol Chem 268, 18844-9.

93. Kim PS, Baldwin RL (1984) Nature 307, 329-34.

94. Kim PS, Baldwin RL (1990) Ann REv Biochem 59, 631-60.

95. Koenig SH, Brown RD III, Spiller M, Chakrabarti V, Pande A (1992) Biophys J 61, 776-85.

96. Kuwabara T (1983) in *Histology: Cell and Tissue Biology*. (Weiss L, ed) 5th ed, Elsevier, New York, pp. 1135-76.

97. Kuwajima K (1989) Proteins 6, 87-103.

98. Laemmli UK (1970) Nature 227, 680-685.

99. Landry SJ, Gierasch LM (1991) Biochemsitry 30, 7359-62.

100. Landry SJ, Jordan R, McMacken R, Gierasch LM (1992) Nature 355, 455-7.

101. Levinthal C (1968) J Chem Phys 65, 44-5.

102. Liang C-J, Hamashita K, Muellengerg, Shichi CG, Kobata A (1979) J Biol Chem 254, 6414-8.

103. Lindley PF, Narebor ME, Summers LJ, Wistow GJ (1985) in *The Ocular Lens* (Maisel H, ed) Marcel Dekker, New York, pp. 123-167.

104. McDermott MJ, Chiesa R, Spector A (1988) Biochem Biophys Res Commun 157, 626-31.

105. McMullin TW, Hallberg RL (1987) Mol Cell Biol 7, 4414-23.

106. Manski WJ, Malinowski KC (1980) J Biol Chem 255, 1572-6.

107. Mayr E-M, Jaenicke R, Glockshuber R (1994) J Mol Biol 235, 84-8.

108. Miranker A, Radford SE, Karplus M, Dobson CM (1991) Nature 349, 633-6.

109. Merck KB, De Haard-Hockman WA, Oude Essink BB, Gloemendal H, DeJong WW (1992) Biochim Biophys Acta 1130, 267-76.

110. Merck KB, Groenen PJTA, Voorter CEM, de Haard-Hoekman WA, Horwitz J, Bluemendal H, de Jong WW (1993) J Biol Chem 268, 1046-1052.

111. Merck KB, Horwitz J, Kersten M, Overkamp P, Gaestel M, Bloemendal H, DeJong WW (1993) Mol Biol Reports 18, 209-15.

112. Miesbauer LR, Zhou X, Yang Z, Yang Z, Sun Y, Smith DL, Smith JB (1994) J Biol Chem 269, 12494-502.

113. National Advisory Eye Council (1993) *Vision Research: A National Plan 1994-1998*. NIH/NEI, Bethesda, MD.

114. Ngo JT, Klisak I, Dubin RA (1989) Genomics 5, 665-9.

115. Nilsson B, Anderson S (1991) Annu Rev Microbiol 45, 607-35.

116. O'Farrell PZ, Goodman HM, O'Farrell PH (1977) Cell 12, 1133-1142.

117. Oas TG, Kim PS (1988) Nature 336, 42-8.

118. Parveen R, Smith JB, Sun Y, Smith DL (1993) J Prot Chem 12, 93-101.

119. Piatigorsky J (1984) Cell 38, 620-1.

120. Piatigorsky J (1987) Invest Ophthalmol Vis Sci 28, 9-28.

121. Piatigorsky J, O'Brien WE, Norman BL (1988) Proc Natl Acad Sci 85, 3479-83.

122. Ptitsyn OB (1991) J Protein Chem 6, 272-93.

123. Quax-Jenken Y, Quax W, Van Rens G, Khan PM, Bloemendal H (1985) Proc Natl Acad Sci, USA 82, 5819-5823.

124. Quax-Jenken Y, Driessen H, Leunissen J, Quax W, DeJong W, Bloemendal H (1985) EMBO J, 4, 2597-602.

125. Radford SE, Dobson CM, Evans PA (1992) Nature 358, 302-7.

126. Rafferty NS (1985) in *The Ocular Lens: Structure, Function, and Pathology*. (Maisel H, ed) Marcel Dekker, New York, pp. 1-60.

127. Rao P, Horwitz J, Zigler S (1993) Biochem Biophys Res Commun 190, 786-93.

128. Rao SC, Rao CM (1994) FEBS Lett 337,269-73.

129. Rothman JE (1989) Cell 59, 591-601.

130. Roy D, Chiesa R, Spector A (1983) Biochem Biophys Res Commun 116, 204-9.

131. Roy D, Dillon J, Chaney W, Spector A (1984) Proc Natl Acad Sci 81, 2878-81.

132. Roy D, Spector A (1978) Exp Eye Res 26, 445-59.

133. Russel P (1984) Invest Ophthalmol Vis Sci 25, 209-12.

134. Schimke RT (1975) in *Intracellular Protein Turnover* Acad Press, NY, pp. 173-86.

134a. Shearer TR, David LL, Anderson RS, Azuma M (1987) Curr Eye Res 6, 289.

135. Shearer TR, Azuma M, David LL, Murachi T (1991) Invest Ophthalmol Vis Sci 32, 533-540.

136. Shearer TR, David LL, Anderson RS, Azuma M (1992) Curr Eye Res 11, 357-369.

137. Shinde U, Inouye M (1993) TIBS 18, 442-6

138. Siezen RJ, Hoenders HJ (1977) Febs Lett 80, 75-80.

139. Silen JL, Agard DA (1989) Nature 341, 462-4.

140. Spector A (1985) in *The Ocular Lens: Structure, Function, and Pathology.* (Maisel H, ed) Marcel Dekker, New York, pp. 405-38.

141. Spector A, Li LK, Augusteyn RC, Schneider A, Freund T (1971) Invest Ophthalmol Vis Sci 10, 677-86.

142. Srivastava OP, Ortwerth BJ (1983) Exp Eye Res 37, 597-612.

143. Srivastava OP, Srivastava K, Silney C (1994) Exp Eye Res, In Press.

144. Streeten BW, Licari PA, Marucci AA, Dougherty RM (1981) Invest Ophthalmol Vis Sci 21, 130-5.

145. Takemoto L, Emmons T (1991) Exp Eye Res 53, 811-813.

146. Takemoto L, Emmons T, Granstrom D, Griffin PR, Shabanowitz J, Hunt DF (1990) Exp Eye Res 50, 695-702.

147. Takemoto L, Emmons T, Horwitz J (1993) Biochem J, 294, 435-8.

148. Tardieu A, Delaye M (1988) Biophys Biophys Chem 17, 47-70.

149. Thompson JA, Augusteyn RC (1988) Curr Eye Res 7 563-9.

150. Thompson JA, Augusteyn RC (1989) Biochim Biophys Acta 994, 246-52.

151. Thompson JA, Siezen RJ, Kaplan ED, Messmer M, Chakrabarti B (1989) Curr Eye Res 8, 139-49.

152. Trokel SL (1962) Invest Ophthalmol Vis Sci 1, 493-501.

153. Uchiumi T, Kimura S, Ogata K (1983) Exp Eye Res 36, 125-134.

154. van der Heuvel R, Hendriks W, Quax W, Bloemendal H (1985) J Mol Biol 185, 273-84.

155. van der Oetelaar PJM, Clauwaert J, van Laethem M, Hoenders HJ (1985) J Biol Chem 260, 14030-4.

156. van der Ouderaa FJ, DeJong WW, Bloemendal H (1973) Eur J Biochem 39, 207-22.

157. van Kleef FSM, Willems-Thijssen W, Hoenders HJ (1976) Eur J Biochem 66, 477-83.

158. van Kleef FSM, Nijiink-Maas M, Hoenders HJ (1974) Eur J Biochem 48, 543-70.

159. Varnum MD, David LL, Shearer T (1989) Exp Eye Res 49, 1053-1065.

160. Vermorken AJM, Bloemendal H (1978) Nature 271, 779.

161. Walsh MT, Sen AC, Chakrabarti B (1991) J Biol Chem 266, 20079-84.

162. Wislocki GB (1952) Am J Anat 91, 233.

163. Wistow G (1985) FEBS Lett 181, 1-6.

164. Wistow G (1993) TIBS 18, 301-6.

165. Wistow G (1993) Exp Eye Res 56, 729-32.

166. Wistow G, Mulders JWM, DeJong WW (1987) Nature 326, 622-4.

167. Wistow G, Piatigorsky J (1987) Science 236, 1554-6.

168. Wistow G, Piatigorsky J (1988) Ann Rev Biochem 57, 479-503.

169. Wright PE, Dyson HJ, Lerner RA (1988) Biochemistry 27, 7167-75.

170. Veretout R, Delaye M, Tardieu A (1989) J Mol Biol 205, 713-8.

171. Yoshida H, Yumoto N, Tsukahara I, Murachi T (1986) Invest Ophthalmol Vis Sci 27, 1269-1273.

THE JOURNAL OF BIOLOGICAL CHEMISTRY
Vol. 268, No. 25, Issue of September 5, pp. 18844-18849, 19
Printed in U.S.

α-Crystallin Chaperone Activity Is Reduced by Calpain II *in Vitro* and in Selenite Cataract*

(Received for publication, March 15, 1993, and in revised form, May 14, 199

Mary J. Kelley‡, Larry L. David, Naoki Iwasaki, Jay Wright, and Thomas R. Shearer

From the Departments of Biochemistry, Oral Molecular Biology, and Ophthalmology, Schools of Dentistry and Medicine, Oregon Health Sciences University, Portland, Oregon 97201

This study reports the first demonstration of a marked reduction in α-crystallin chaperone activity in an experimental model of cataract, and the study implicates activation of the cysteine protease calpain II (EC 3.4.22.17) as the *in vivo* protease responsible for decreased chaperone activity. Chaperone activity of normal α-crystallin from lenses of young rats was assayed by measuring attenuation of heat-induced aggregation and scattering of βL-crystallin. α-Crystallin from the nucleus of lenses with selenite cataract showed specific selective proteolysis, and chaperone activity was diminished. Proteolysis of α-crystallin from selenite cataract lenses was mimicked by incubating normal α-crystallin with calpain II, and this also resulted in loss of chaperone activity. Two-dimensional gel electrophoresis and peptide mapping were used to identify four partially degraded αA- and αB-crystallin polypeptides following incubation of normal α-crystallin with calpain. Similar partially degraded αA and αB polypeptides were found in selenite cataract. Previous experiments indicated that α-crystallin chaperone activity decreases because of removal of the COOH terminus. Our experiments support this observation and suggest that calpain proteolysis of α-crystallin at the COOH terminus may result in a loss of chaperone activity in selenite cataract.

The transparency and refractive power of the lens in mammalian eyes are maintained by a highly ordered array of structural proteins designated α-, β-, and γ-crystallins. Based on sequence homologies, β- and γ-crystallins belong to the same evolutionary superfamily, whereas the α-crystallins are related to the small heat shock protein family (1–4). The chaperone activity of α-crystallin was found to be as effective as some small heat shock proteins in preventing heat denaturation of proteins (5). A recent hypothesis therefore states that the chaperone activity of α-crystallin may be important in helping to prevent denaturation of crystallins in lens (6, 7). Such denatured insoluble crystallins are a hallmark of experimental cataracts in lens (8). Opaque cataract is the universal response of the lens to a wide variety of insults including excess sugar, UV irradiation, trauma, toxic chemicals, and aging. Protein denaturation during cataract form tion is particularly detrimental to the lens because the le has little protein turnover. Thus, it is important to determir which factors influence α-crystallin chaperone activity in len

Aging in bovine lenses was recently shown to reduce crystallin chaperone activity (9). α-Crystallins undergo clea age at their COOH termini during aging of the lens (10 however, the specific *in vivo* proteases causing the loss of t COOH terminus of α-crystallin are unknown. Furthermor no data have been published on whether or not α-crystalli chaperone activity is reduced in cataract.

The experimental model of cataract produced by an ove dose of selenite in the young rat was used in the present stu to investigate changes in chaperone activity during catara formation, because the model involves proteolysis of α- an β-crystallins (11). Loss of NH_2-terminal extensions on crystallins may lead to their insolubilization and to productio of light scattering opacity (12). Calpain II, a calcium-depen ent nonlysosomal cysteine protease found in all vertebra cells studied, is believed to be responsible for most of t proteolysis in selenite cataract (13), and this protease has al been implicated in other models of cataract in rat lens utilizing calcium ionophore A23187 (14), galactose (15), xylo (14), and diamide (16). Although α-crystallins are not inso ubilized during formation of selenite cataract, they do under partial degradation, both during cataract formation (17) an after incubation with calpain II (18). Therefore, calpain II a likely endogenous protease that may contribute to loss chaperone activity in rat lens. Thus, the purposes of t present study were to determine if the chaperone activity α-crystallin is lost during the formation of the selenite cat ract and to determine if *in vitro* incubation with purifie calpain II can also cause the loss of chaperone activity of crystallin.

MATERIALS AND METHODS

Production of Selenite Cataract—Cataracts were induced in 1 day-old Sprague-Dawley rats from B & K International (Fremor CA) following a single subcutaneous injection of 30 μmol of sodiu selenite/kg of body weight. Five days after injection, cortex a nucleus of lenses were isolated by dissection, as described previous (17). Animals used in this study were treated in accordance with t Declaration of Helsinki and appropriate National Institutes of Heal recommendations.

Gel Filtration of Crystallins—To obtain α- and βL-crystallin cortical and nuclear regions from 40 lenses were homogenized buffer I containing 20 mM imidazole (pH = 6.8), 0.1 mM EGTA, mM dithioerythritol, and 0.01% azide. Homogenates were centrifug at 8000 × *g* for 15 min at room temperature to prevent cold precip tation of crystallins. Following centrifugation, the supernatant w applied to a 2.5 × 90-cm Bio-Gel A1.5 M gel filtration column (Bi Rad) and eluted with 20 mM Tris buffer (pH = 7.5) containing 1 m EGTA, 1 mM EDTA, 10 mM 2-mercaptoethanol, and 100 mM Na

* This research was funded by Grants EY07755 (to L. L. D.) and EY05786 and EY03600 (to T. R. S.) from the National Eye Institute. The costs of publication of this article were defrayed in part by the payment of page charges. This article must therefore be hereby marked "*advertisement*" in accordance with 18 U.S.C. Section 1734 solely to indicate this fact.

‡ To whom correspondence should be addressed: Oregon Health Sciences University, 611 S.W. Campus Dr., Portland, OR 97201. Tel.: 503-494-8774; Fax: 503-494-8918.

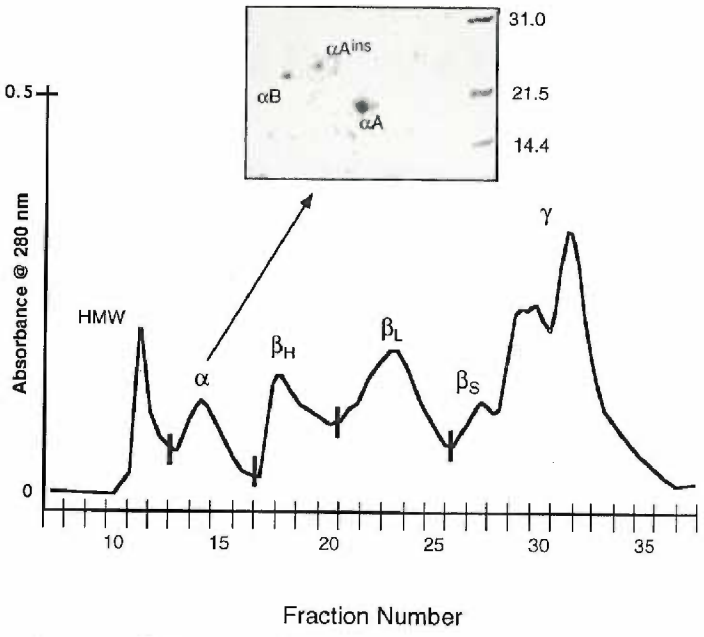

FIG. 1. **Gel filtration chromatography of water-soluble proteins from lens cortex of 14-day-old rats.** *Heavy vertical bars* on this representative chromatogram enclose α-crystallin and βL-crystallin peaks. The *inset* shows a portion of a two-dimensional electrophoretic gel of the proteins in the α-crystallin peak, indicating αA, αB, and αA insert polypeptides.

at 25 ml/h flow rate. After pooling various fractions (Fig. 1), α- and βL-crystallins were concentrated by ultrafiltration (YM-5 membrane, Amicon, Beverly, MA), and the gel filtration buffer was exchanged for buffer I. Protein concentrations were determined by the Bio-Rad dye-binding reagent (Bio-Rad) using bovine serum albumin as standards.

Proteolysis of Lens Proteins with Calpain—Calpain II was purified from porcine cardiac muscle as described previously (12). Use of porcine cardiac muscle calpain II was appropriate, because it degraded crystallin at similar sites as calpain purified from rat lens (19). To proteolyze α-crystallin, 17 units of purified calpain II were incubated with 0.48 mg of normal α-crystallin and 2 mM $CaCl_2$ in a total volume of 0.4 ml of buffer I at 37 °C. The reaction was stopped after 1 h by the addition of 0.1 ml of 25 mM EGTA.

Chaperone Experiments—Heat-induced aggregation of βL-crystallin was measured by the increase in light scattering at 340 nm in an enzyme-linked immunosorbent assay plate reader. Normal βL-crystallin (200 μg/ml) was incubated at 64 °C in a total volume of 0.25 ml of buffer I containing 0.08 M NaCl. The wells were normalized to correct for uneven heating across the plate. The measurement of the light scatter of the same βL-crystallin solution in all of the individual wells (columns 1 and 12 not used) was the basis of this normalization. To test chaperone effects, either 25, 50, or 75 μg/ml α-crystallin were added to the βL-crystallin prior (5 min at 37 °C) to heat-induced aggregation.

Electrophoresis—One-dimensional SDS-PAGE[1] (20) of lens proteins was performed on 12% (0.75 mm thick) gels. Low and broad range molecular weight standards were used (Bio-Rad) at 6.2 μg of protein/lane. Two-dimensional electrophoresis using a nonequilibrium pH gradient in the first dimension and SDS-PAGE with 12% gels in the second was conducted as described previously (13, 21). Gels were stained with Coomassie Blue, and blots were stained with Ponceau S before being subjected to computer image analysis (Image 1.44, National Technical Service, Springfield, VA) following digital flat bed scanning (LaCie Silverscanner, Beaverton, OR) using green lamp illumination, 200 dots/inch resolution, and 256 gray levels/pixel.

Tryptic Mapping—Following incubation with calpain, putative breakdown products of αA- and αB-crystallins were identified by tryptic mapping. The lenses of 14-day-old rats were d homogenized at a ratio of 1 mg of lens wet weight/2.5 μ The lens homogenates were centrifuged at 8000 × *g* fc 25 °C to remove the insoluble protein. Soluble lens pro ml) was incubated for 60 min at 37 °C in buffer I contain of calpain II/mg of lens protein and 1.2 mM $CaCl_2$ and c 8000 × *g* for 15 min. The supernatant was removed, dried centrifuge, and frozen at −70 °C. Aliquots (250 μg) of the proteolyzed with calpain and nonproteolyzed control s then subjected to two-dimensional gel electrophoresis. from four gels were blotted onto PVDF membranes (I Millipore, Bedford, MA), stained, excised, subjected to tion with trypsin, and separated by reverse phase HPLC terminal sequence analysis was performed as describe (13). The molecular weights of αA-crystallin tryptic fra measured using fast atom bombardment mass spectros scribed previously (22).

[1] The abbreviations used are: PAGE, polyacrylamide gel electrophoresis; PVDF, polyvinylidene difluoride; HPLC, high performance liquid chromatography.

RESULTS

Chaperone Activity of Rat Lens α-Crystallins—α Crystallins were isolated from the soluble protein 14–15-day-old rat lens cortex by gel filtration (Fi PAGE demonstrated that α-crystallin was compos major polypeptides (Fig. 2, *lane 2*), and βL-cry composed of two major and two minor polypeptid *lane 8*). Based on their migration during SDS-PAG dimensional electrophoresis, the α-crystallin p

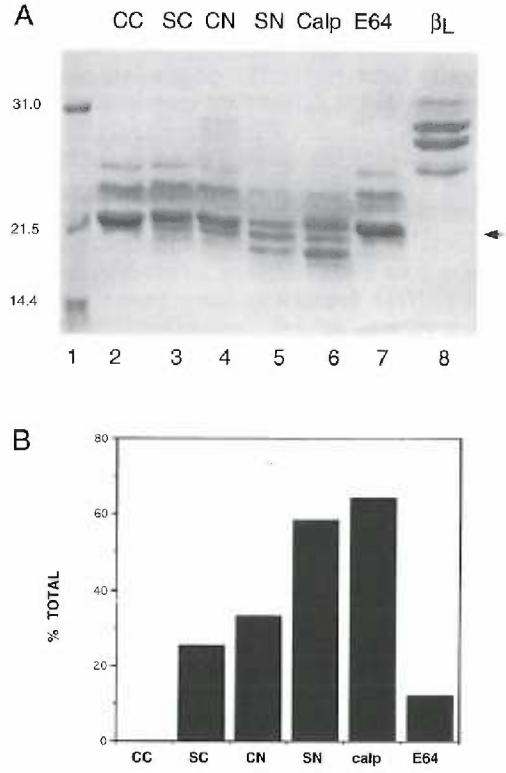

FIG. 2. *A*, SDS-PAGE of α-crystallin preparations. *La* ular mass standards labeled in the margin in kilodaltons crystallin from control cortex (*CC*); *lane 3*, α-crystallin fr cortex (*SC*); *lane 4*, α-crystallin from control nucleus (C α-crystallin from selenite nucleus (*SN*); *lane 6*, α-crys control cortex incubated with calpain (*CALP*); *lane 7*, from control cortex incubated with both calpain and protease inhibitor, E64 (*E64*); *lane 8*, βL-crystallin (*βL*) is the control cortex by gel filtration and used in the h aggregation and scattering assay. All sample lanes were l 5 μg of protein/lane. Note the appearance of proteolytic below the *arrow*, especially in *lanes 5* and *6*. *B*, percer crystallin fragments. Percentages were calculated by de scanning of the gel shown in *A* and dividing the densit below 20 kDa by the total density of each lane × 100.

were identified as αA, αB, and αA insert (Fig. 1, *box*) (23). The α-crystallin fractions from lens cortex and nucleus were first tested for their ability to act as chaperones. Heating βL-crystallin from the cortex of rat lens in the absence of α-crystallin caused aggregation as measured by an increase in light scattering at 340 nm (Fig. 3, *beta-L*). The extent of aggregation of βL-crystallin was directly related to both the concentration of βL-crystallin and duration of heating (Fig. 3, *inset*).

Addition of normal α-crystallin from the lens cortex of young rats caused a marked protective effect against the heat-induced aggregation and scattering of βL-crystallin (Fig. 3, *beta-L/CC*). This was similar to the chaperone activity of α-crystallin observed in other species (6, 7). The results of the chaperone activity of α-crystallin depended upon two factors, the temperature, and the purity of the preparation. If the temperature was too high, or if the preparation was not very pure, then the α-crystallin sample was a less effective chaperone. The chaperone activity of α-crystallin from the cortex of rat lens shown in Fig. 3 was 91% effective against heat-induced aggregation and scattering of βL-crystallin at 30 min and 82% effective even after 60 min of heating at 64 °C (Fig. 3). The proportions of α- and βL-crystallin subunits in Fig. 2 were used to calculate a weighted average molecular mass of the α-crystallin monomer to be 21 kDa and of the βL-crystallin monomer to be 29 kDa. By using these values, the molar ratio of βL- to α-crystallin subunits in Fig. 3 was approximately 2:1, but the chaperone effect of cortical α-crystallin was appreciable even at a molar ratio of βL- to α-crystallin 6:1. Note that α-crystallin from the nucleus of rat lens w also an effective chaperone for the first 30 min of heating βL-crystallin (Fig. 3, *beta-L/CN*). However, after 30 min, crystallin from the nucleus tended to lose chaperone effe tiveness faster than α-crystallin from the cortex.

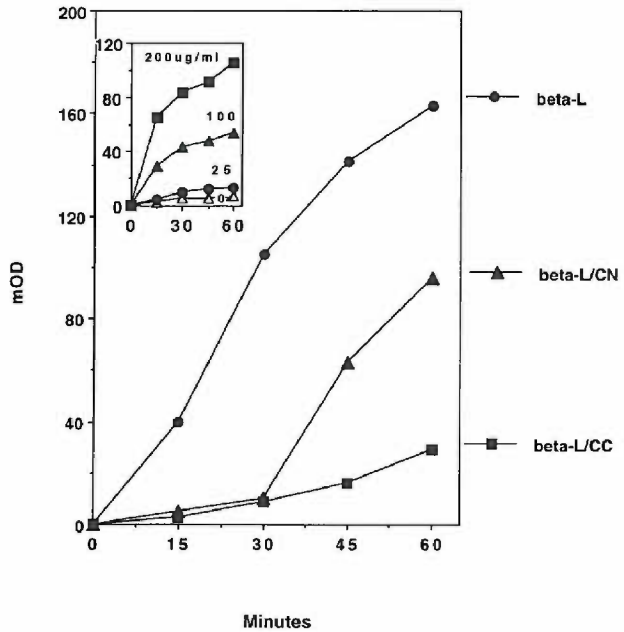

FIG. 3. **Rate of heat-induced aggregation and scattering of βL-crystallin (200 μg/ml) in the presence (75 μg/ml) and absence of α-crystallin isolated from the lens cortex and nucleus of control 14-day-old rats.** Control cortical α-crystallin (*CC*) was more effective than control nuclear α-crystallin (*CN*) in preventing the heat-induced aggregation and scattering of βL-crystallin. βL-Crystallin without α-crystallin aggregates and precipitates most rapidly. The *inset* shows a time course of heat-induced aggregation and scattering of successively higher concentrations of βL-crystallin at 64 °C. The *y* axis (optical density (*mOD*) increase 1000) is the increase in light scattering measured at 340 nm and the *x* axis is incubation time (min) for both figures. The higher concentrations of βL-crystallin showed increased precipitation and light scatter during heating. For all subsequent aggregation assays, 200 μg/ml βL-crystallin was used. Mean range for multiple determinations (n = 2–4) for all points on this figure was ± 10%. At each time point, none of the individual values within a group overlapped individual values in another group.

Chaperone Activity of α-Crystallins from Selenite Cataract

In order to test if the chaperone effect of α-crystallin w altered in a model of cataract, α-crystallins were also isolat from the lens cortex and nucleus of rats with dense nucle selenite cataracts. After 30 min at 64 °C, the α-crystallin fro the nucleus of lenses with selenite cataract showed marked reduced chaperone activity (Fig. 4*A*, *SN*). By contrast, the crystallin from control cortex (*CC*), selenite cortex (*SC*), a control nucleus (*CN*) were all effective chaperones (Fig. 4*A* although the α-crystallin from the control cortex (*CC*, F 4*A*) was slightly more effective than the others at low concentrations.

Correlations between proteolysis and chaperone activi were made by subjecting the α-crystallin from the lens cortic and nuclear regions of control and selenite treated rats SDS-PAGE (Fig. 2). The chaperone-defective α-crystall aggregates from the cataractous nucleus of selenite-treat (*SN*) rats showed specific selective proteolysis of αA, αB, a αA insert polypeptides. In addition, new proteolytic fragmen appeared at approximately 18 and 19 kDa (Fig. 2*A*, *lane 5* The proteolytic fragments of α-crystallins at 18 and 19 kI comprised approximately 58% of the total α-crystallin isolat from the selenite cataractous nucleus (Fig. 2*B*). Control n cleus (*CN*) and selenite cortex (*SC*), which exhibited slight reduced chaperone activity, showed lesser levels of proteolys (Fig. 2*A*, *lanes 3* and *4*) with fragments comprising only and 33% of the total protein (Fig. 2*B*).

Chaperone Activity of α-Crystallin Incubated with Purifi

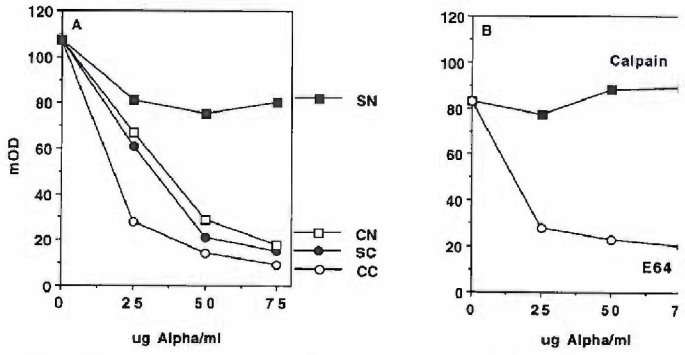

FIG. 4. *A*, comparison of the chaperone activity of normal a selenite cataract α-crystallins. α-Crystallins from selenite nucle (*SN*), selenite cortex (*SC*), control nucleus (*CN*), and control cort (*CC*) were used at the concentrations indicated to suppress the hea induced aggregation and scattering of 200 μg/ml βL-crystallin 64 °C. α-Crystallins from selenite nucleus (*SN*) were ineffecti chaperones when compared with the other groups shown. The mea range for duplicate determinations for each point within this expe ment was ± 8%. None of the individual values at 25, 50, and 75 μg α-crystallin from the selenite nucleus overlapped with any value fro the control nucleus, selenite cortex, or control cortex groups. treatment of α-crystallin with calpain decreased chaperone activit Prior to incubation with 200 μg/ml βL-crystallin at 64 °C for 30 mi α-crystallin was incubated for 1 h at 37 °C in the presence of calpai both with and without the protease inhibitor E64. The α-crystall treated with calpain proved to be an ineffective chaperone of β crystallin. E64, however, inhibited calpain proteolysis and allow the α-crystallin to act as a chaperone to prevent precipitation of β crystallin. The mean range for replicates within this representati experiment was ± 3%. None of the individual values at 25, 50, a 75 μg of α-crystallin overlapped between the calpain and E64 grou

Calpain II—Proteolysis observed in selenite cataract is caused by activation of calcium-activated protease, calpain II, present in rat lens (13). Thus, it was conceivable that the loss of chaperone activity observed in selenite cataract was due to proteolysis of α-crystallin by calpain. In order to test this hypothesis, normal α-crystallin from the clear cortical region of rat lenses was incubated with purified calpain II (Fig. 2, *lane 6*). This resulted in a pattern of proteolysis similar to that observed in selenite cataract (Fig. 2, *lane 5*), with similar proportions of proteolytic fragments below 20 kDa (Fig. 2*B*). As a control, the cysteine protease inhibitor E64 was added at the beginning of the incubation in order to inhibit calpain. This resulted in an α-crystallin preparation which showed only minor proteolysis (Fig. 2*A*, *lane 7* and Fig. 2*B*), resembling normal α-crystallin. The α-crystallin preparation resulting from incubation of α-crystallin with calpain showed markedly reduced chaperone activity (*calpain curve*, Fig. 4*B*). This was compared with the chaperone activity of α-crystallin incubated with calpain inhibited by E64 (*E64 curve*, Fig. 4*B*), which retained effective chaperone activity.

Unlike βL-crystallin, normal intact α-crystallin showed no appreciable increase in light scattering when heated to 64 °C. However, the α-crystallin incubated with calpain showed increased light scattering when heated (data not shown). Some loss of thermal stability was also noted for α-crystallin from the cataractous nucleus of rats with selenite cataract.

Nature of α-Crystallin Cleavage—In order to gain insight into specific changes occurring on α-crystallin leading to loss of chaperone activity, control soluble protein from rat lens, and soluble protein incubated with calpain II were separated by two-dimensional electrophoresis, and the polypeptides were electrotransferred onto PVDF membranes. Since αA and αB were NH_2-terminally blocked, the identity of the intact αA and αB polypeptides (Fig. 5*A*) was confirmed by *in situ* trypsinization on the membrane surface and separation of the resulting tryptic fragments by HPLC (Fig. 6, *αA* and *αB*). Sequence analysis of two of the resulting peaks confirmed the identity of these polypeptides as αA and αB. A peak eluting at 48 min from the αA digest (Fig. 6, *αA*) was subjected to eight cycles of amino acid sequence analysis. The peak contained two polypeptides with the sequences ALGPFYPS and XFSPQDLT. These matched the partial sequences of two tryptic fragments from rat αA crystallin (residues 13–20 and 79–86) (24). The identity of the residue marked *X* could not be determined because of histidine at this position. Mass spectroscopy confirmed the identity of these fragments and detected peptides with the masses of 1006.5 and 1171.5 in this peak. These masses differed from the predicted masses of residues 13–20 and 79–86 of αA by 0.0 and 0.9 atomic mass units, respectively. A peak eluting at 56 min from the αB digest (Fig. 6, *αB*) contained a fragment with the sequence APSXIDTGLS. This sequence corresponded to residues 57–66 of hamster αB (25). The identity of the residue marked *X* could not be determined because of the presence of tryptophan at this position. Following incubation with calpain, the spots corresponding to undegraded αA and αB decreased in concentration and several fragments appeared which were tentatively identified as αA and αB breakdown products (Fig. 5*B*, *αA-1*, *αA-2*, *αA-3*, and *αB-1*). These partially degraded polypeptides were trypsinized on the membrane surface and the resulting fragments were separated by HPLC (Fig. 6, *αA-1*, *αA-2*, *αA-3*, and *αB-1*). The tryptic maps of αA-1, αA-2, and αA-3 were similar to the tryptic map of undegraded αA. Similarly, the tryptic map of the partially degraded polypeptide αB-1 was similar to the tryptic map of undegraded αB. This confirmed

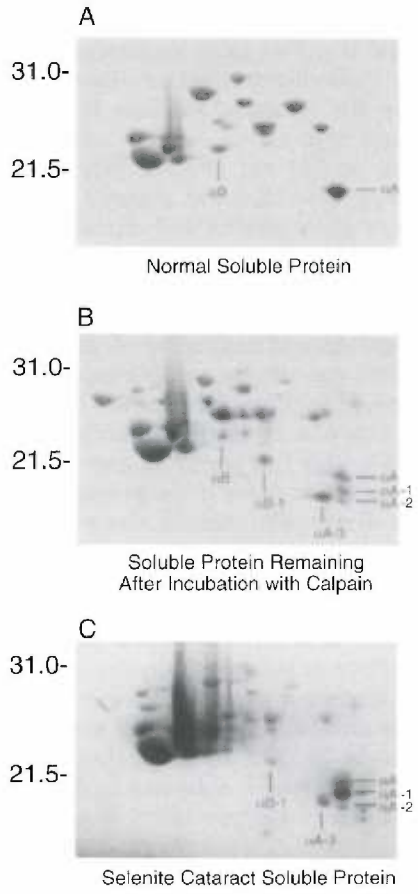

FIG. 5. **Two-dimensional electrophoresis of sol proteins from 14-day-old rats.** *A*, soluble protein from (control); *B*, soluble protein from whole lens remaining bation with calpain, and *C*, soluble protein from the lens rats treated with selenite. The positions of intact αA an peptides are indicated in *A*. These polypeptides were id sequencing tryptic fragments as shown in Fig. 6. Calpair produced partially degraded αA and αB polypeptides ir *αA-1*, *αA-2*, *αA-3*, and *αB-1* (*B*). These polypeptides wer by comparison of their tryptic maps with the tryptic ma αA and αB polypeptides (Fig. 6). Soluble proteins from of rats with selenite-induced cataract contained partiall polypeptides (*C*, *αA-1*, *αA-2*, *αA-3*, and *αB-1*). These p migrated to the same position as the partially degraded polypeptides produced by calpain (*B*).

that the polypeptides *αA-1*, *αA-2*, and *αA-3* in Fig derived from partial cleavage of αA and that the p αB-1 was derived from partial cleavage of αB. NH sequence analysis of polypeptides αA-1, αA-2, αA-3 1 indicated that all remained NH_2-terminally bloc is consistent with earlier reports that calpain cleav αB at their COOH terminus (26). Polypeptides mi the same positions as αA-1, αA-2, αA-3, and αB-1 found in the nucleus of rats with selenite cataract Therefore, the loss of residues on the COOH termi and αB was related to loss of chaperone activity, bo following calpain incubation, and *in vivo* followin formation.

DISCUSSION

The major findings in the present study were th one activity of α-crystallin isolated from selenite ca reduced and that the lens protease calpain may be r for the diminished chaperone activity. We hypoth α-crystallins may stabilize β-crystallins and the maintain lens transparency. Previous work has sho

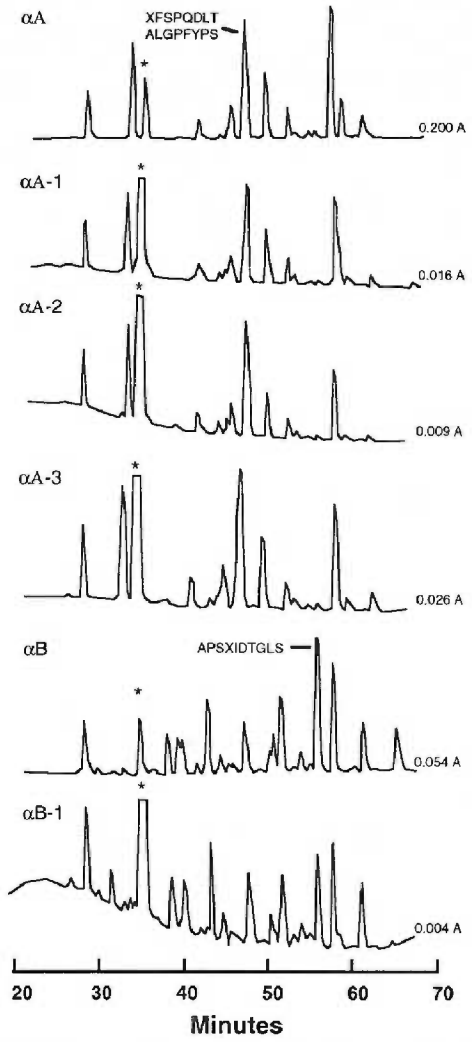

FIG. 6. **HPLC separation of tryptic fragments of αA- and αB-crystallins and their partial degradation products produced by calpain.** Polypeptides marked αA and αB in Fig. 5*A*, and *αA-1*, *αA-2*, *αA-3*, and *αB-1* in Fig. 5*B*, were transferred to PVDF membrane. The polypeptide spots were excised, trypsinized on the membrane surface, and the resulting fragments were separated by HPLC. Intact αA and αB polypeptides were identified by partial amino acid sequence of the indicated tryptic fragments. Fragments with the sequence ALGPFYPS and XFSPQDLT corresponding to residues 13–20 and 79–86 of αA (24) were both present in the peak eluting at 48 min. The residue indicated by *X* could not be detected because of the presence of histidine at this position. The sequence APSXIDTGLS corresponding to residues 57–66 of hamster αB (25) was present in the peak eluting at 56 min. The residue indicated by *X* could not be detected because of the presence of tryptophan at this position. The polypeptides αA-1, αA-2, and αA-3 were identified as partially degraded αA based on the similarity of their tryptic maps (compare *αA* with *αA-1*, *αA-2*, and *αA-3*). The polypeptide αB-1 was identified as a partially degraded αB (compare *αB* with *αB-1*). The *asterisk* denotes the trypsin peak, and the *numbers* on the *right side* of each chromatogram are the absorbance values of the largest peak, excluding the trypsin peak.

crystallin chaperone activity diminishes upon aging of bovine lenses (9). Opacities appearing in lenses from young rats with selenite cataract may result from a similar but more rapid loss of chaperone activity. Five days after an injection of selenite, the lens nucleus showed both opacity and loss of α-crystallin chaperone activity. In contrast, the chaperone activity of α-crystallins from the clear cortex of the lenses from rats injected with selenite was only slightly reduced. Moreover, the loss of chaperone activity in the various lens regions could be related to partial proteolysis of α-crystallins (Fig. 2).

Several pieces of evidence from the present investigatio support the hypothesis that calpain II is probably responsib for proteolysis and the loss of chaperone activity in seleni cataract. First, incubation of intact α-crystallin with calpai markedly reduced chaperone function, and addition of E64, calpain inhibitor, blocked this effect (Fig. 4*B*). Second, th pattern of limited proteolysis of α-crystallins from seleni cataract was similar to that produced by incubation of calpai with α-crystallin *in vitro*. In both cases, the proteolysis wa characterized by decreases in αA and αB crystallin polype tides and appearance of three fragments of αA and on fragment of αB that migrated similarly during two-dimer sional electrophoresis (Fig. 5).

Calpain appeared to decrease chaperone activity in a mar ner similar to that occurring with aging by removal of portion of the COOH terminus of α-crystallins (10, 27). Th three partially degraded αA and one partially degraded α fragments remained NH_2-terminally blocked following ca pain proteolysis. To obtain these fragments, a 1–2-kDa de crease in molecular mass must have occurred by removal of portion of the COOH terminus. Yoshida *et al.* (26) found tha calpain caused limited degradation of bovine α-crystallins b cleaving αA at the carboxyl side of residues 162 and 163 an αB at the carboxyl side of residues 163 and 170. This suggeste that removal of 11–12 residues or less at the COOH terminu of αA and αB will decrease chaperone activity. Limited diges tion with trypsin, in a separate study, also suggested tha removal of 16 and 12 residues from the COOH terminus c αA and αB, respectively, caused loss of chaperone activit (28). The reason why removal of such a limited number c residues produces loss of chaperone function is unknown. I is possible that removal of the COOH terminus causes a los of chaperone activity by destabilizing α-crystallin aggregate

To our knowledge, these are the first data to show tha chaperone function is reduced in a model of cataract and t attribute the effect to a specific enzyme found in the len Activity of calpain II in young rat lens is much higher tha in humans (29). Therefore, partial degradation of α-crystalli in human lenses during aging and cataract could involve protease other than calpain or a mechanism other than pro teolysis. The present data, however, do confirm that a loss c chaperone activity accompanies cataract formation in an an imal model. They also provide a rationale to determine if similar process occurs during human cataract.

Acknowledgments—We acknowledge Debra McMillen of the Inst tute of Molecular Biology, University of Oregon for sequencing dat used in this paper. We also thank Drs. Jean and David Smith of th Department of Medicinal Chemistry and Pharmacognosy, Purdu University for performing mass spectroscopy analysis of α-crystalli

REFERENCES

1. Lindley, P. F., Narebor, M. E., Summers, L. J., and Wistow, G. J. (198 in *The Ocular Lens* (Maisel, H., ed) pp. 123–124, Marcel Dekker, Inc New York
2. Cotlier, E. (1981) in *Alder's Physiology of the Eye* (Moses, R. A., ed) p 284–285, C. V. Mosby Co., St. Louis, MO
3. Harding, J. (1991) in *Cataract: Biochemistry, Epidemiology, and Pharma cology* (Harding, J., ed) pp. 30–33, Chapman and Hall Ltd., London
4. de Jong, W. W., Leunissen, J. A. M., Leenen, P. J. M., Zweers, A., an Versteeg, M. (1988) *J. Biol. Chem.* **263,** 5141–5149
5. Jakob, U., Gaestel, M., Engel, K., Buchner, J. (1993) *J. Biol. Chem.* **26** 1517–1520
6. Horwitz, J. (1992) *Proc. Nat. Acad. Sci. U. S. A.* **89,** 10449–10453
7. Merck, K. B., Groenen, P. J. T. A., Voorter, C. E. M., de Haard-Hoekma W. A., Horwitz, J., Bloemendal, H., de Jong, W. W. (1993) *J. Biol. Chen* **268,** 1046–1052
8. Harding, J. (1991) in *Cataract: Biochemistry, Epidemiology, and Pharma cology* (Harding, J., ed) p. 191, Chapman and Hall Ltd., London
9. Horwitz, J., Emmons, T., and Takemoto, L. (1992) *Curr. Eye Res.* **11,** 81 822
10. Takemoto, L., and Emmons, T. (1991) *Exp. Eye Res.* **53,** 811–813
11. Shearer, T. R., David, L. L., Anderson, R. S., and Azuma, M. (1992) *Cur Eye Res.* **11,** 357–369

12. David, L. L., Wright, J. W., and Shearer, T. R. (1992) *Biochim. Biophys. Acta,* **1139,** 210–216
13. David, L. L., Shearer, T. R., and Shih, M. (1992) *J. Biol. Chem.* **268,** 1937–1940
14. Shearer, T. R., Azuma, M., David, L. L., and Murachi, T. (1991) *Invest. Ophthalmol. & Visual Sci.* **32,** 533–540
15. Azuma, M., Shearer, T. R., Matsumoto, T., David, L. L., and Murachi, T. (1990) *Exp. Eye Res.* **51,** 393–401
16. Azuma, M., and Shearer, T. (1992) *FEBS Lett.* **307,** 313–317
17. David, L. L., and Shearer, T. R. (1984) *Invest. Ophthalmol. & Visual Sci.* **25,** 1275–1283
18. David, L. L., and Shearer, T. R. (1986) *Exp. Eye Res.* **42,** 227–238
19. David, L. L. amd Shearer, T. R. (1993) *FEBS Lett.*, in press
20. Laemmli, U. K. (1970) *Nature* **227,** 680–685
21. O'Farrell, P. Z., Goodman, H. M., and O'Farrell, P. H. (1 1133–1142
22. Parveen, R., Smith, J. B., Sun, Y., and Smith, D. L. (19 *Chem.* **12,** 93–101
23. Uchiumi, T., Kimura, S., and Ogata, K. (1983) *Exp. Eye Res.*
24. DeJong, W., Van Der Ouderaa, F. J., Versteeg, M., Groene Amelsvoort, M., and Bloemendal, H. (1975) *Eur. J. Bioch* 242
25. Quax-Jenken, Y., Quax, W., Van Rens, G., Khan, P. M., an H. (1985) *Proc. Nat. Acad. Sci., U. S. A.* **82,** 5819–5823
26. Yoshida, H., Yumoto, N., Tsukahara, I., and Murachi, T. *Ophthalmol. & Visual Sci.* **27,** 1269–1273
27. Emmons, T., and Takemoto, L. (1992) *Exp. Eye Res.* **55,** 55
28. Takemoto, L., Emmons, T., and Horwitz, J. (1993) *Biochem.*
29. Varnum, M. D., David, L. L., and Shearer, T. (1989) *Exp.* 1053–1065